Electronic Supplementary Material (ESI) for Organic & Biomolecular Chemistry.

Supporting Information

Greener Liquid-Phase Synthesis and ACE Inhibitory Structure-activity Relationship of Anti-SARS Octapeptide

Haidi Li, Jin Ren, Junyou Li, Zixin Zhang, Ninghui Chang, and Chuanguang Qin*

Shaanxi Key Laboratory of Polymer Science & Technology, OME Key Laboratory of Supernormal Material Physics & Chemistry, School of Chemistry and Chemical Engineering, Northwestern Polytechnical University, Xi'an 710129, P. R. China;

E-mail: qinchg@nwpu.edu.cn

Table of Contents

1. Abbreviations.

ACE: angiontens converting enzyme

Anti-SARS: anti-(severes acute respiratory syndrome)

DCM: dichloromethane

DEA: diethylamine

DIEA: N, N-diisopropylethylamine

DMAP: 4-dimethylaminopyridine

EA: ethyl acetate

EDC•HCl: 1-ethyl-3-(3-dimethylaminopropyl) carbodiimide hydrochloride

HHL: Hippury-L-Histidyl-L-Leucine

Hip: hippuric acid

HOBt: 1-hydroxybenzotriazole

MeCN: acetonitrile

MeOH: methanol

NCS: N-chlorosuccinimide

PE: petroleum ether

Py: pyridine

TDPBP: tri (4'-diphenyl phosphonyloxyl benzoylphenyl) phosphonate

TEA: triethylamine

TFA: trifluoroacetic acid

THF: tetrahydrofuran

Tis: triisopropylsilane

2. Synthesis of tri (4'-diphenyl phosphonyloxyl benzoylphenyl) Phosphate (TDPBP) Derivatives.

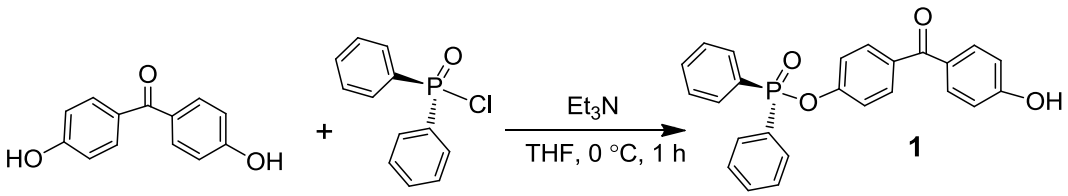

Synthesis of (a, 4-(4'-hydroxybenzoyl) phenyl diphenylphosphinate)

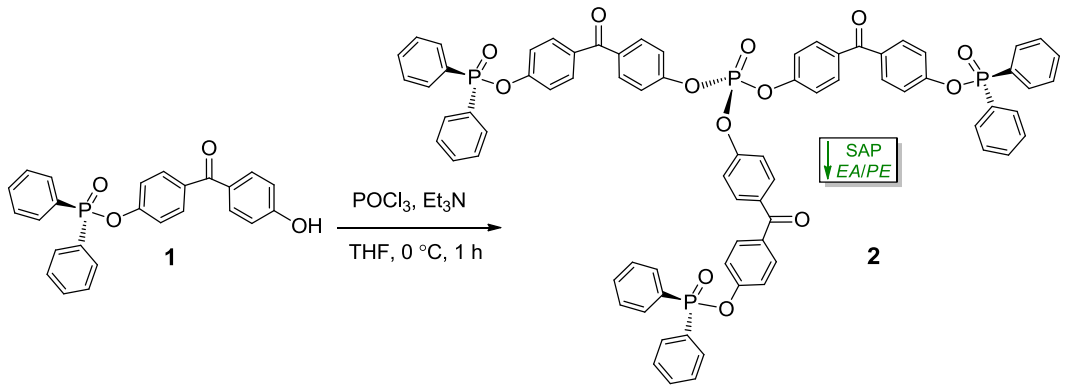

Synthesis of (b, tri(4'-diphenylphosphonyloxylbenzoyl phenyl) phosphonate)

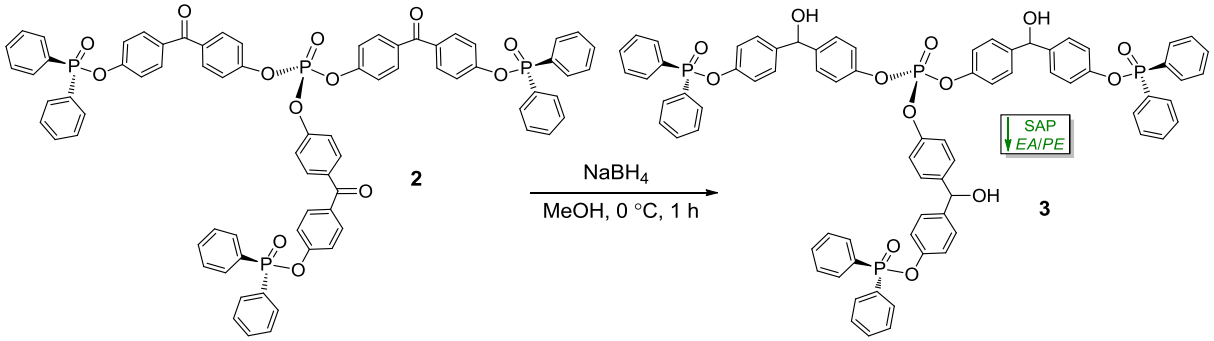

Synthesis of (c, tri(4-((4-((diphenylphosphoryl)oxy)phenyl)(hydroxy)methyl)phenyl) phosphonate, TDPBP-OH).

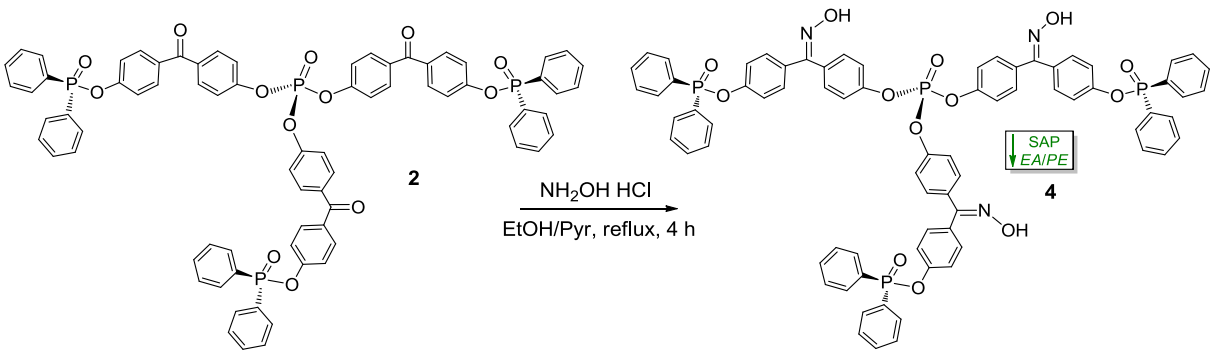

Synthesis of (4, bis(4-((E)-(4-((diphenylphosphoryl)oxy)phenyl) (hydroxyimino)methyl)phenyl) (4-((Z)-(4-((diphenylphosphoryl) oxy)phenyl) (hydroxyimino) methyl) phenyl) phosphate, TDPBP=N-OH).

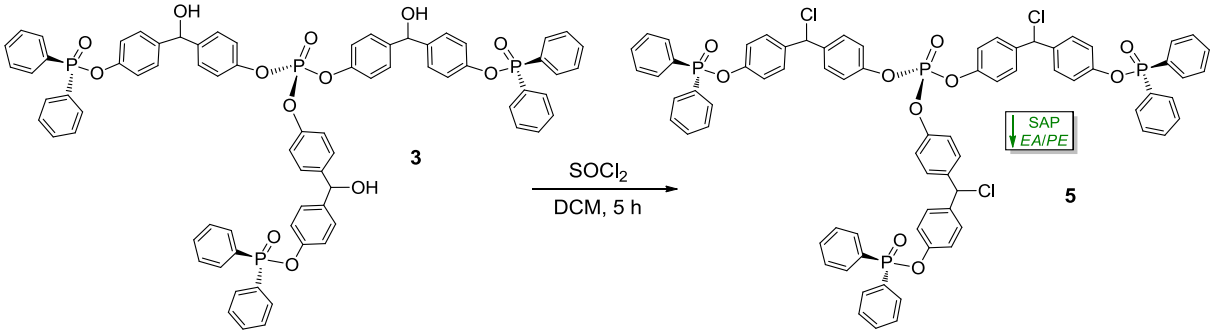

Synthesis of (5, tri(4-(chloro(4-((diphenylphosphoryl)oxy)phenyl)methyl)phenyl) phosphate, TDPBP-Cl).

3. Synthesis of anti-SARS octapeptide (2).

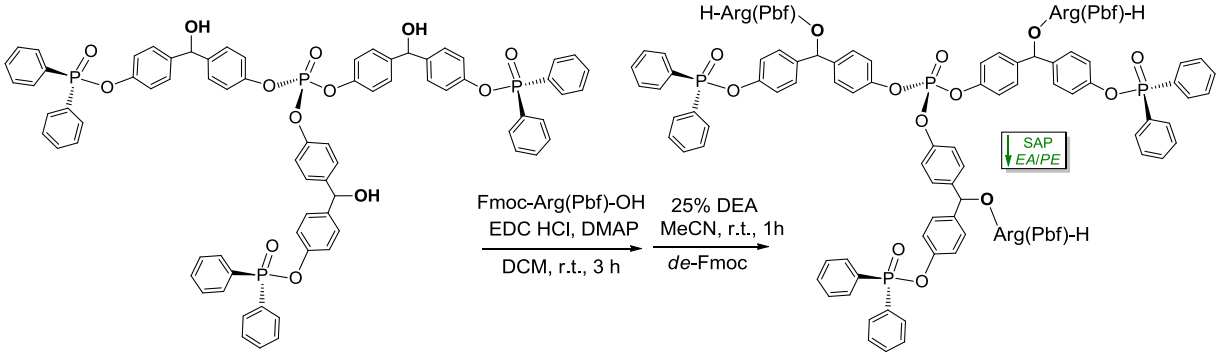

Synthesis of [Fmoc-Arg(Pbf)-O]$_3$-TDPBP

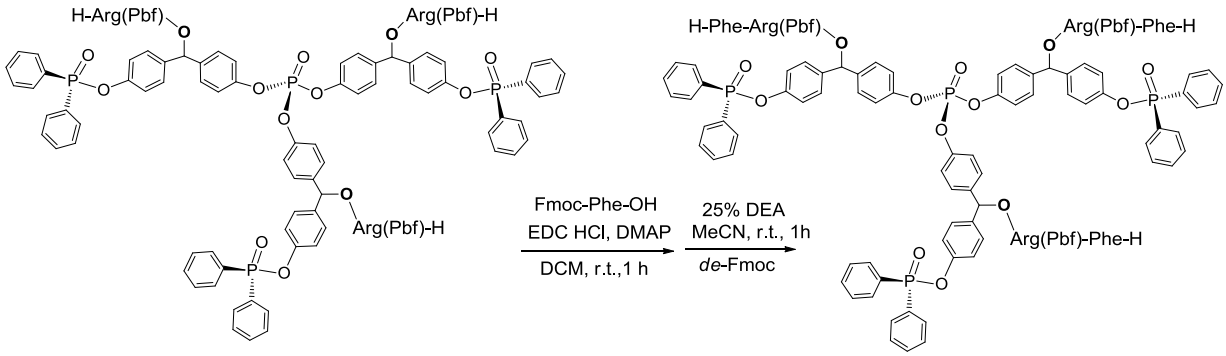

Synthesis of [Fmoc-Phe-Arg(Pbf)-O]$_3$-TDPBP

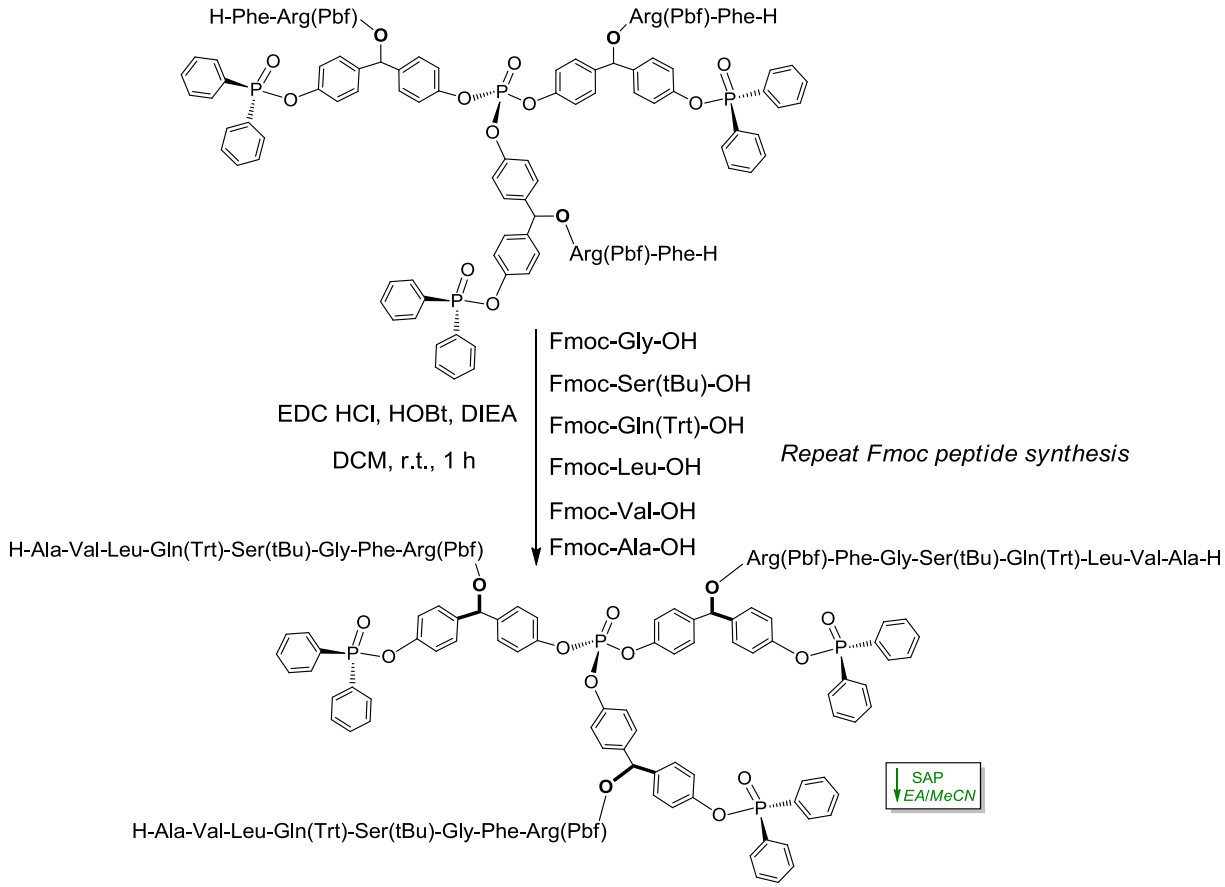

Extension of TDPBP attached octapeptide

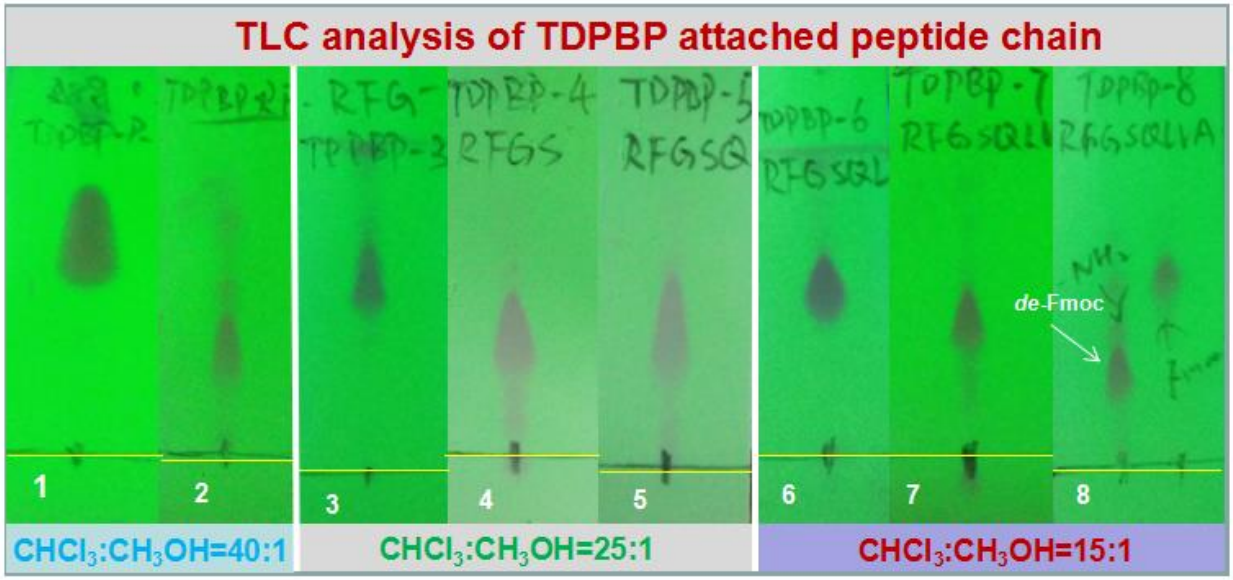

Figure S1: TLC analysis of the TDPBP attached peptide intermediate products.

1:[Fmoc-Arg(Pbf)-O]$_3$-TDPBP; **2**:[Fmoc-Phe-Arg(Pbf)-O]$_3$-TDPBP;

3:[Fmoc-Gly-Phe-Arg(Pbf)-O]$_3$-TDPBP; **4**:[Fmoc-Ser(tBu)-Gly-Phe-Arg(Pbf)-O]$_3$-TDPBP;

5:[Fmoc-Gln(Trt)-Ser(tBu)-Gly-Phe-Arg(Pbf)-O]$_3$-TDPBP;

6:[Fmoc-Leu-Gln(Trt)-Ser(tBu)-Gly-Phe-Arg(Pbf)-O]$_3$-TDPBP;

7:[Fmoc-Val-Leu-Gln(Trt)-Ser(tBu)-Gly-Phe-Arg(Pbf)-O]$_3$-TDPBP;

8:[Fmoc-Ala-Val-Leu-Gln(Trt)-Ser(tBu)-Gly-Phe-Arg (Pbf)-O]$_3$-TDPBP and

[NH$_2$-Ala-Val-Leu-Gln(Trt)-Ser(tBu)-Gly-Phe-Arg (Pbf)-O]$_3$-TDPBP;

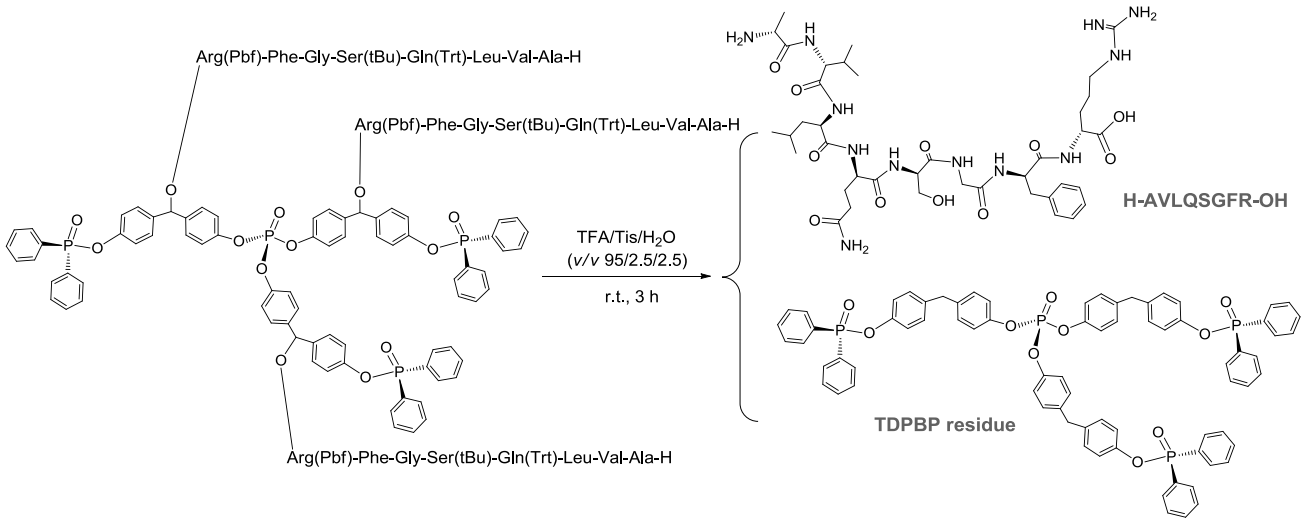

Shear of the octapeptide from the TDPBP support

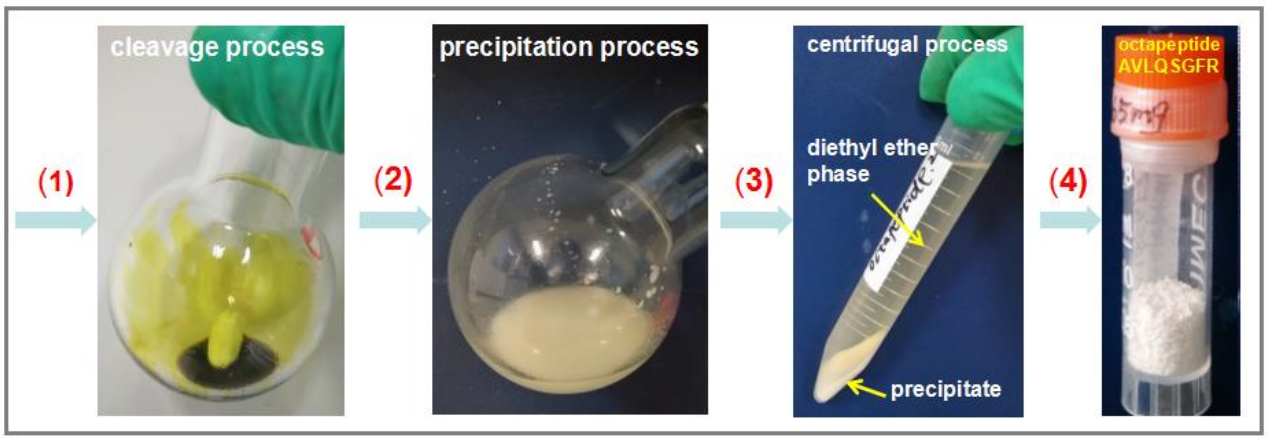

Figure S2. The optical photograph for cleavage and precipitation (purification) processes: (**1**) TFA/ Tis/ H_2O (3 mL, *v/v*, 95/2.5/2.5) cleavage process, r.t., 3 h; (**2**) Cold diethyl ether for precipitation process; (3) Centrifugal process to obtain the octapeptide precipitate process (the precipitate was repeated to add the cold diethyl ether and ultrasonic-assisted for 3 times to obtained the depurative target anti-SARS octapeptide AVLQSGFR)

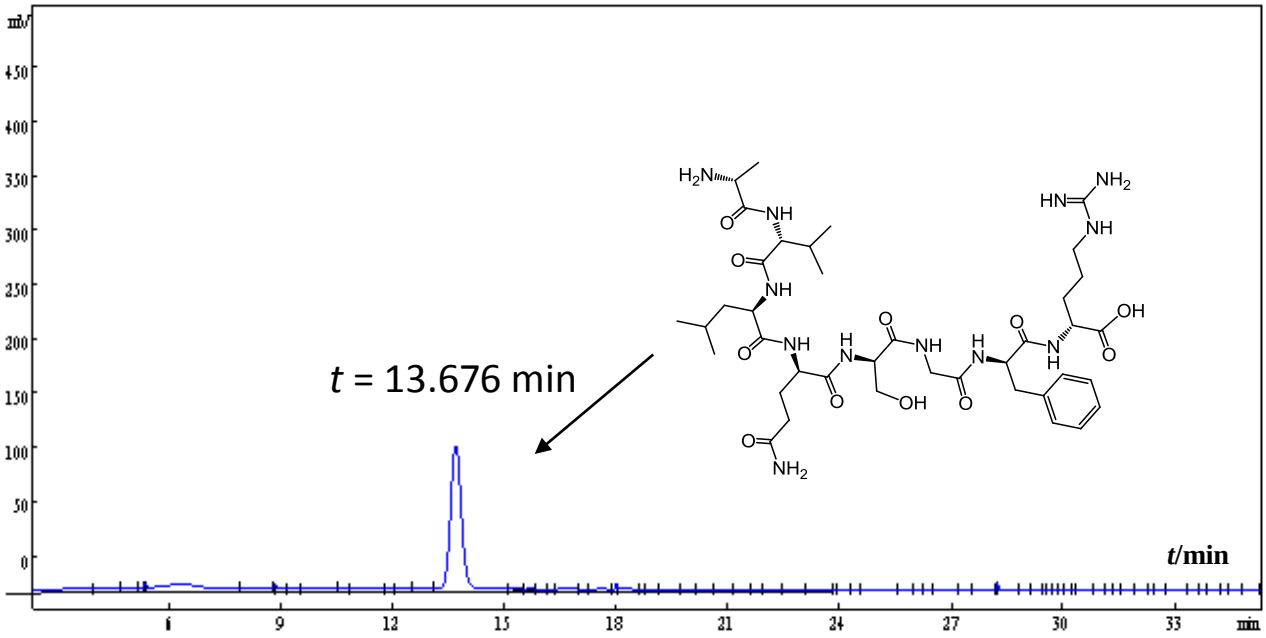

Figure S3. HPLC analysis of anti-SARS octapeptide (**2**). HPLC conditions: LC 3000 HPLC System with CXTH-3000 work station Column, Kromasil C18, NC-2546-06251151; 250×4.6 mm; 25 °C.

t *(min)*	Flow Rate *(mL/min)*	Elution		*UV detection* *λ (nm)*
		H_2O (0.1% TFA)	CH_3OH	
0.0	1.0	90	10	220
5.0	1.0	90	10	
40.0	1.0	0	100	
45.0	1.0	90	10	

4. Synthesis of octapeptide Ala-scanning sequence analogues.

The amide octapeptide (**1**) was syntesized by SPPS with Rink Amide-AM Resin (0.51 mmol/g, 100-200 mesh). The DIC/HOBt coupling reagent system, Pip/DMF (*v/v*, 1/4) *de*-Fmoc reagent system, and TFA/Tis/H_2O (*v/v*, 95/2.5/2.5) cleavage system were used to perform the synthsis work.

Using the Wang resin (0.85 mmol/g, 100-200 mesh) and coupling reagent system DIC/HOBt/NMP, and *de*-Fmoc reagent Pip/DMF (*v/v*, 1/4), the cleavage system TFA/Tis/H_2O (*v/v*, 95/2.5/2.5) to perform the synthesis work of octapeptide Ala-scanning analogues octapeptide (**3~9**), H-AVLQSGFA-OH (**3**), H-AVLQSGAR-OH (**4**), H-AVLQSAFR-OH (**5**), H-AVLQAGFR-OH (**6**), H-AVLASGFR-OH (**7**), H-AVAQSGFR-OH (**8**), H-AALQSGFR-OH (**9**).

HPLC analysis of the synthetic anti-SARS octapeptide (2) and amide octapeptide (1), Ala-scanning octapeptide (3-9) analogues.

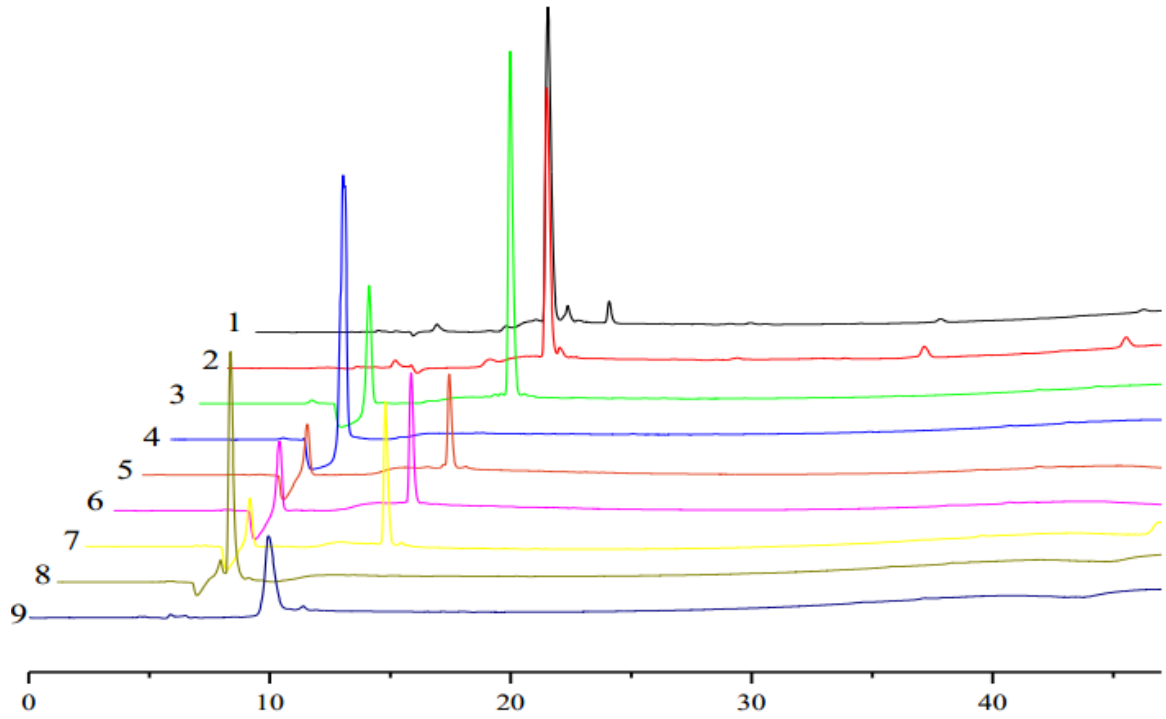

Figure S4. HPLC analysis of anti-SARS octapeptide and its **Ala** scanning sequence analogues.

HPLC conditions: Waters 2996-2695 system, Column: Kromasil, NC-2546-06251151; 4.6 mmi.d.×250 mm, 5 μm; 25 °C.

t (*min*)	Flow Rate (*mL/min*)	Elution		*UV detection*
		H_2O (0.1% TFA)	ACN	*λ (nm)*
0.0	0.5	80	20	220
2.0	0.5	80	20	
27.0	0.5	20	80	
37.0	0.5	0	100	

Table S1. The synthetic anti-SARS octapeptide (**2**), anti-SARS amide octapeptide (**1**) and **Ala** scanning sequence octapeptide analogues (**3**) to (**9**).

entry	octapeptide sequence (**1**~**9**)	retention time (t/min)	ESI MS calcd.	ESI MS found. $[M+H]^+$	yield (%)	purity (%)
1	H-AVLQSGFR-NH_2	11.45	875.5	875.5	75.4	98.0
2	**H-AVLQSGFR-OH**	13.26	876.6	877.4	94.9	97.8
3	H-AVLQSGF**A**-OH	12.94	792	793	93.9	99.8
4	H-AVLQSG**A**R-OH	7.19	801	802	94.8	99.5
5	H-AVLQS**A**FR-OH	12.77	891	892	92.7	98.7
6	H-AVLQ**A**GFR-OH	12.36	861	862	96.6	99.3
7	H-AVL**A**SGFR-OH	12.47	820	821	93.1	97.6
8	H-AV**A**QSGFR-OH	7.21	835	836	98.2	94.8
9	H-A**A**LQSGFR-OH	9.97	849	850	92.4	95.2

Waters Quattro Premier XE electrospray mass spectrometer for the anti-SARS octapeptide (2) and its octapeptide (3-9) Ala scanning sequence ESI MS analysis.

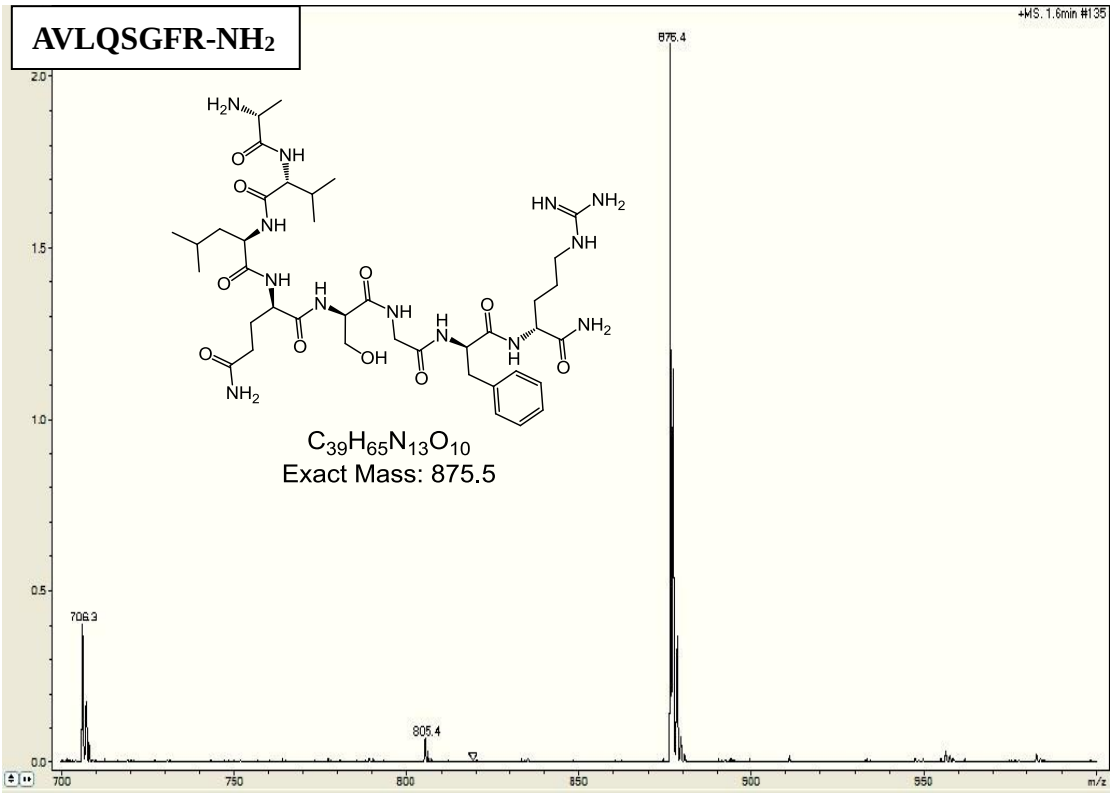

Octapeptide (**1**) ESI MS

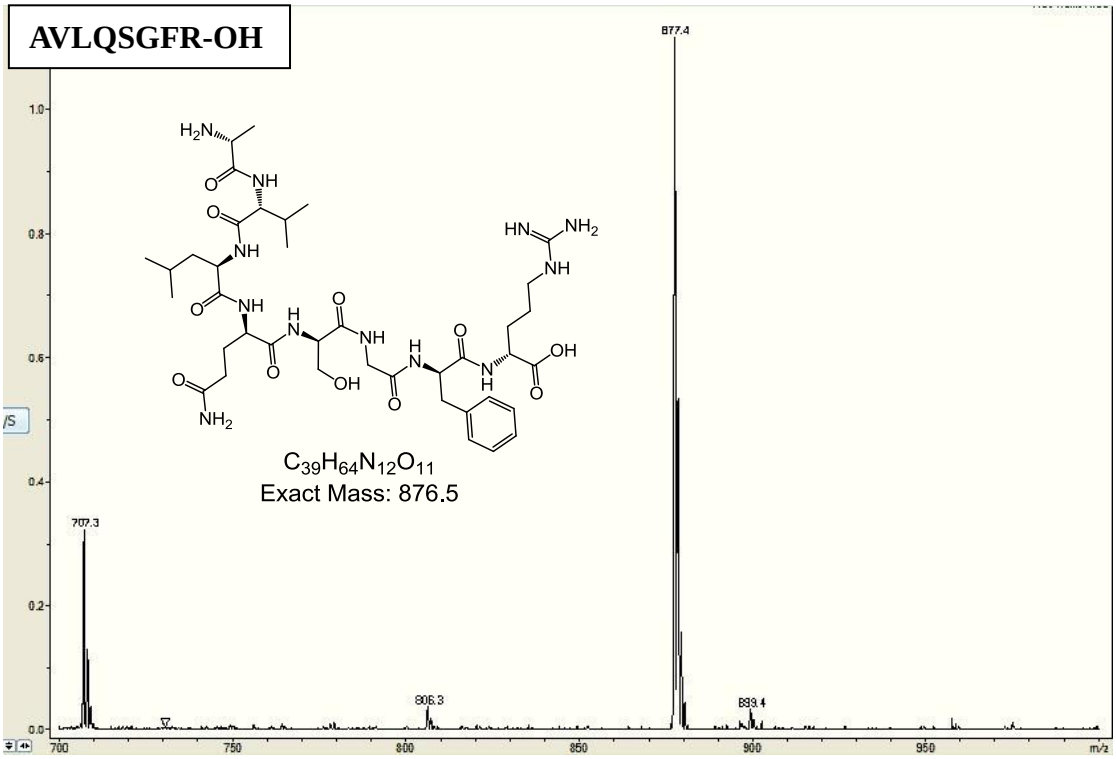

Octapeptide (**2**) ESI MS

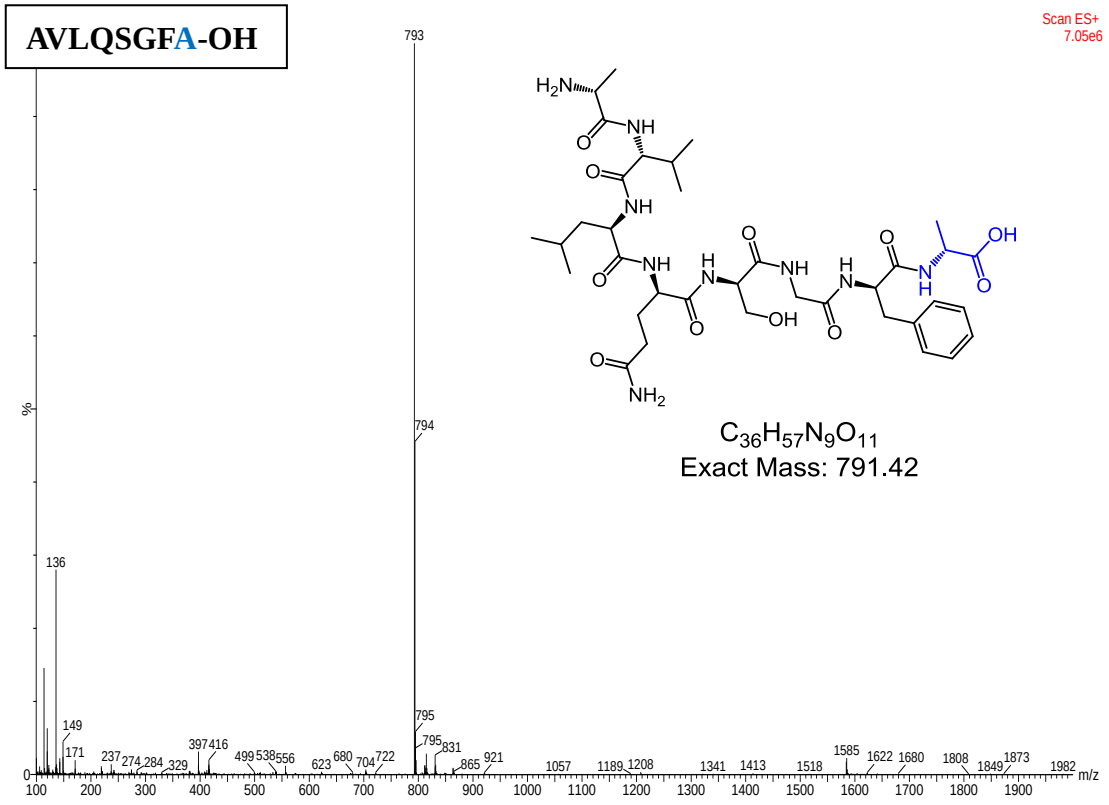

Octapeptide (**3**) ESI MS

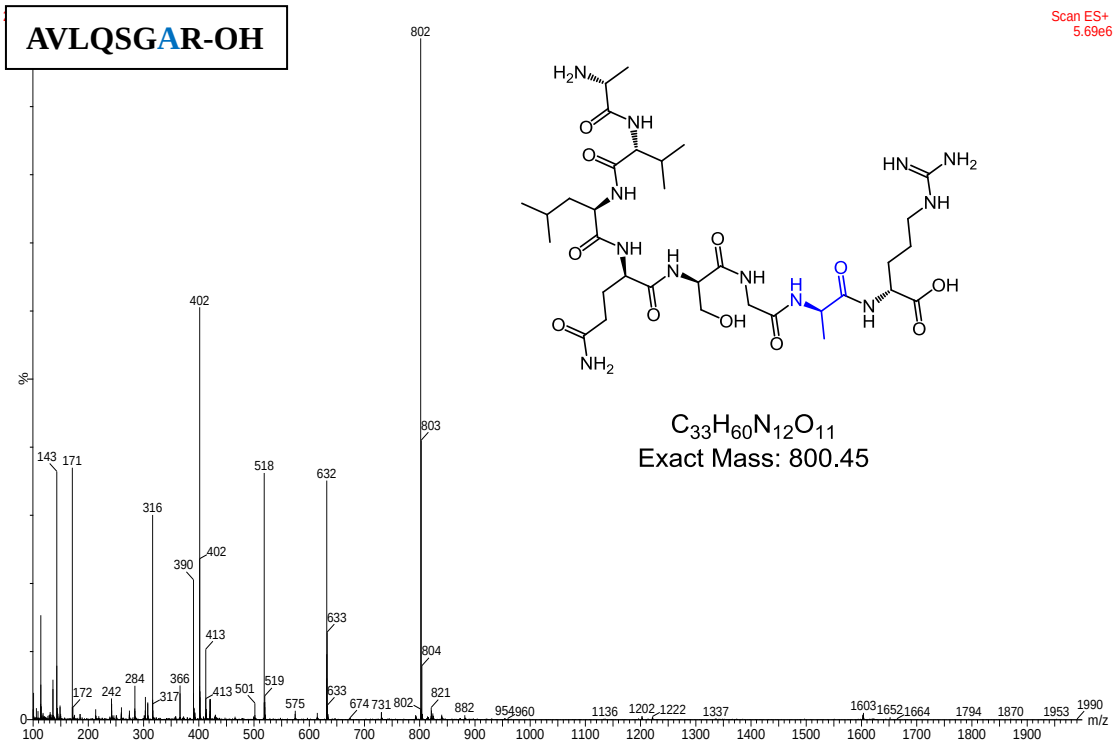

Octapeptide (**4**) ESI MS

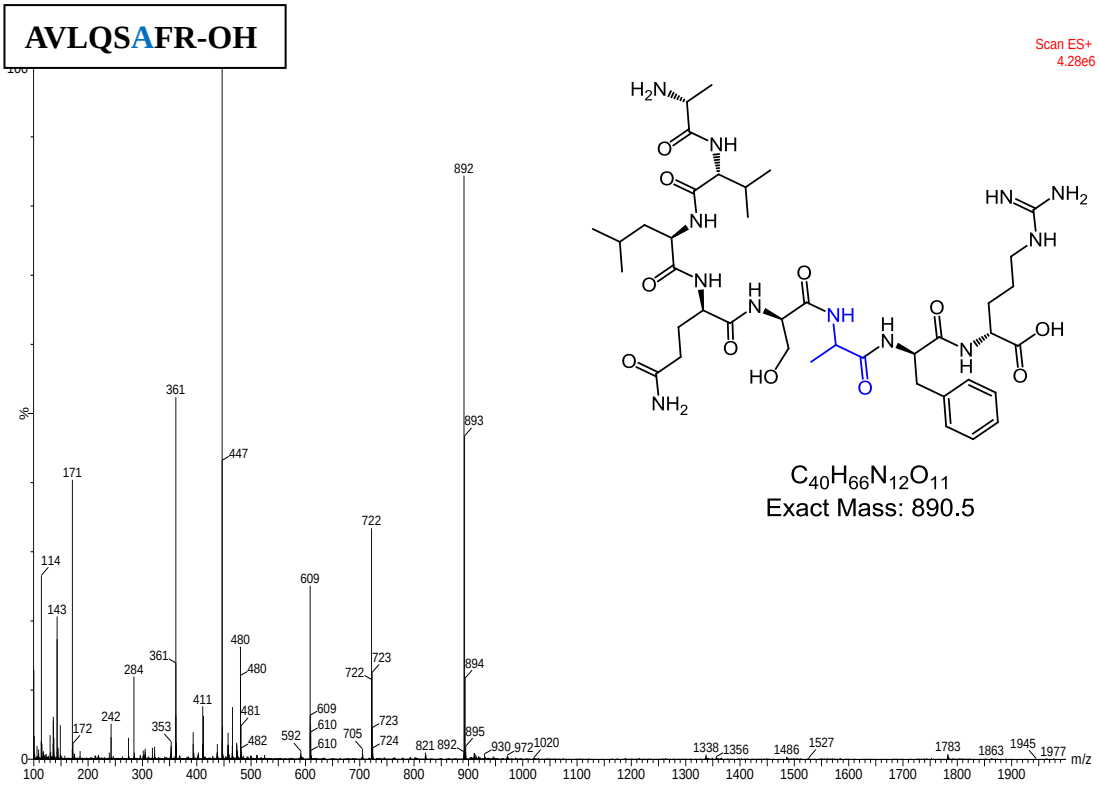

Octapeptide (**5**) ESI MS

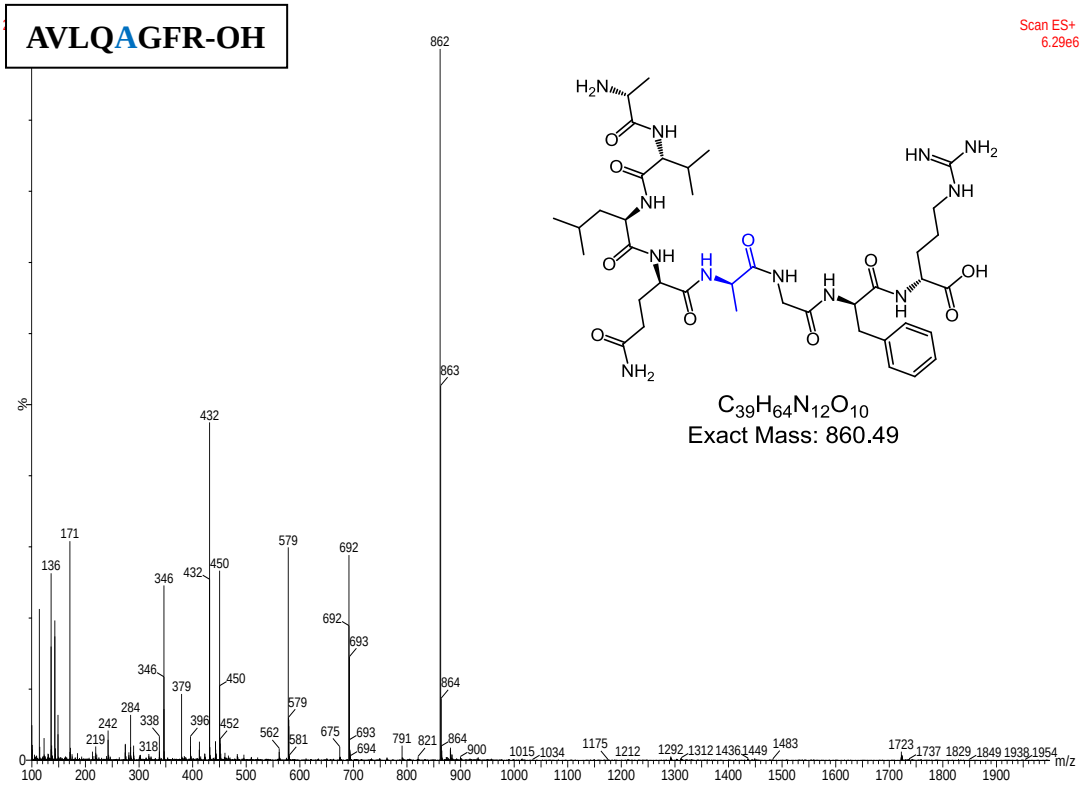

Octapeptide (**6**) ESI MS

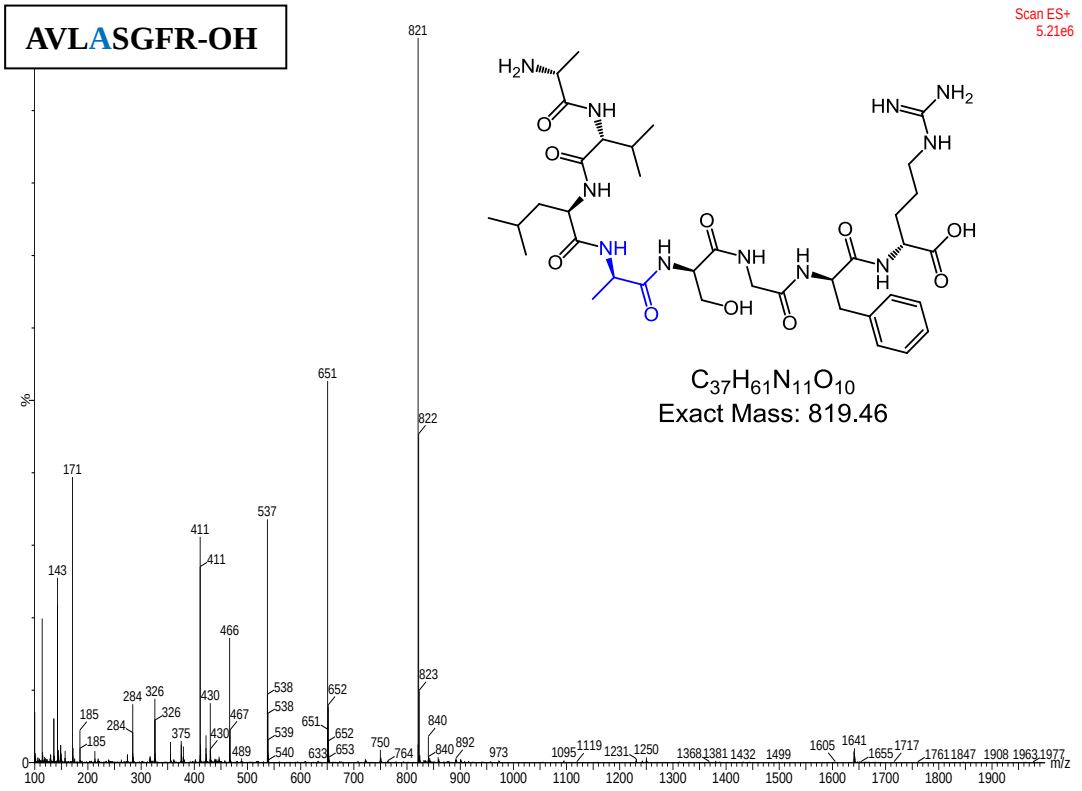

Octapeptide (**7**) ESI MS

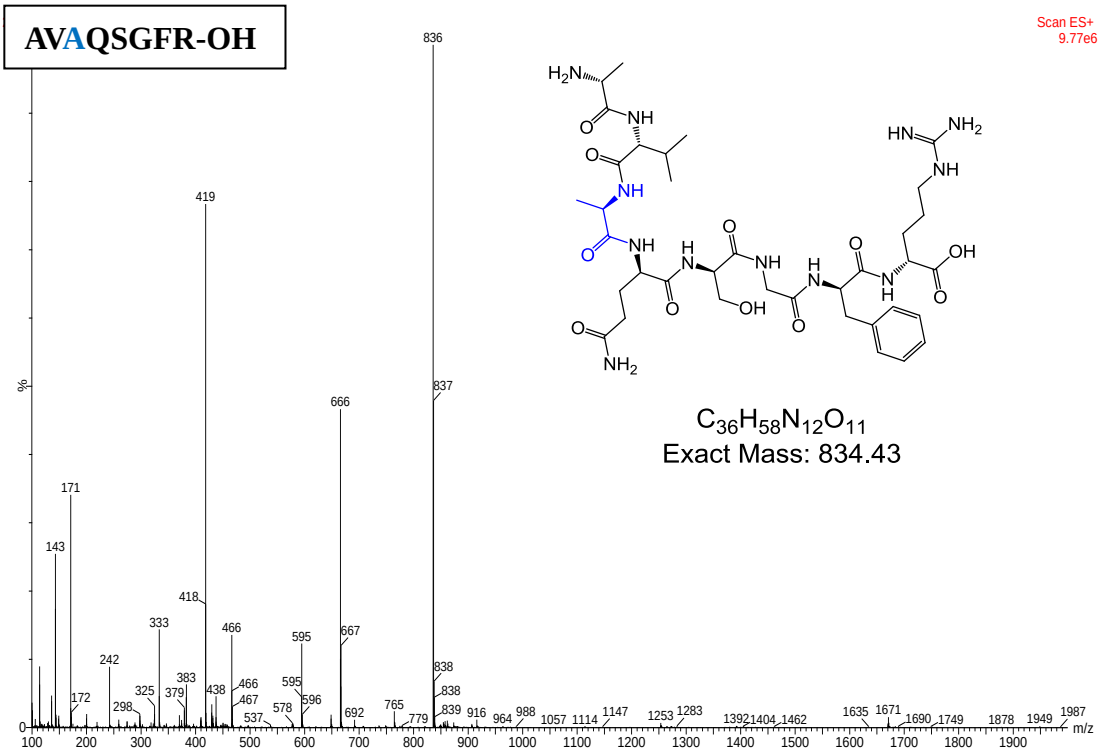

Octapeptide (**8**) ESI MS

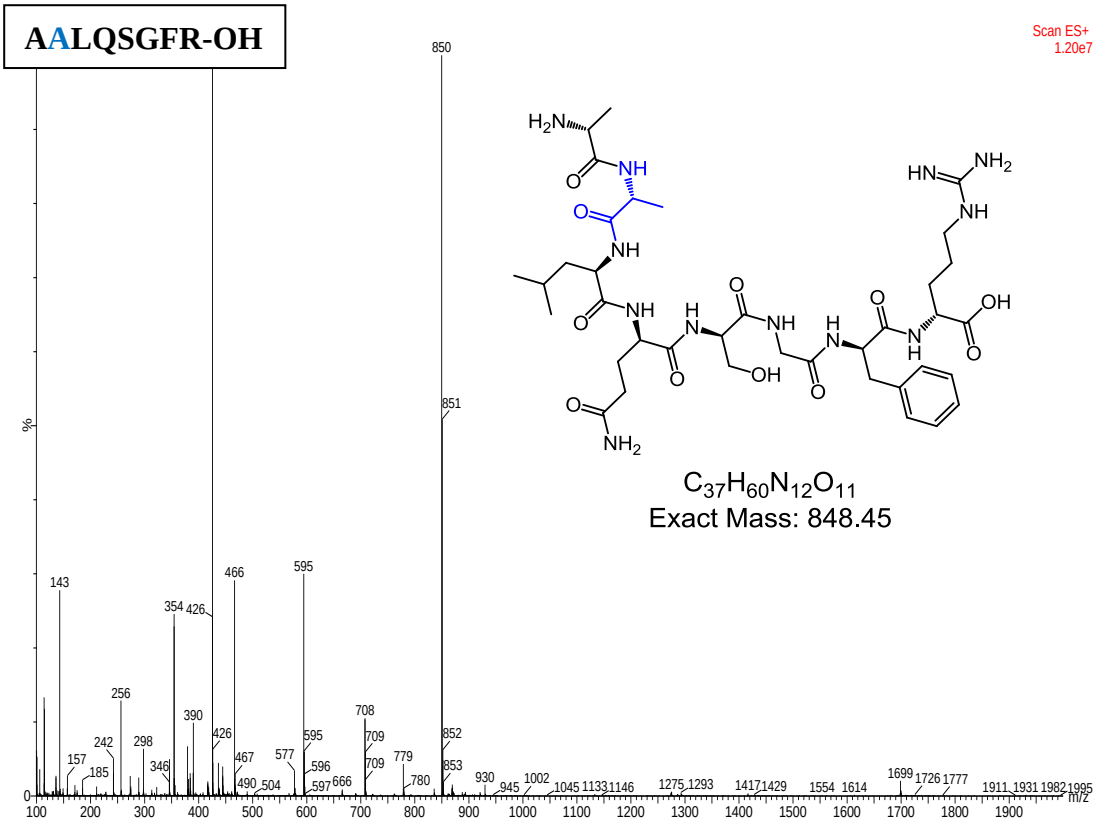

Octapeptide (**9**) ESI MS

5 The molecular stability of octapeptide (2) and its Ala scanning sequences analogues.

Chemoffice 2008 software was used to calculate the minimum energy and the number of intramolecular hydrogen bonds for preliminary molecular structural stability analysis of the synthesized ACE inhibitory ocpeptide.

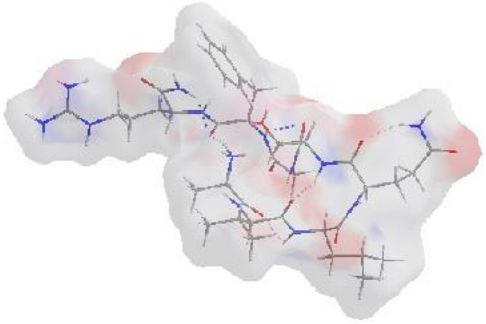

1 AVLQSGFR-NH_2

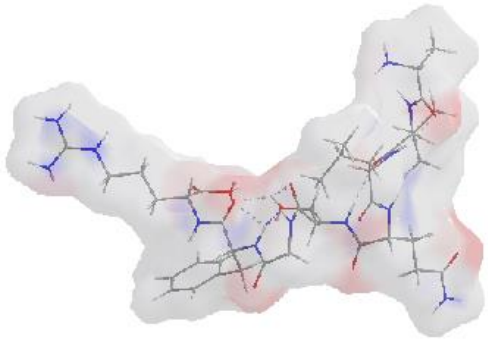

2 AVLQSGFR-OH

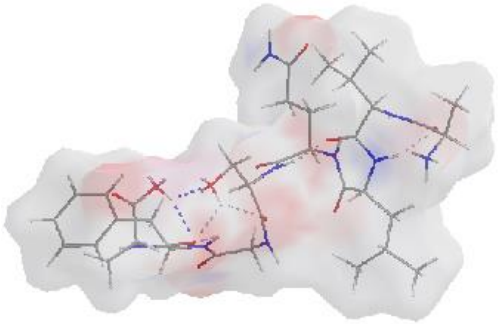

3 AVLQSGF**A**-OH

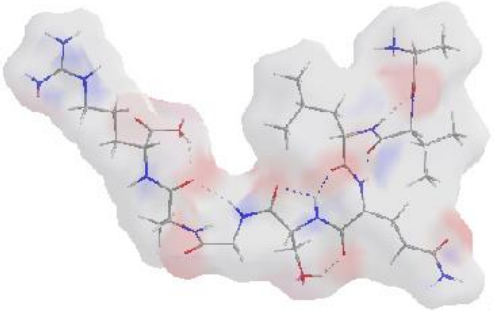

4 AVLQSG**A**R-OH

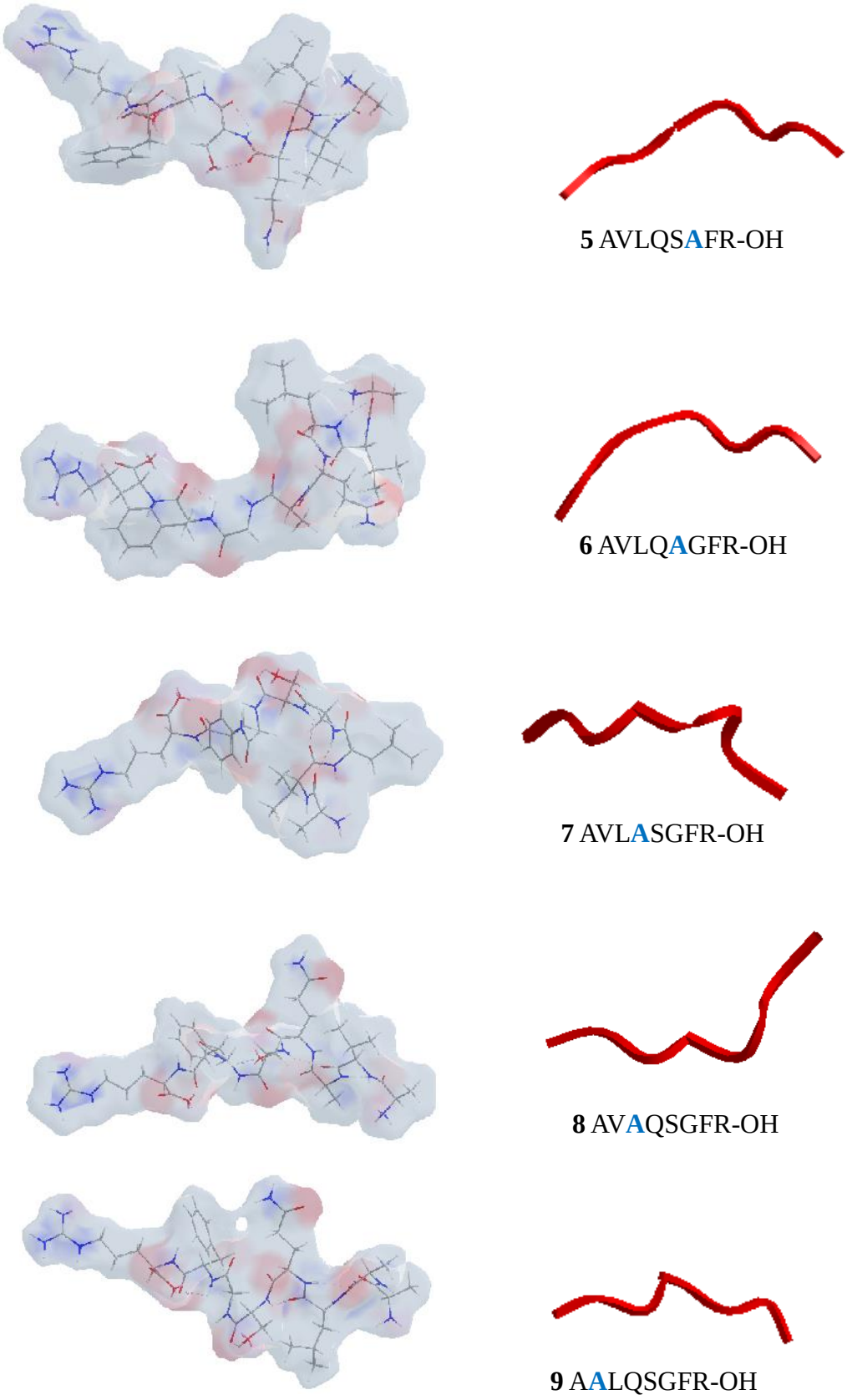

Fig. S5 Molecular surface (left) and model display (right) of anti-SARS octapeptide (**2**), anti-SARS amide octapeptide (**1**) and Ala scanning sequence analogues (**3**) to (**9**).

Table S2 The minimum steric energy and intramolecular hydrogen bond of anti-SARS octapeptide (**2**), anti-SARS amide octapeptide (**1**) and Ala scanning sequence analogues (**3**) to (**9**).

enter	octapeptide sequence (1~9)	steric Energy	intramolecular hydrogen bonds
1	H-AVLQSGFR-NH_2	-48.817	6
2	**H-AVLQSGFR-OH**	**-39.895**	**6**
3	H-AVLQSGF**A**-OH	-36.870	8
4	H-AVLQSG**A**R-OH	-19.388	7
5	H-AVLQS**A**FR-OH	-30.358	5
6	H-AVLQ**A**GFR-OH	-28.635	3
7	H-AVL**A**SGFR-OH	-38.358	3
8	H-AV**A**QSGFR-OH	-42.482	3
9	H-A**A**LQSGFR-OH	-40.428	5

Octapeptide (**1**) had the lowest structural energy, and octapeptide (**4**) has the highest structural energy. The structure of anti-SARS amide octapeptide (**1**) was relatively stable. When Phe-2 (F) in the sequence of anti-SARS octapeptide (**2**) was replaced by Ala (A) to form the octapeptide (**4**), the molecular structure became unstable. This showed that Phe has a more significant influence on the stability of the molecular structure. The intramolecular hydrogen bonds were mainly concentrated at Ser-4. When Ser-4 was replaced by Ala to form the octapeptide (**6**), the molecular structural stability deteriorated and the number of intramolecular hydrogen bonds decreases.

6. In vitro ACE inhibitory activity and stability study of anti-SARS octapeptide (2).

Table S3. The related solution preparation.

entry	prepare solution	concentration	remark
1	Dilute HCl	1.0 mol·L^{-1}	-
2	Boric acid buffer (contain 0.3 mol·L^{-1} NaCl)	0.1 mol·L^{-1}	pH 8.3
3	ACE	100 mU·mL^{-1}	-
4	Hippury-L-Histidyl-L-Leucine (HHL)	5.5 mmol·L^{-1}	-
5	Captopril (positive control)	1.0 mg·ml^{-1}	-
6	Octapeptide (final concentration)	1.0 mg·ml^{-1}	-

$$IR = A-B/A \times 100\% \qquad \textbf{Equation 1}$$

***IR*:** the inhibition rate (%) of ACE inhibitory peptide.

A: the peak area of Hip in the blank control group.

B: the peak area of Hip in the ACE inhibitory peptide group.

In vitro ACE inhibitory evaluation of the Octapeptide (2) and amide octapeptdie (1).

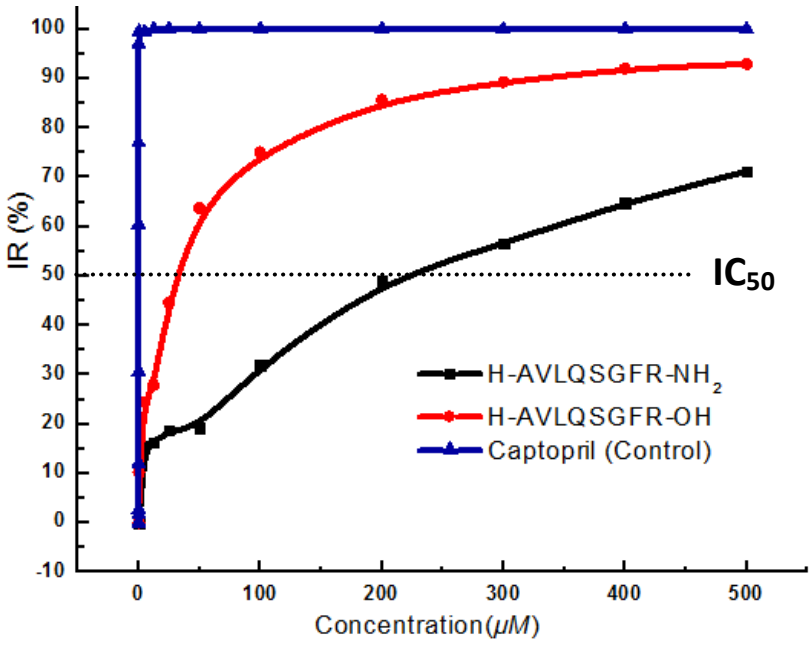

Figure S6. The Inhibitory Effect of anti-SARS octapeptide (**2**), acylamino peptide and Captopril at different concentrations against ACE. Positive control captopril, IC_{50} was 9.2×10^{-3} μmol·L^{-1} (*Ref* report 7.5×10^{-4}~2.2×10^{-2} μmol·L^{-1}).

The temperature influence on anti-SARS octapeptide (2) stability.

Treating the anti-SARS octapeptide (**2**) (AVLQSGFR) (0.1 mg/mL) at different temperatures (20 °C, 40 °C, 60 °C, 80 °C, and 100 °C) for 2 h. The solution returns to room temperature and then tested the ACE inhibitory depended on the above method.The results portrait the subtle change of ACE inhibitory of anti-SARS octapeptide (2) with different temperatures, boasting excellent thermal stability within 100°C.

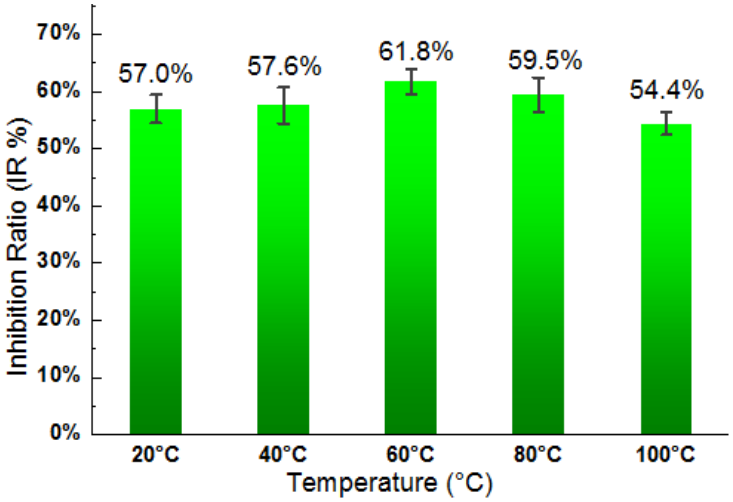

Figure S7. ACE inhibitory of octapeptide (**2**) after treating with various temperatures for 2 h.

The ACE itself influence on anti-SARS octapeptide stability.

The anti-SARS octapeptide (**2**) with a concentration of 0.5 mg·mL^{-1} was treated with ACE (6 mU/mg·peptide) at 37 °C for 3 h. The reaction was quenched by inactivating the ACE at 95 °C for 15 min, and then tested the ACE inhibitory activity of the octapeptide (**2**).

Before and after treating octapeptide (**2**) with ACE, the inhibition rate changed slightly, the difference in inhibitory activity was not significant, which indicates that octapeptide was a real inhibitor and will not be affected by ACE itself while maintaining the original activity of anti-SARS octapeptide (**2**).

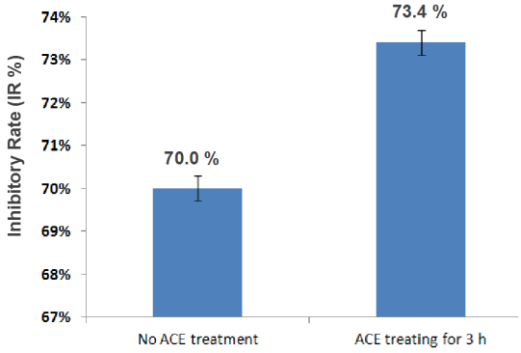

Figure S8. ACE inhibitory of anti-SARS octapeptide (**2**) after treating with ACE for 2 h.

7. Quantitative structure-activity relationship (QSAR) study of of amide octapeptide (1) and anti-SARS octapeptide (2).

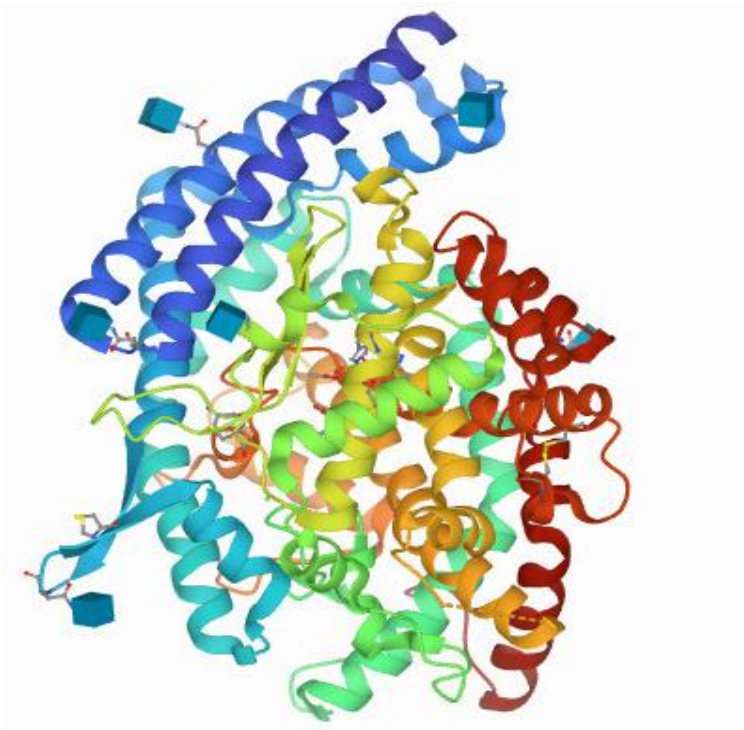

Crystal Structure of Human Angiotensin Converting Enzyme (Native).

ACE-lisinopril complex (1O8A. PDB)

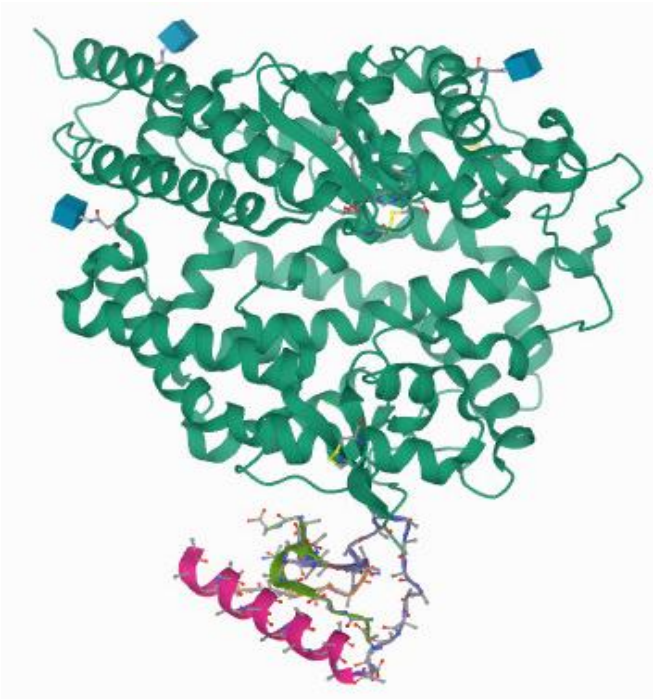

Native Human Angiotensin Converting Enzyme-Related Carboxypeptidase (ACE2) crystal complex (PDB ID: 1R42)

Figure S9. The three-dimensional structure of ACE1 and ACE2

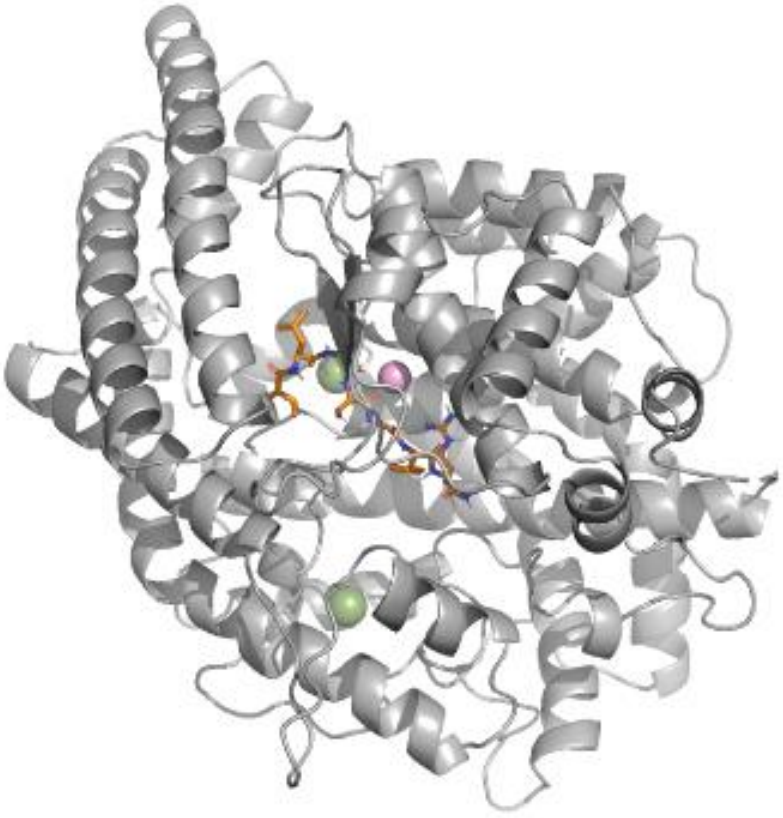

ACE-ligand1-complex (PDB: 1O8A)

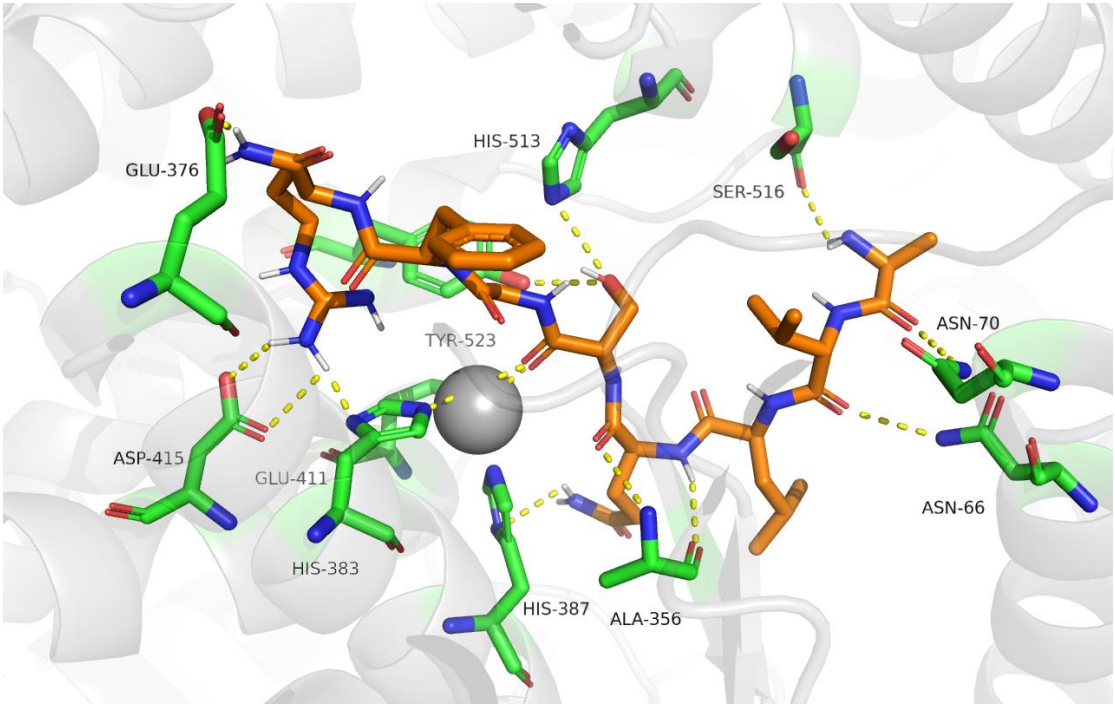

ACE-ligand1-complex (PDB: 1O8A)

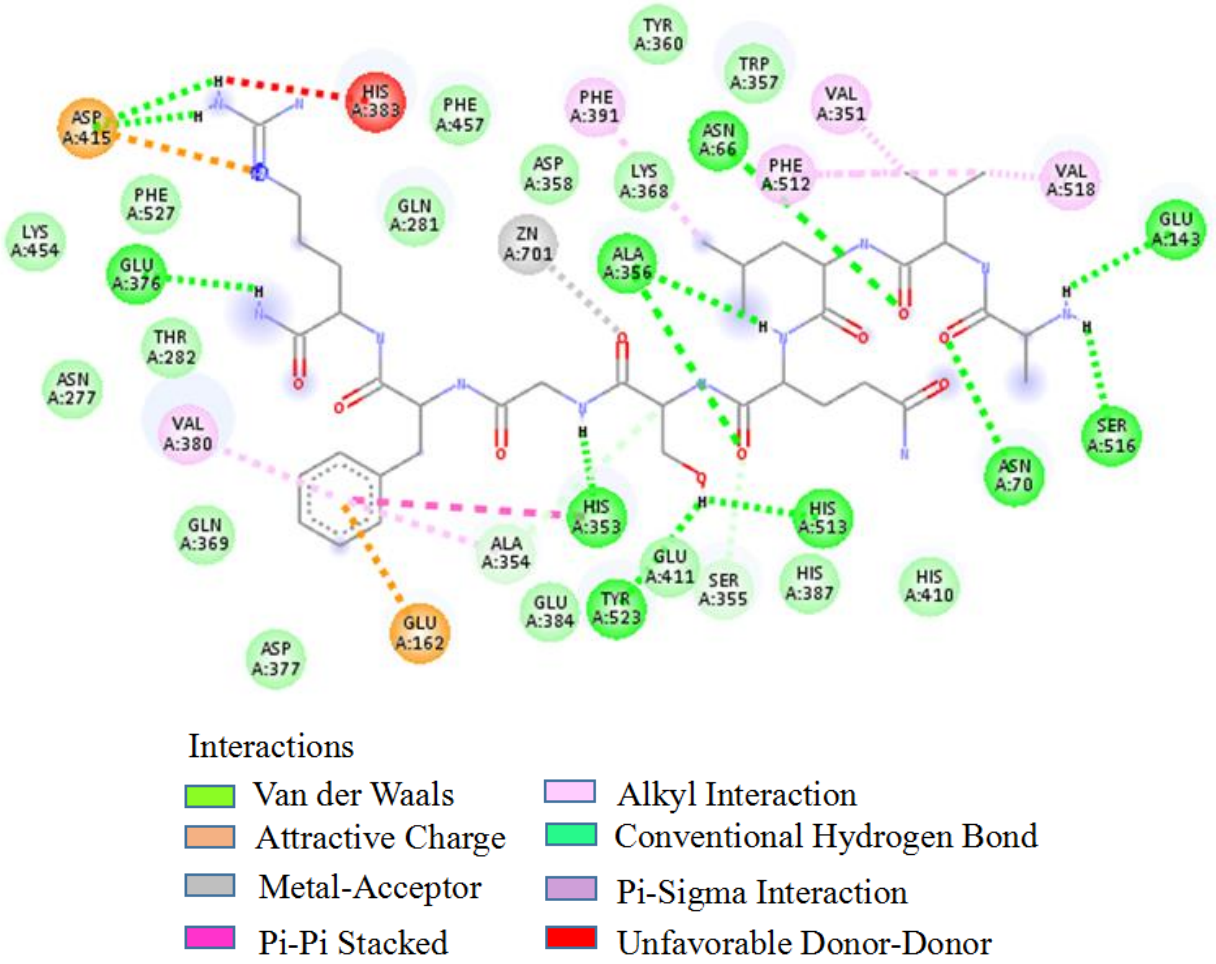

Figure S10. The best ranked docking pose of amide octapeptide **1** (Ligand 1: AVLQSGFR-NH_2) binding with ACE1 (PDB: 1O8A). Full view of ACE1 (PDB: 1O8A, Dark gray)-ligand1 (AVLQSGFR-NH_2, Dark orange) complex; Binding mode of ACE1 (Light grey and green) with Ligand 1 (H-AVLQSGFR-NH_2, Dark orange); All kinds of interactions between ACE1 residues and atoms or atomic groups on Ligand.

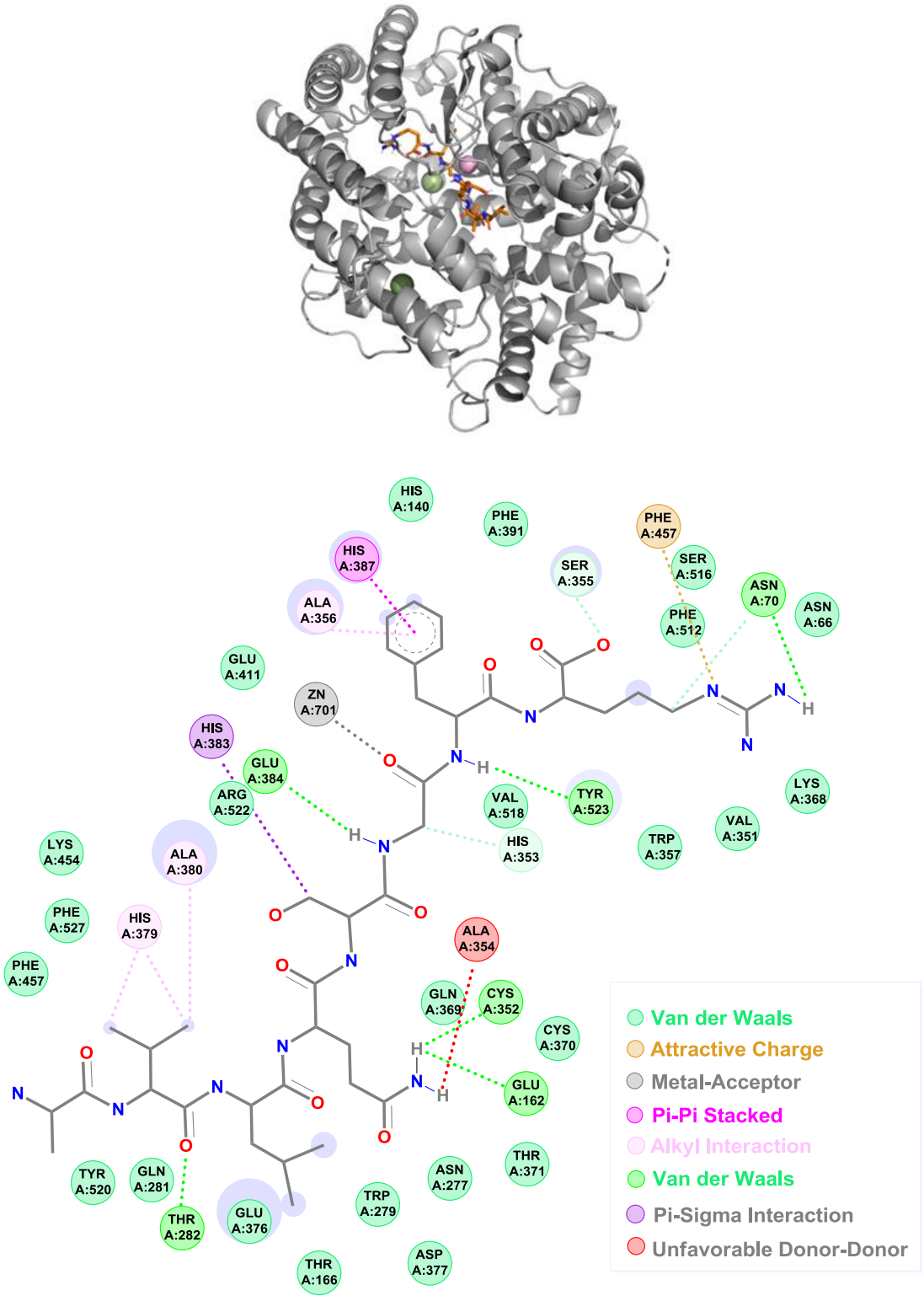

Figure S11. Binding mode of **ACE1** (Light grey and green) with Ligand 2 (H-AVLQSGFR-OH, Dark orange) and all kinds of interactions between **ACE1** residues and atoms or atomic groups on Ligand.

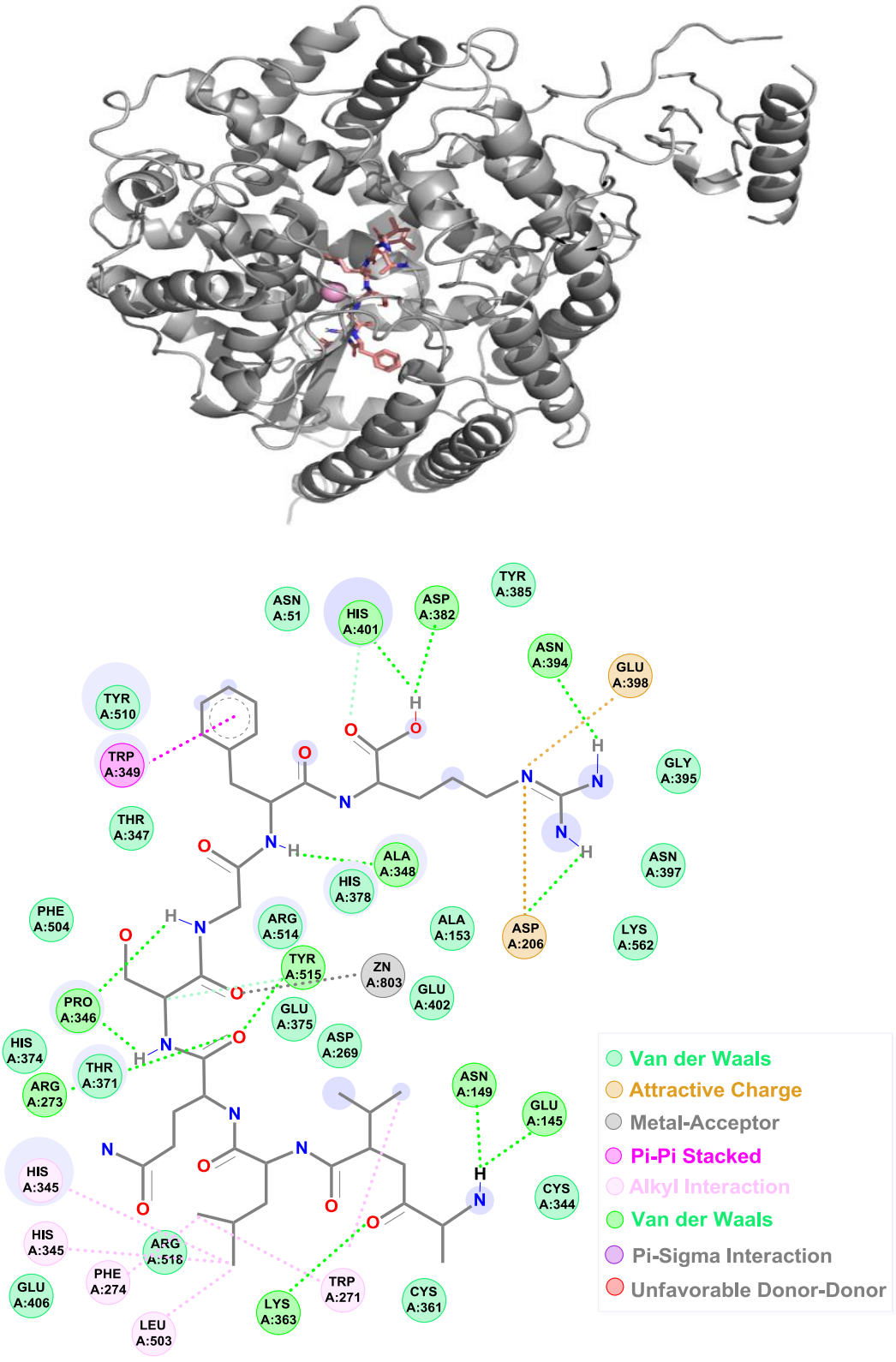

Figure S12. Binding mode of **ACE2** with Ligand 2 (H-AVLQSGFR-OH) and all kinds of interactions between **ACE2** residues and atoms or atomic groups on Ligand 2.

Remark: Other related octapeptide (**1**) and octapeptide (**3-9**) [ligands (**1**, **3-9**)] docking with ACE2 (PDB: 1R42) diagrams are reserved as unpublished data, if necessary, it can be obtained from the corresponding author.

References

[1] Feng, G. F.; Liu,W.; Peng, Y.-X.; Zhao, B.; Huang, W.; Dai, Y.-F. Cavity partition and functionalization of a [2+3] organic molecular cage by inserting polar P=O bonds, *Chem. Commun.*, **2016,** *52*, 9267-9270.

[2] Degrado, W. F.; Kaiser, E. T. Polymer-bound oxime esters as supports for solid-phase peptide synthesis. Preparation of protected peptide fragments, *J. Org. Chem*., 1980, **45**, 1295-1300.

[3] Degrad, W. F.; Kaiser, E. T. Solid-phase synthesis of protected peptides on a polymer-bound Oxime: preparation of segments comprising the sequence of a cytotoxic 26-peptide analogue, *J. Org. Chem*., **1982,** *14*, 3258-3261.

[4] He, C.; Zhang, X.-H.; Huang, R.-F.; Pan, J.; Li, J.-Q.; Ling, X.-G.; Xiong, Y.; Zhu, X.-M. Synthesis of structurally diverse diarylketones through the diarylmethyl sp3 C-H oxidation, Tetrahedron Lett., 2014, 55, 4458-4462.

[5] Wu, J. P.; Ding, H.S. Characterization of inhibition and stability of soy-protein-derived angiotensin I-converting enzyme inhibitory peptides. *Food Res Int.* **2002,** *35*, 367-375.

[6] Cushman, D. W.; Cheung, H.S. Spectrophotometric assay and properties of the angiotensin-conerting enzyme of rabbit lung. *Biochem Pharmacol.* **1971,** *20*, 1637-1648.

[7] Wu, Q.; Jia, J.; Yan, H.; Du, J.; Gui, Z. A novel angiotensin-I converting enzyme (ACE) inhibitory peptide from gastrointestinal protease hydrolysate of silkworm pupa (Bombyx mori) protein: Biochemical characterization and molecular docking study. *Peptides,* **2015,** *68*,17-24.

[8] Wang, Z.; Zhang, S.; Jin, H.; Wang, W.; Huo, J.; Zhou, L.; Wang, Y.; Feng, F.; Zhang, L. Angiotensin-I-converting enzyme inhibitory peptides: Chemical feature based pharmacophore generation. *Euro. J. Med. Chem.* **2011,** *46*, 3428-3433.

- **Compounds NMR Spectra and HRMS (ESI) Spectra**

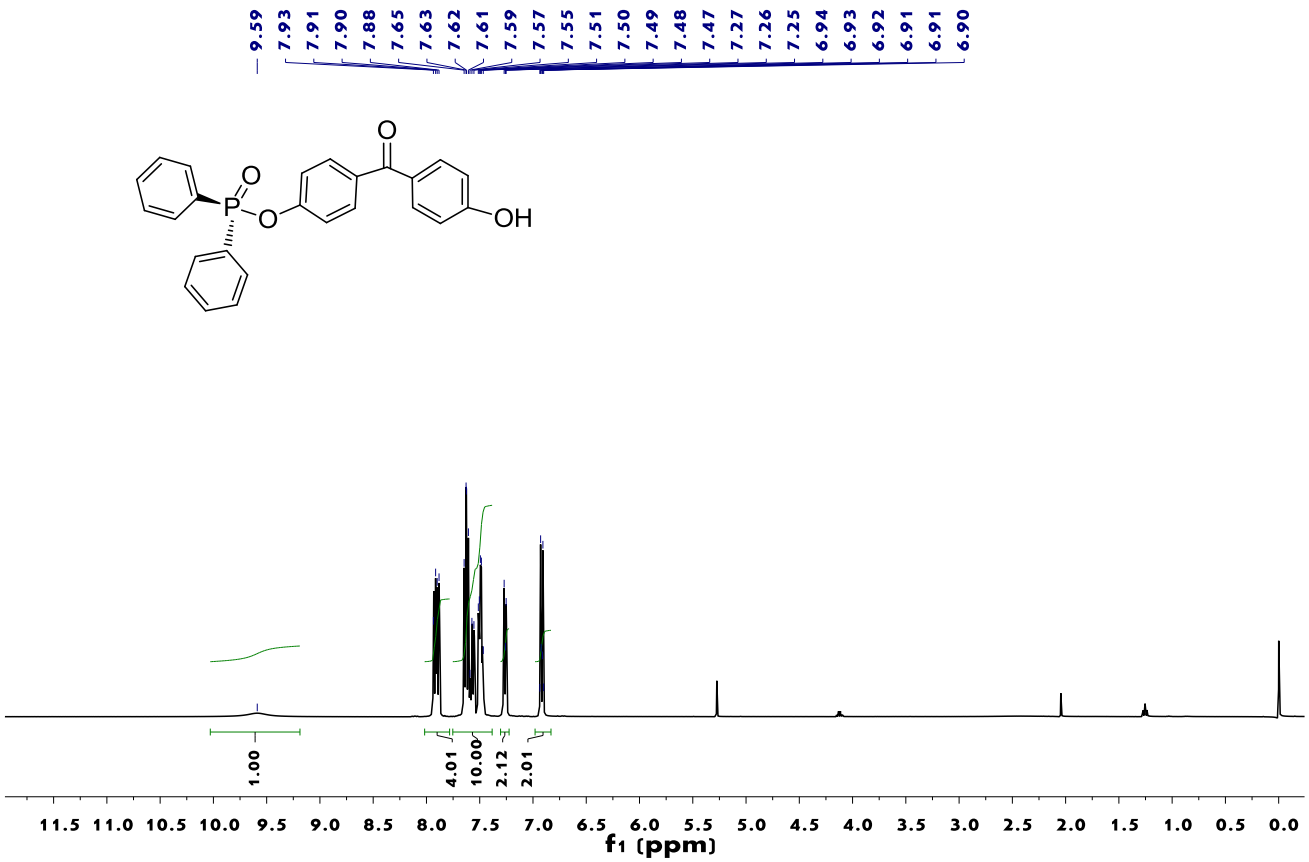

a, 4-(4'-hydroxybenzoyl) phenyl diphenylphosphinate ^{1}H NMR (400 MHz, $CDCl_3$)

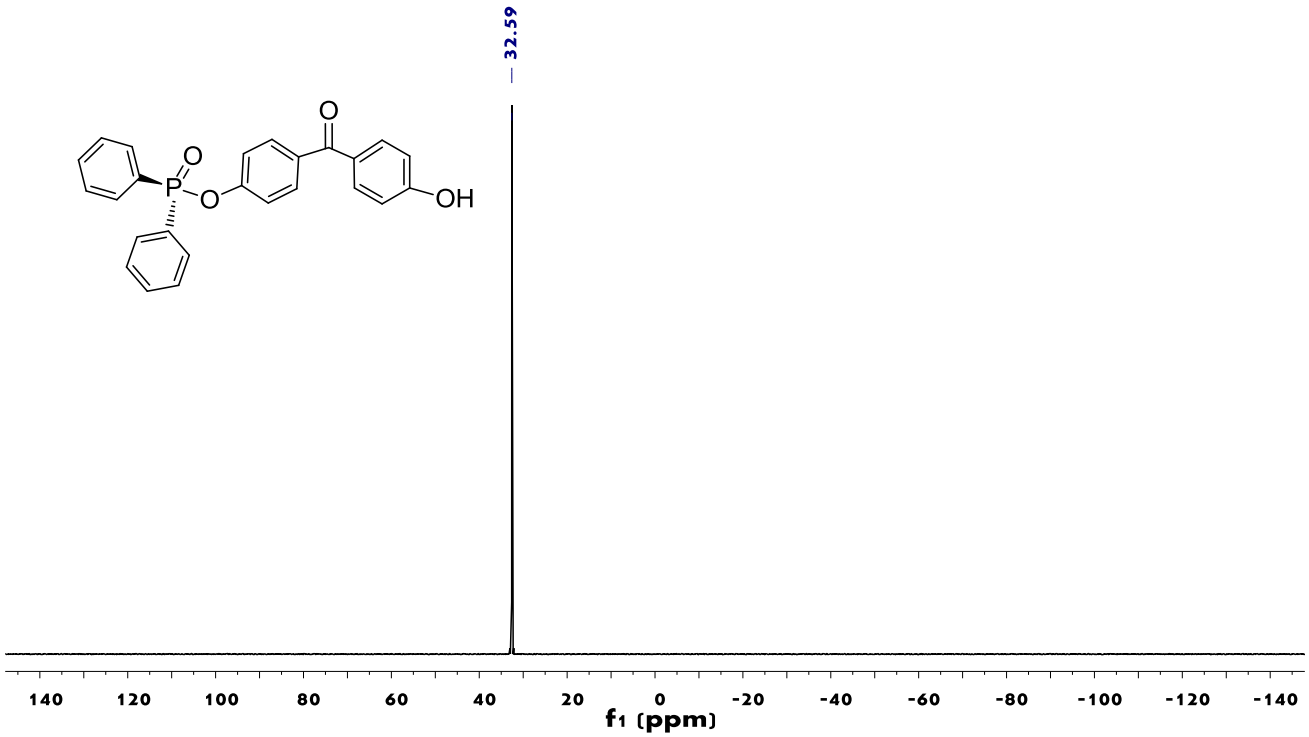

a, 4-(4'-hydroxybenzoyl) phenyl diphenylphosphinate ^{31}P NMR (162 MHz, $CDCl_3$)

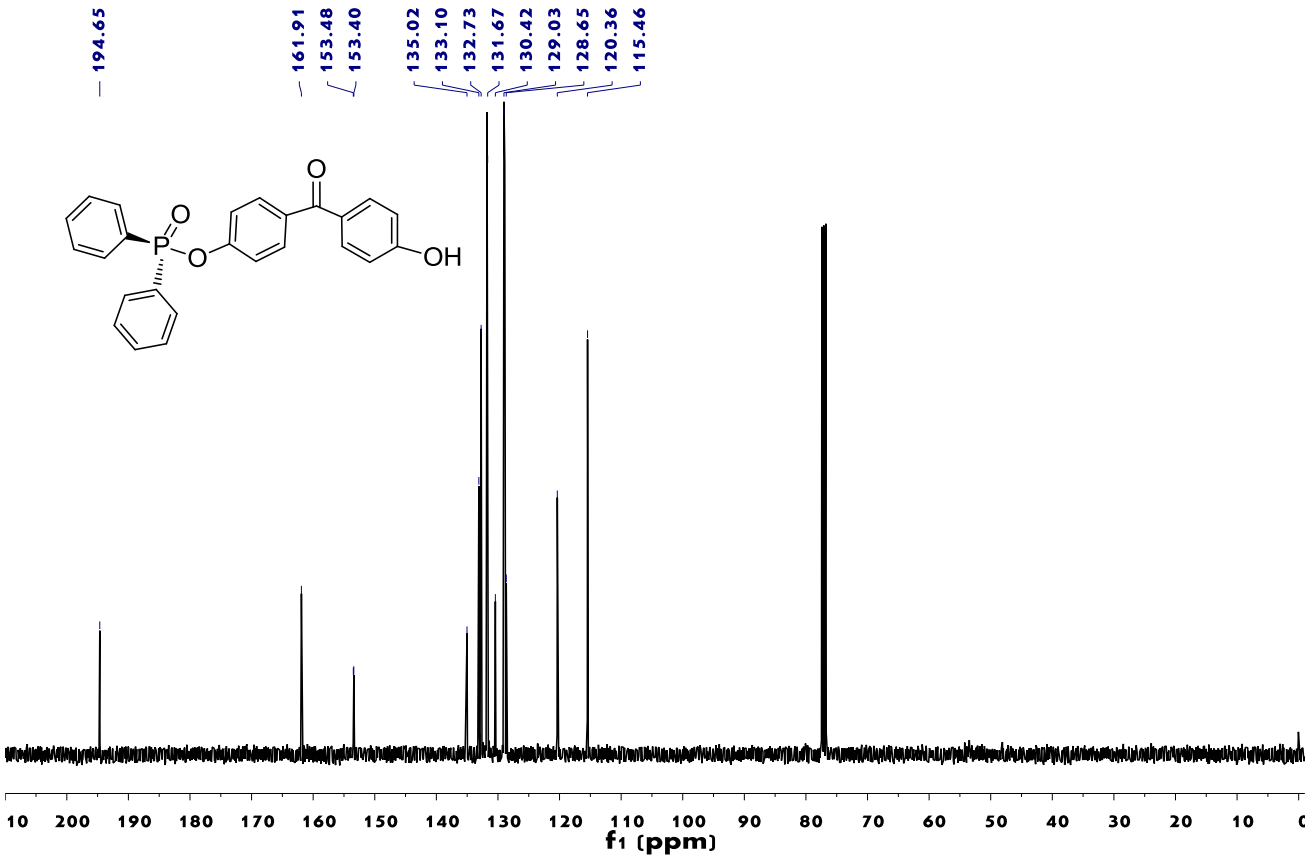

a, 4-(4'-hydroxybenzoyl) phenyl diphenylphosphinate ^{13}C NMR (100 MHz, $CDCl_3$)

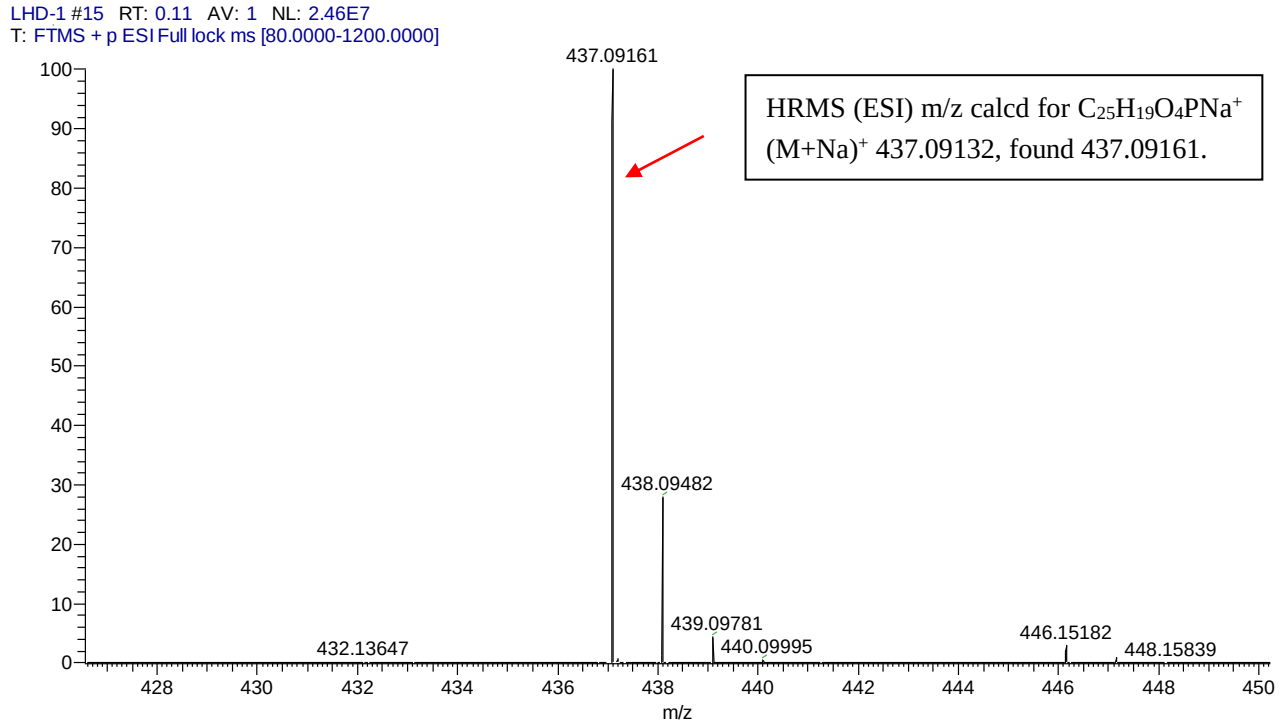

a, 4-(4'-hydroxybenzoyl) phenyl diphenylphosphinate HRMS (ESI)

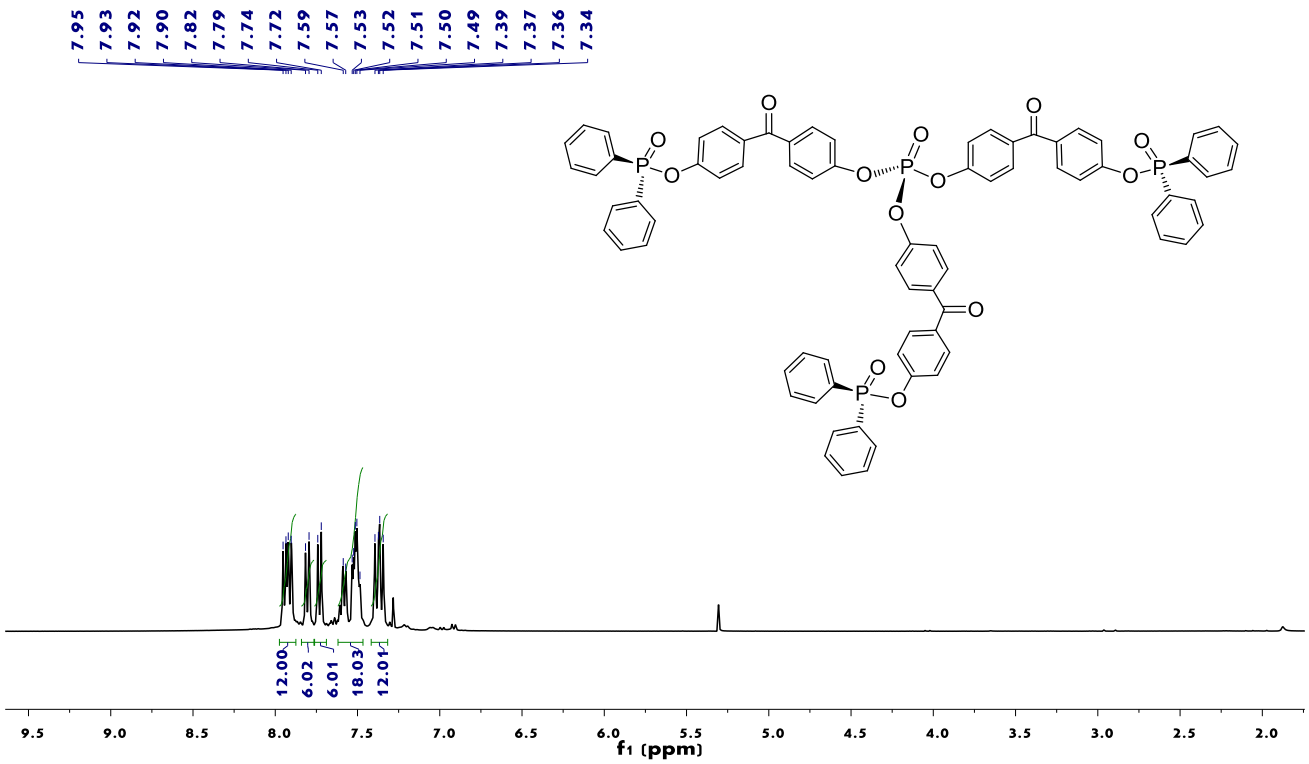

b, tri(4'-diphenylphosphonyloxylbenzoyl phenyl) phosphonate ^{1}H NMR (400 MHz, $CDCl_3$)

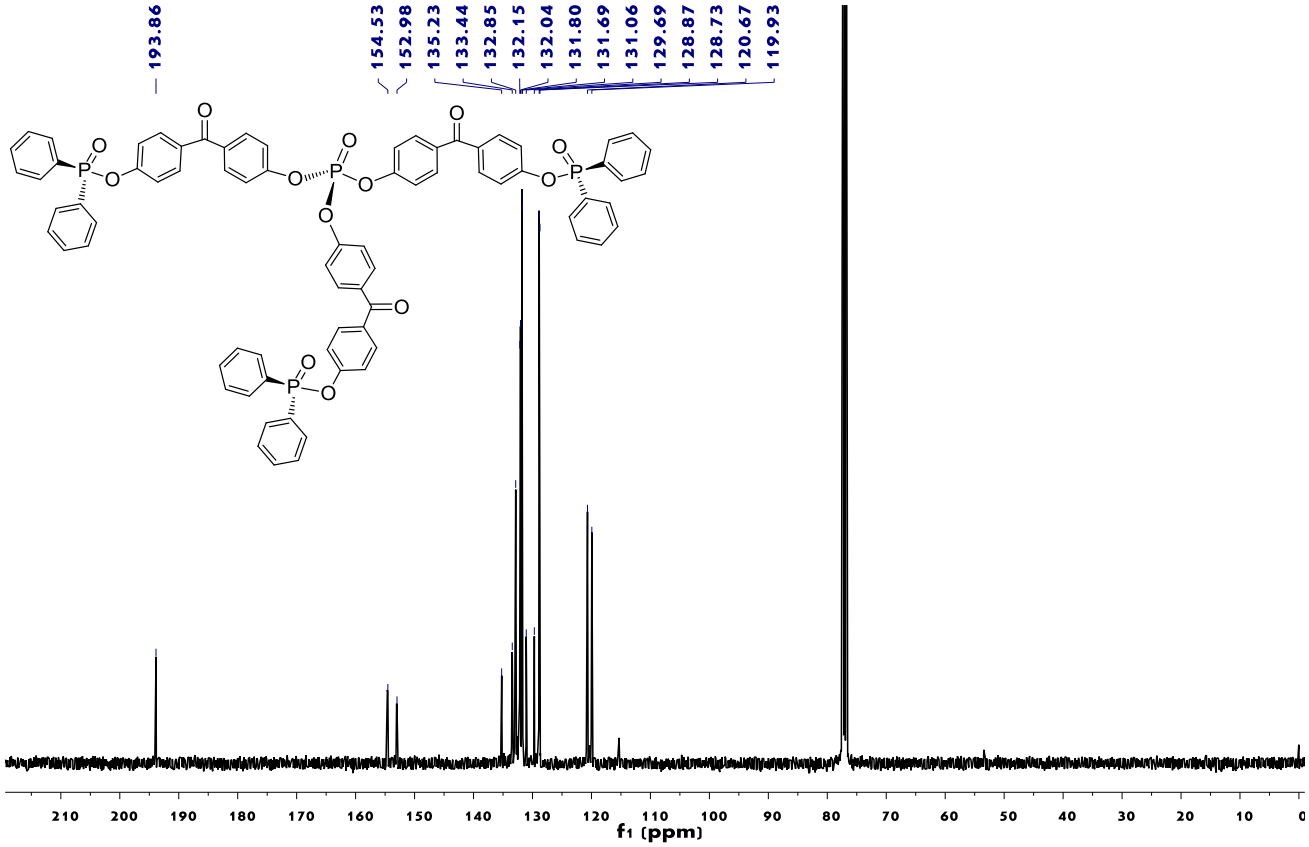

b, tri(4'-diphenylphosphonyloxylbenzoyl phenyl) phosphonate ^{13}C NMR (100 MHz, $CDCl_3$)

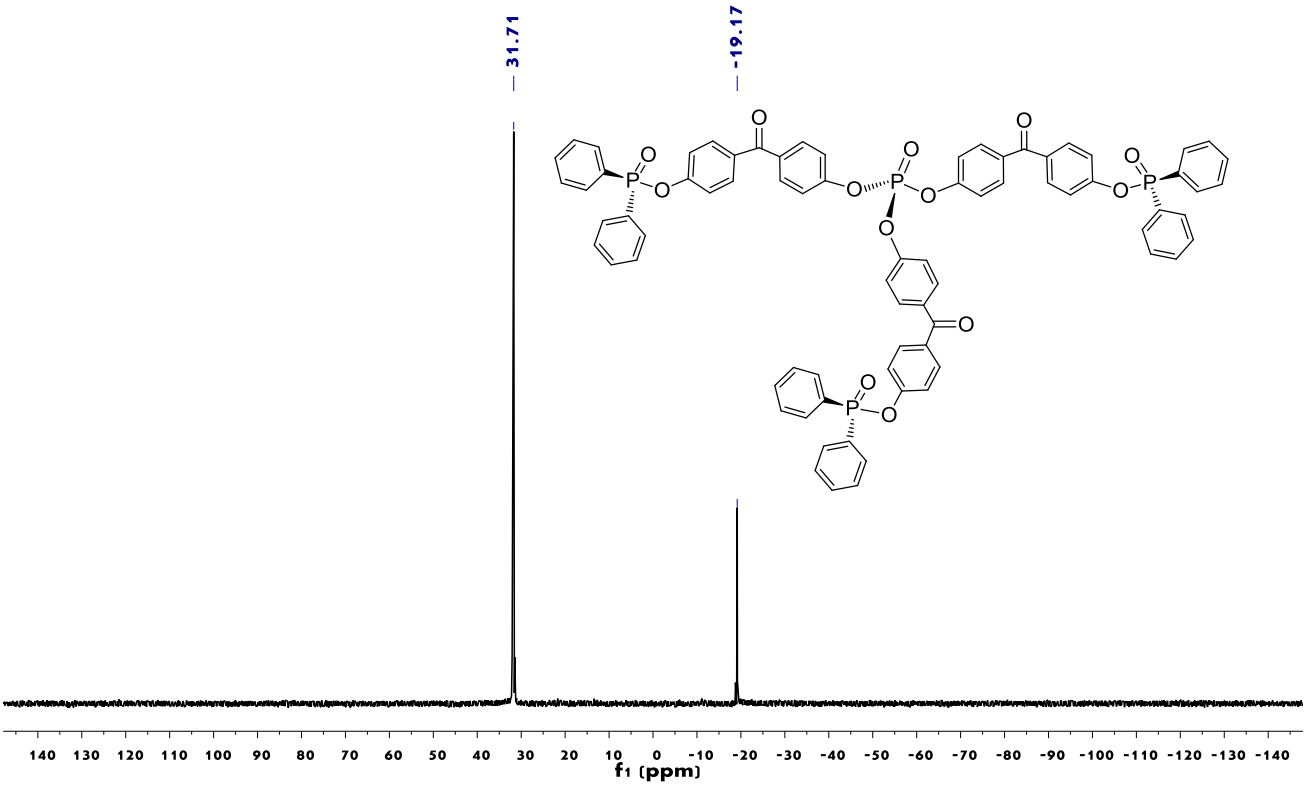

b, tri(4'-diphenylphosphonyloxylbenzoyl phenyl) phosphonate ^{31}P NMR (162 MHz, $CDCl_3$)

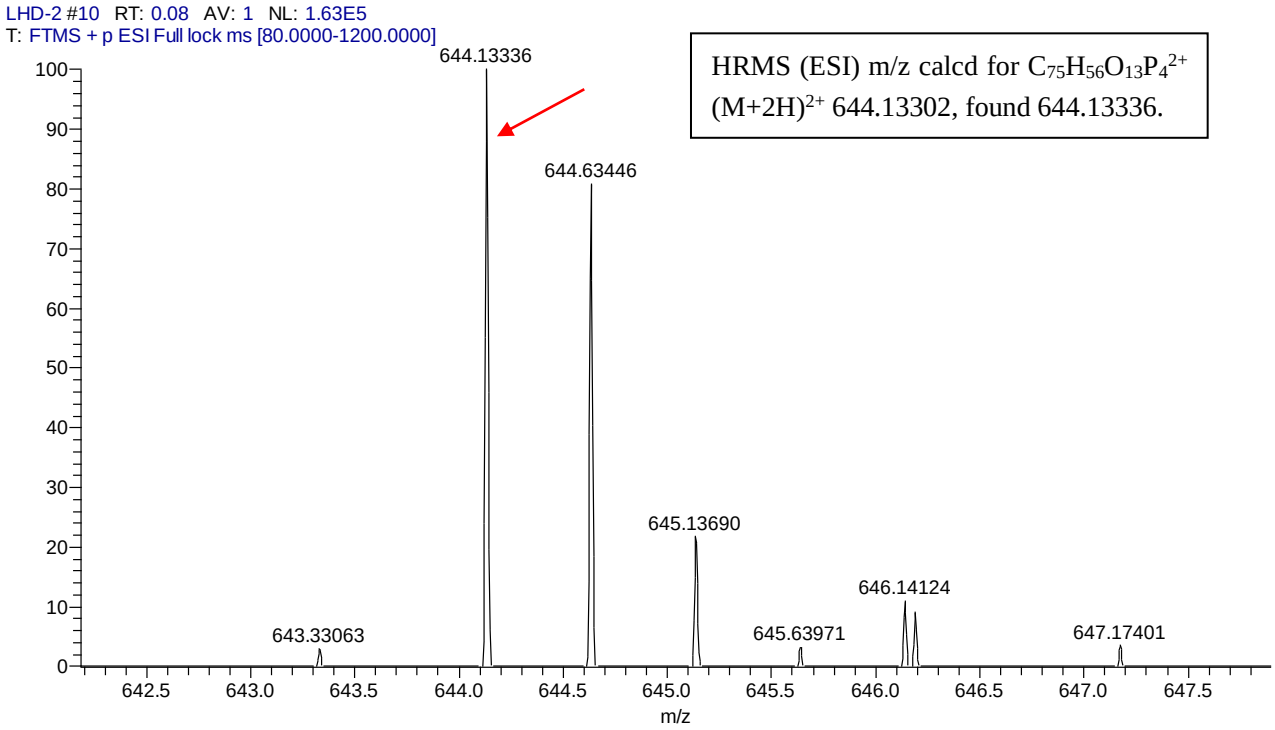

HRMS (ESI) m/z calcd for $C_{75}H_{56}O_{13}P_4^{2+}$ $(M+2H)^{2+}$ 644.13302, found 644.13336.

b, tri(4'-diphenylphosphonyloxylbenzoyl phenyl) phosphonate HRMS (ESI)

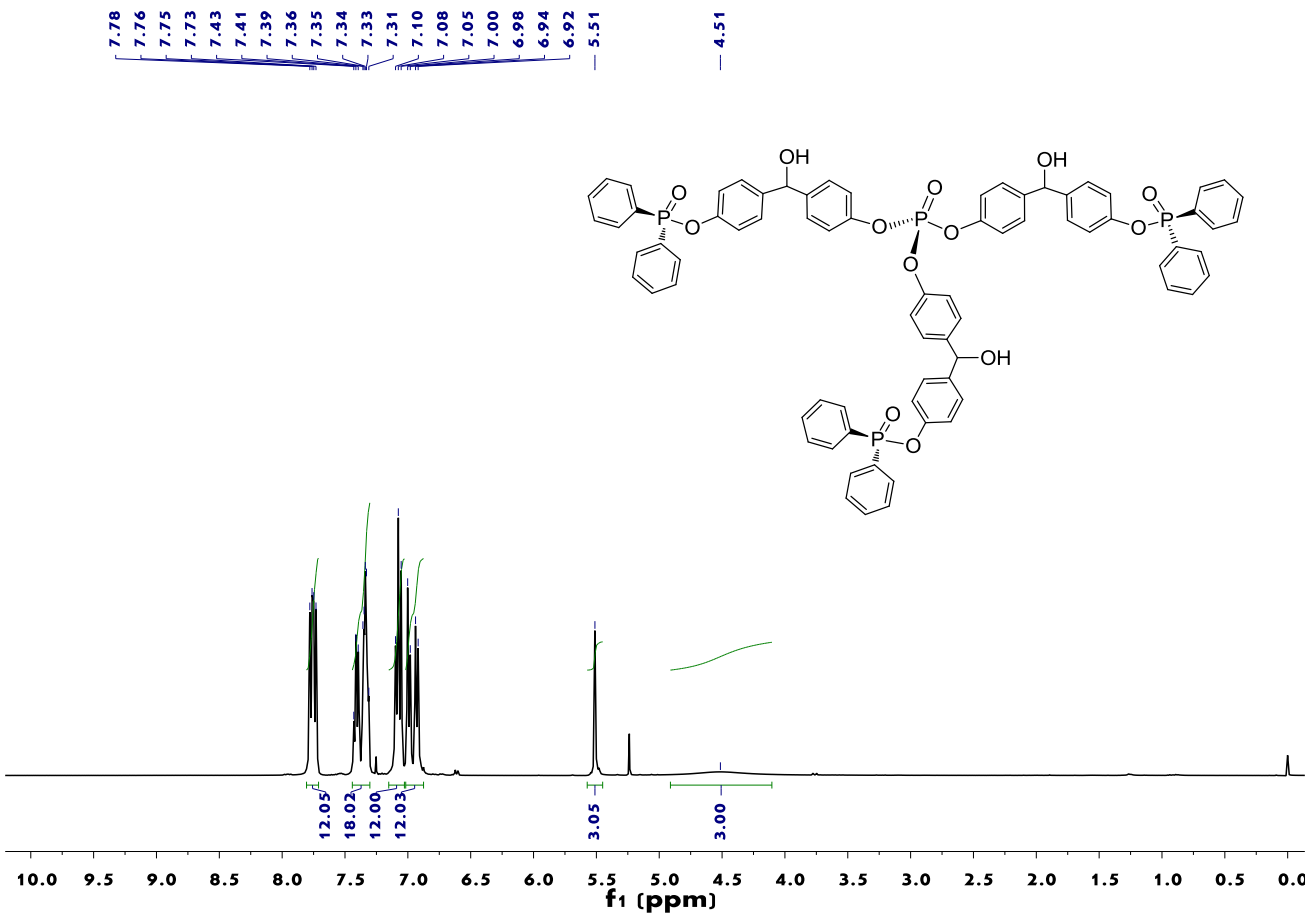

c, TDPBP-OH ^{1}H NMR (400 MHz, $CDCl_3$)

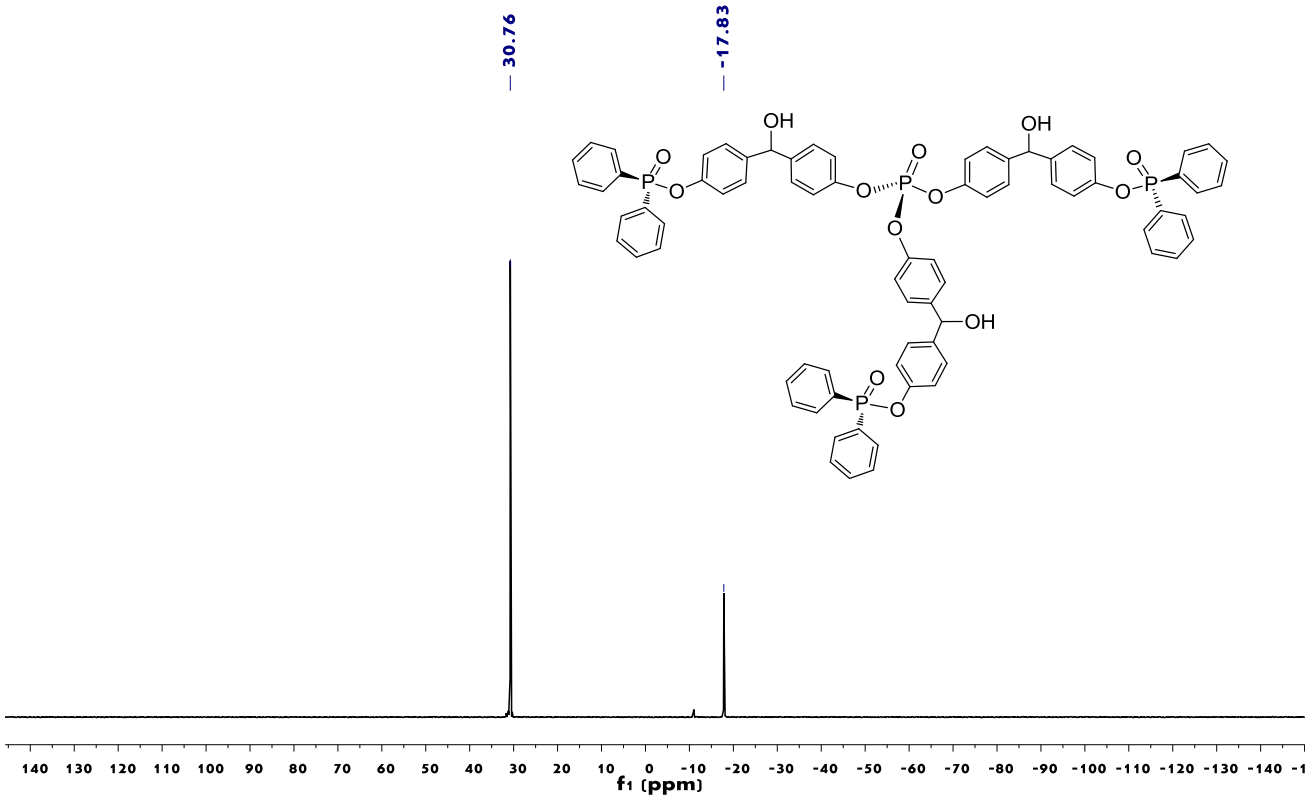

c, TDPBP-OH ^{31}P NMR (162 MHz, $CDCl_3$)

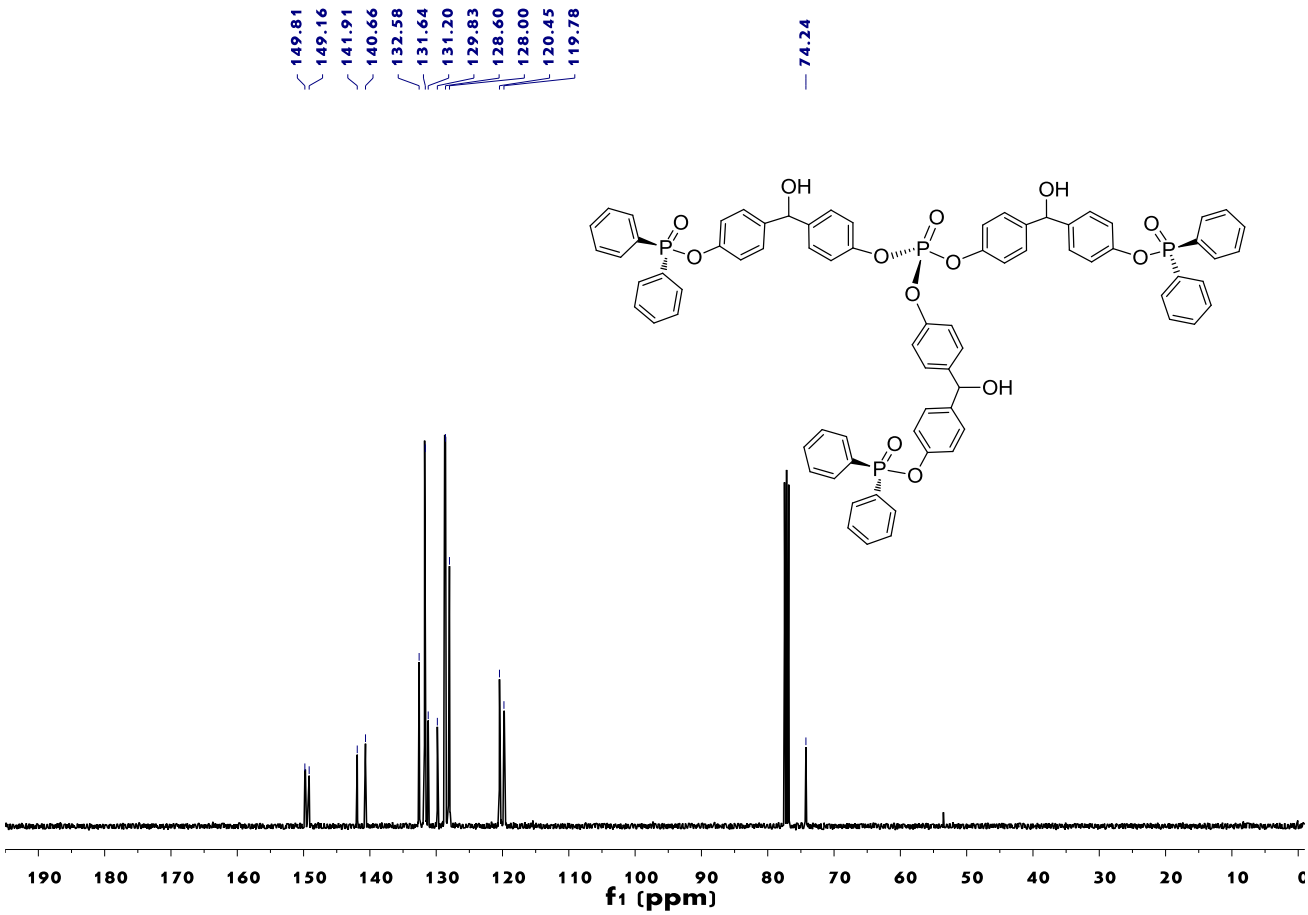

c, TDPBP-OH ^{13}C NMR (100 MHz, $CDCl_3$)

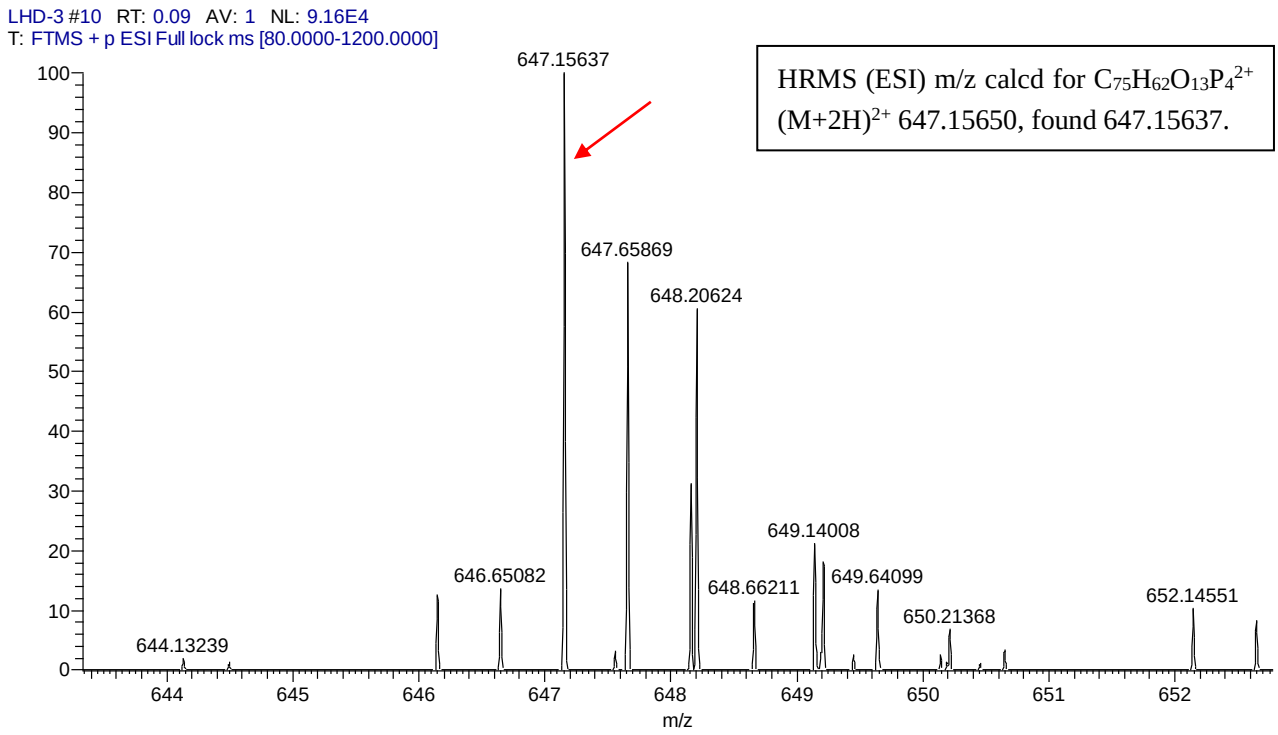

HRMS (ESI) m/z calcd for $C_{75}H_{62}O_{13}P_4^{2+}$ $(M+2H)^{2+}$ 647.15650, found 647.15637.

c, TDPBP-OH HRMS (ESI)

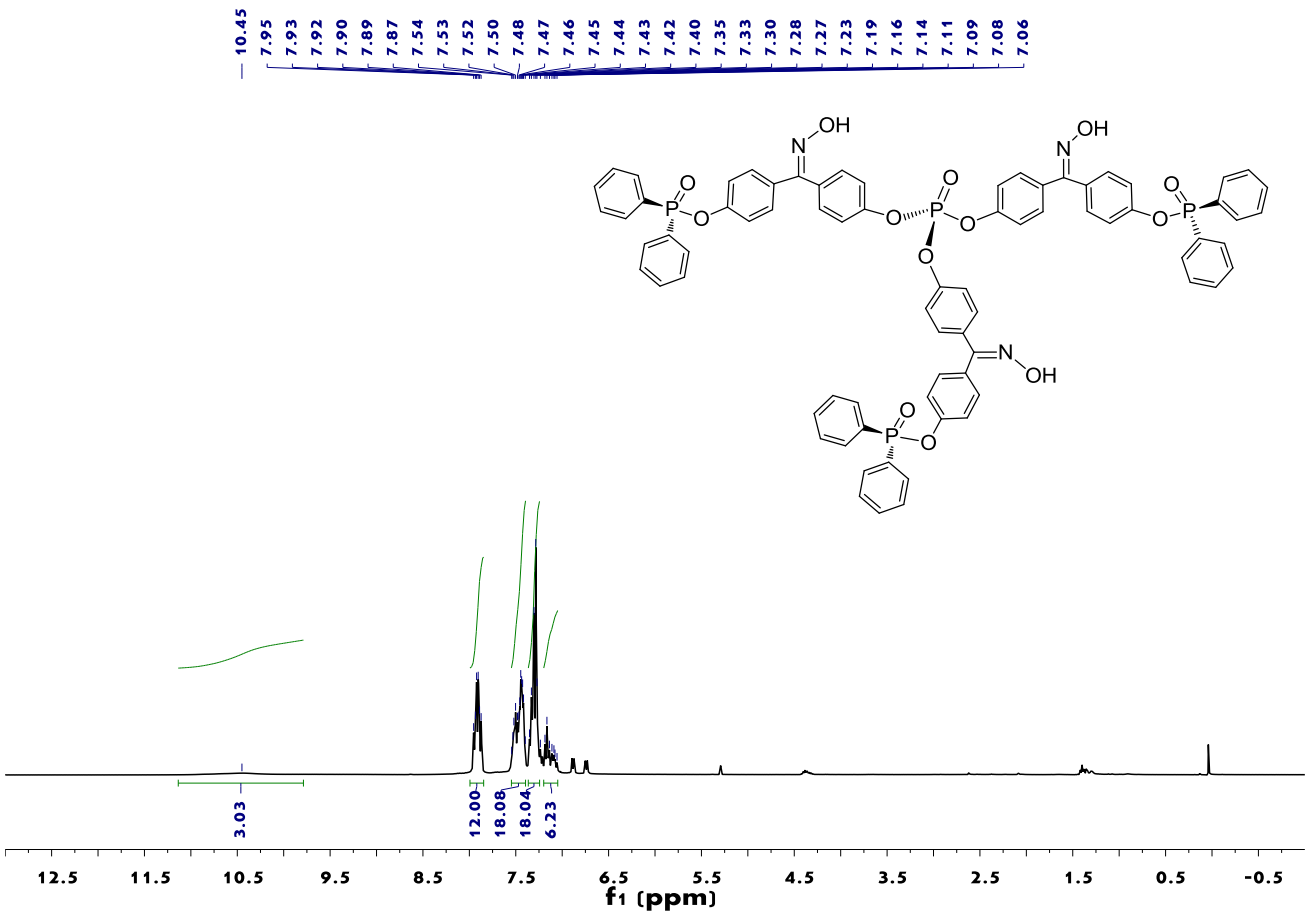

d, **TDPBP=N-OH** ^{1}H NMR (400 MHz, $CDCl_3$)

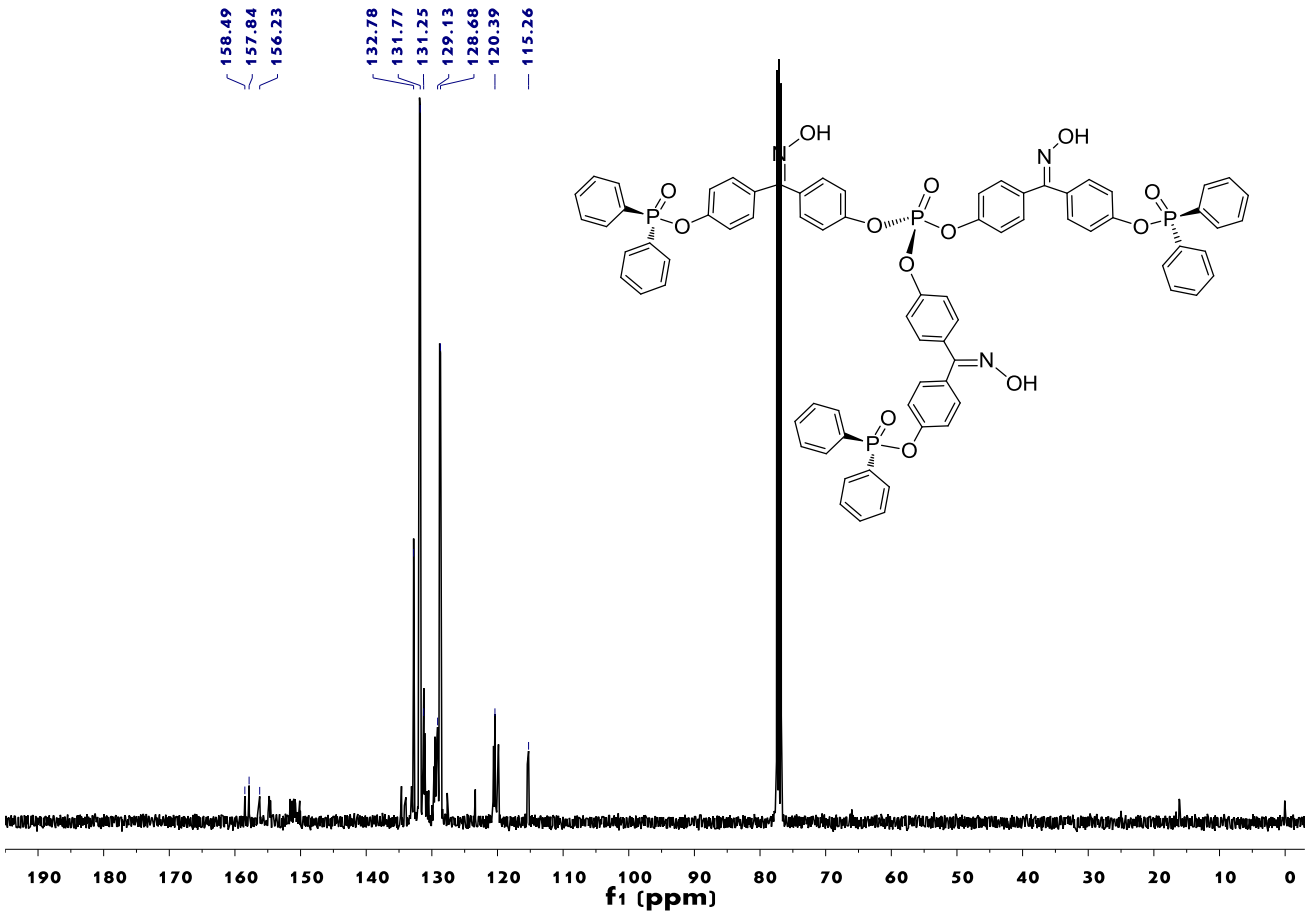

d, **TDPBP=N-OH** ^{13}C NMR (100 MHz, $CDCl_3$)

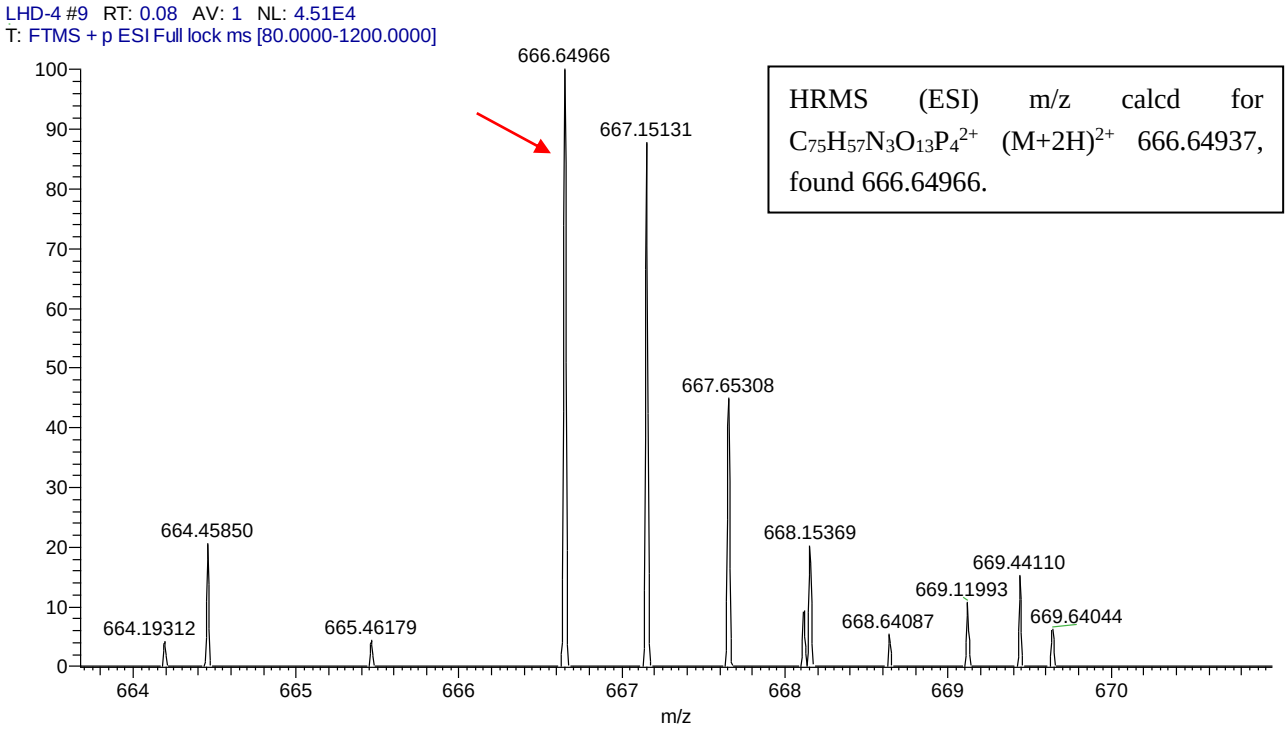

d, **TDPBP=N-OH** HRMS (ESI)

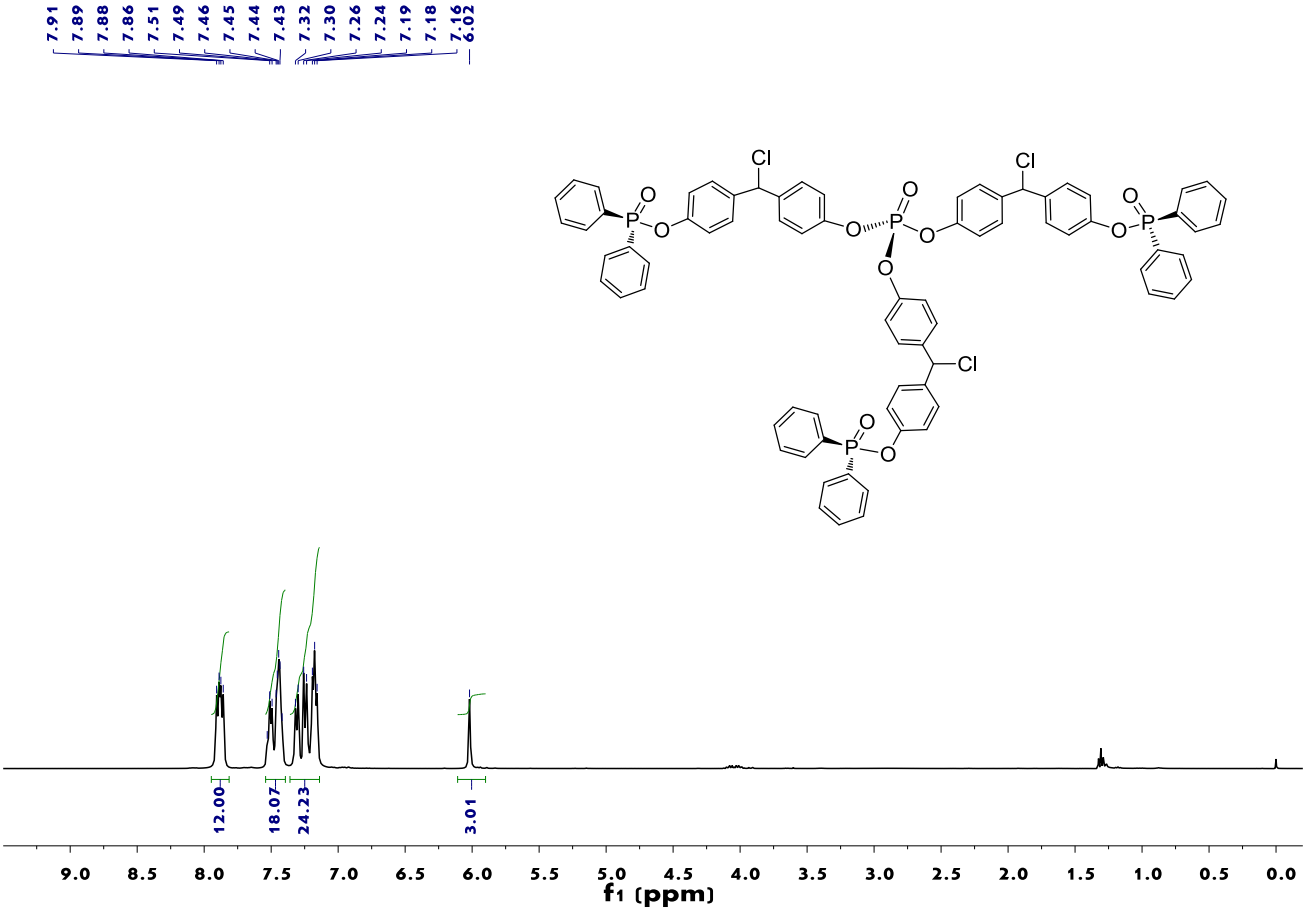

e, TDPBP-Cl ^{1}H NMR (400 MHz, $CDCl_3$)

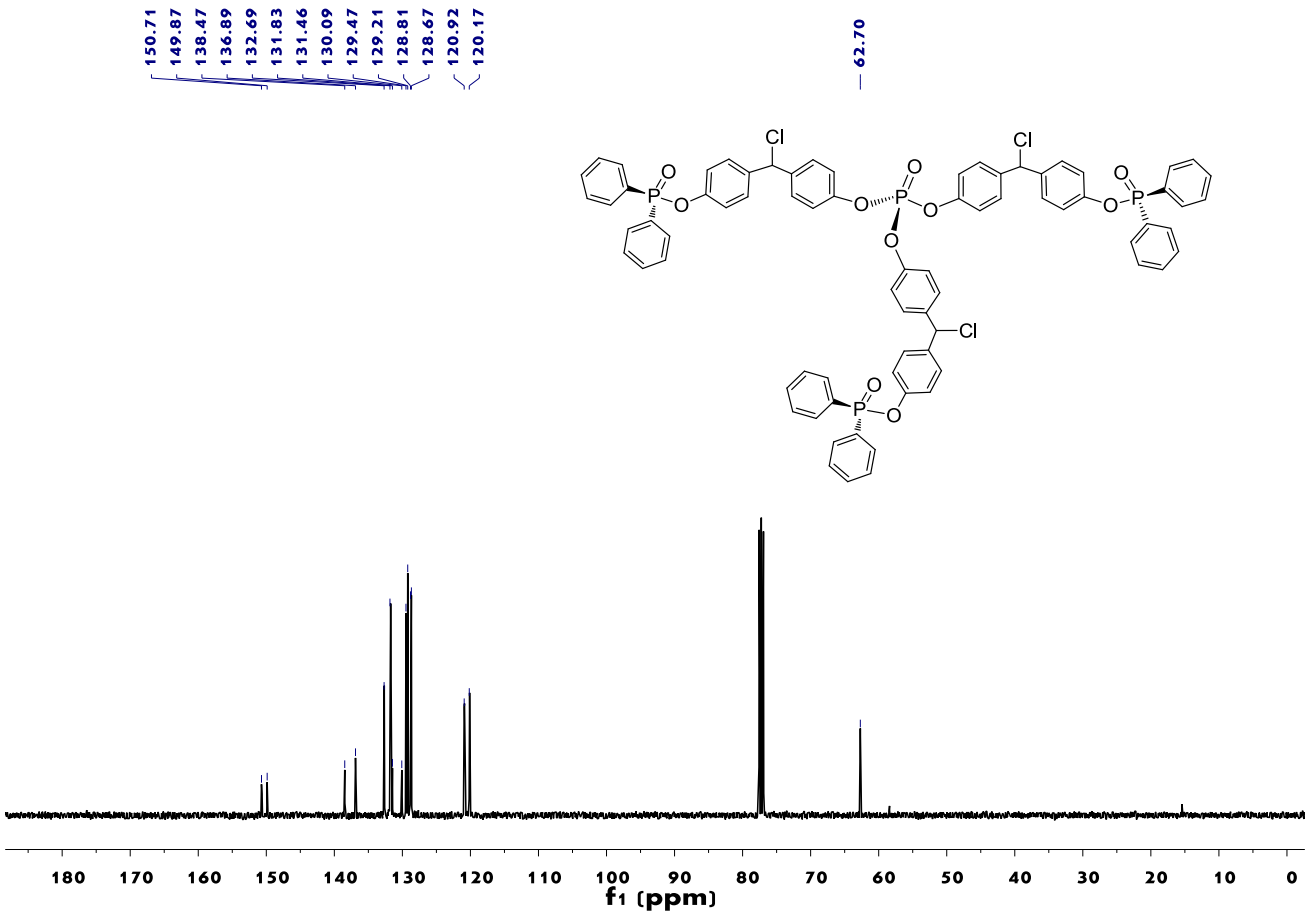

e, TDPBP-Cl ^{13}C NMR (100 MHz, $CDCl_3$)

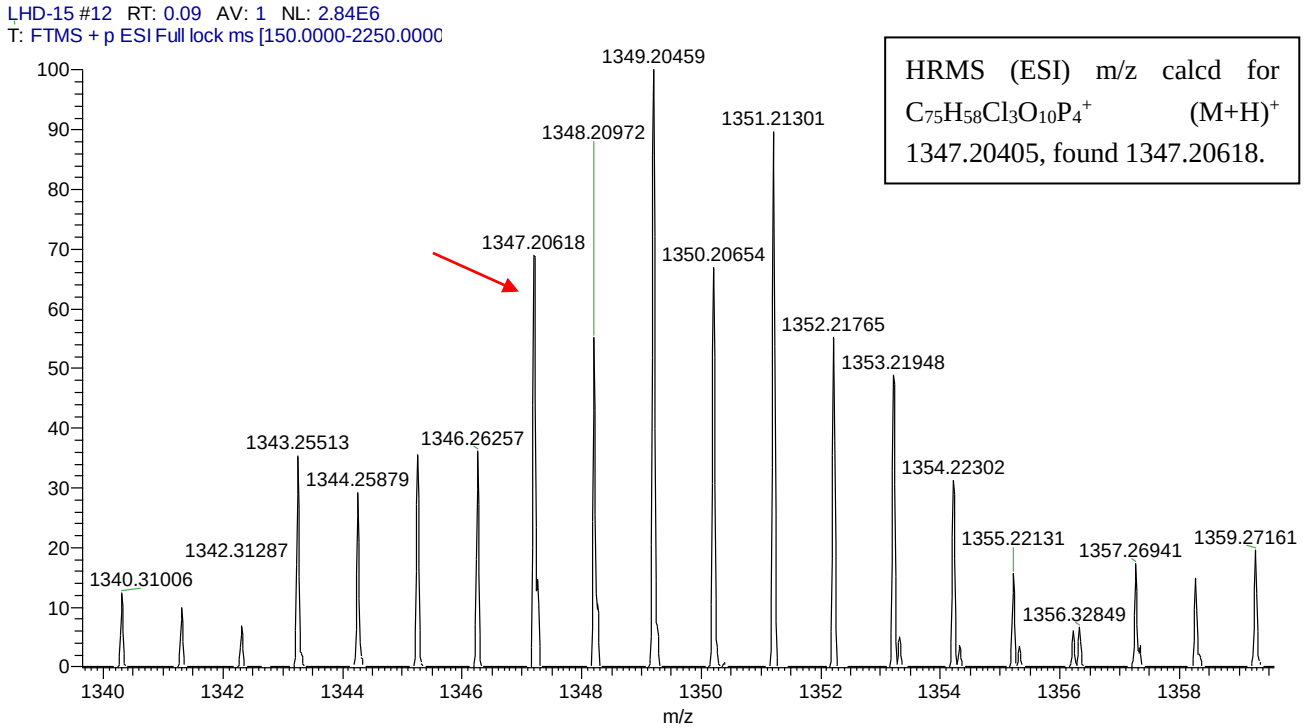

HRMS (ESI) m/z calcd for $C_{75}H_{58}Cl_3O_{10}P_4^+$ $(M+H)^+$ 1347.20405, found 1347.20618.

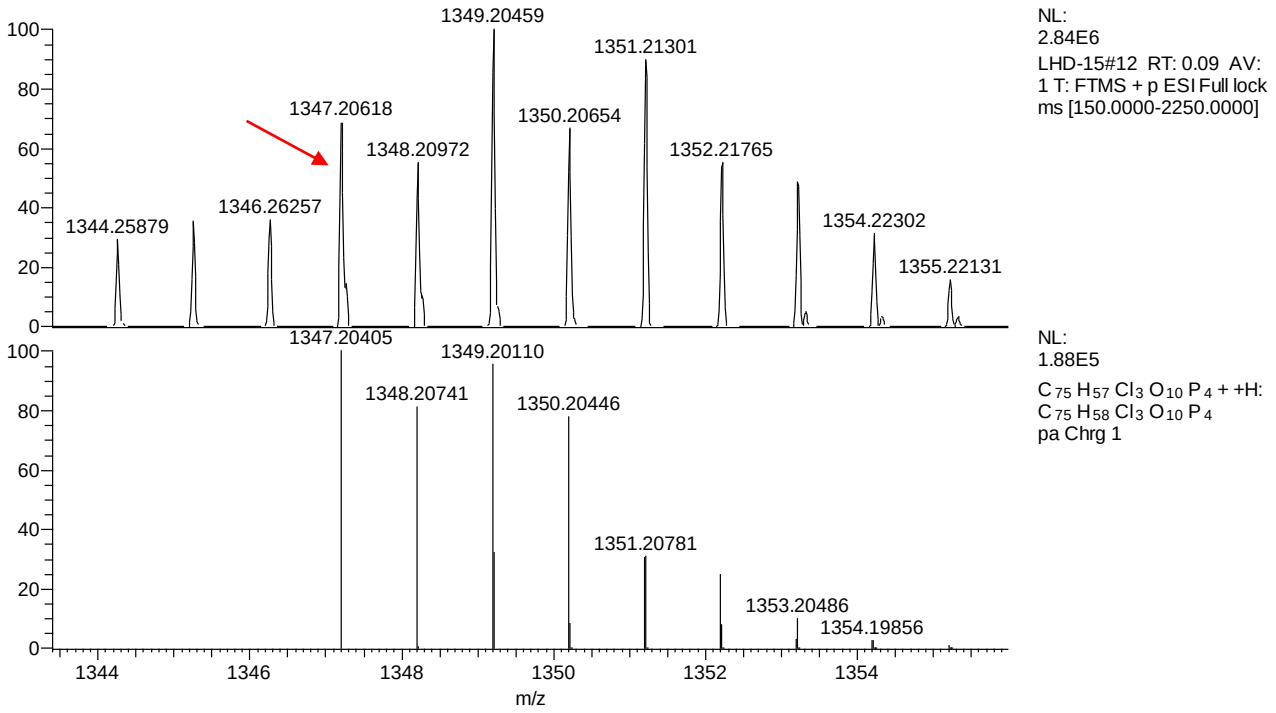

e, TDPBP-Cl HRMS (ESI)

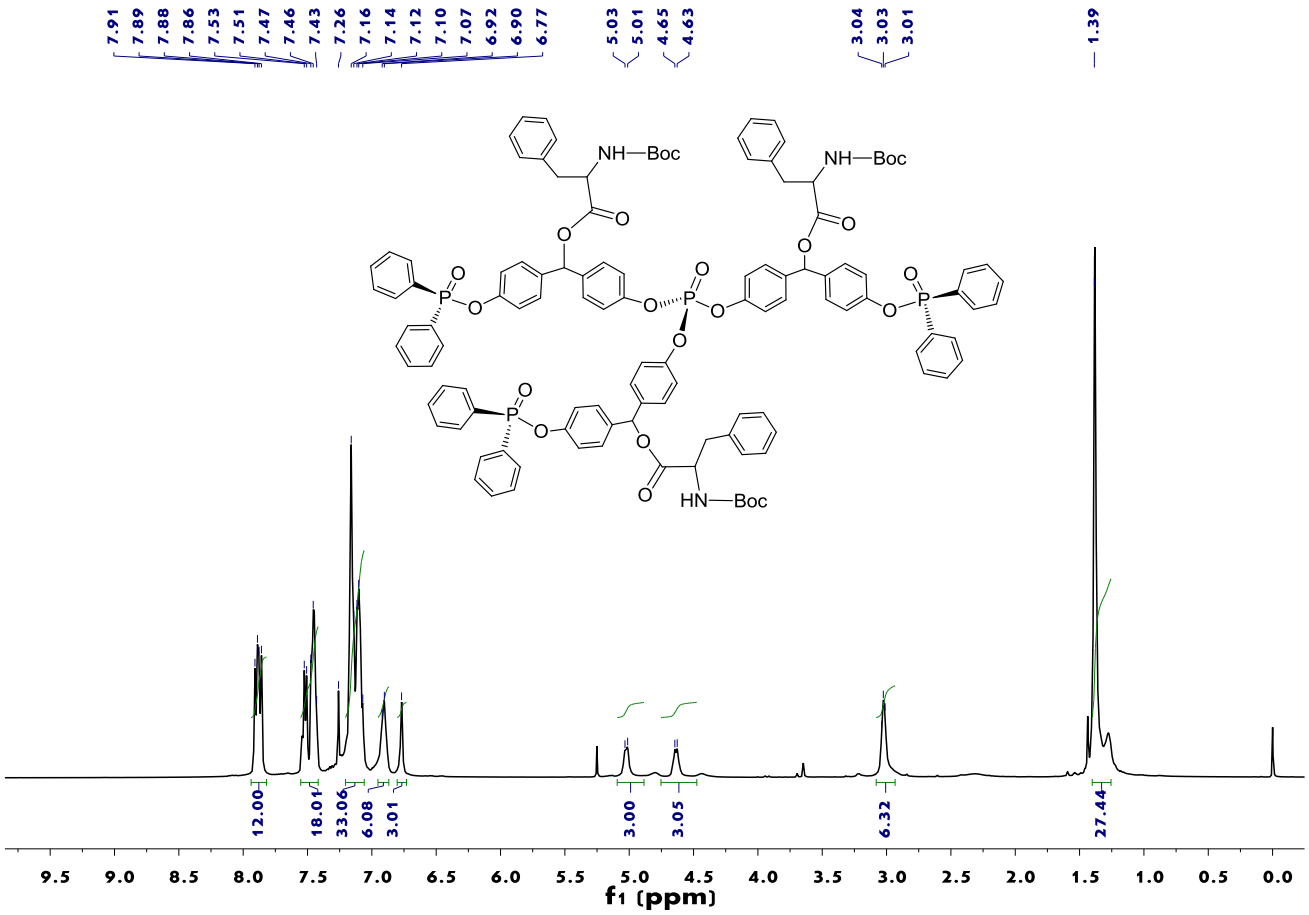

(Boc-Phe-O)$_3$-**TDPBP** ^{1}H NMR (400 MHz, $CDCl_3$)

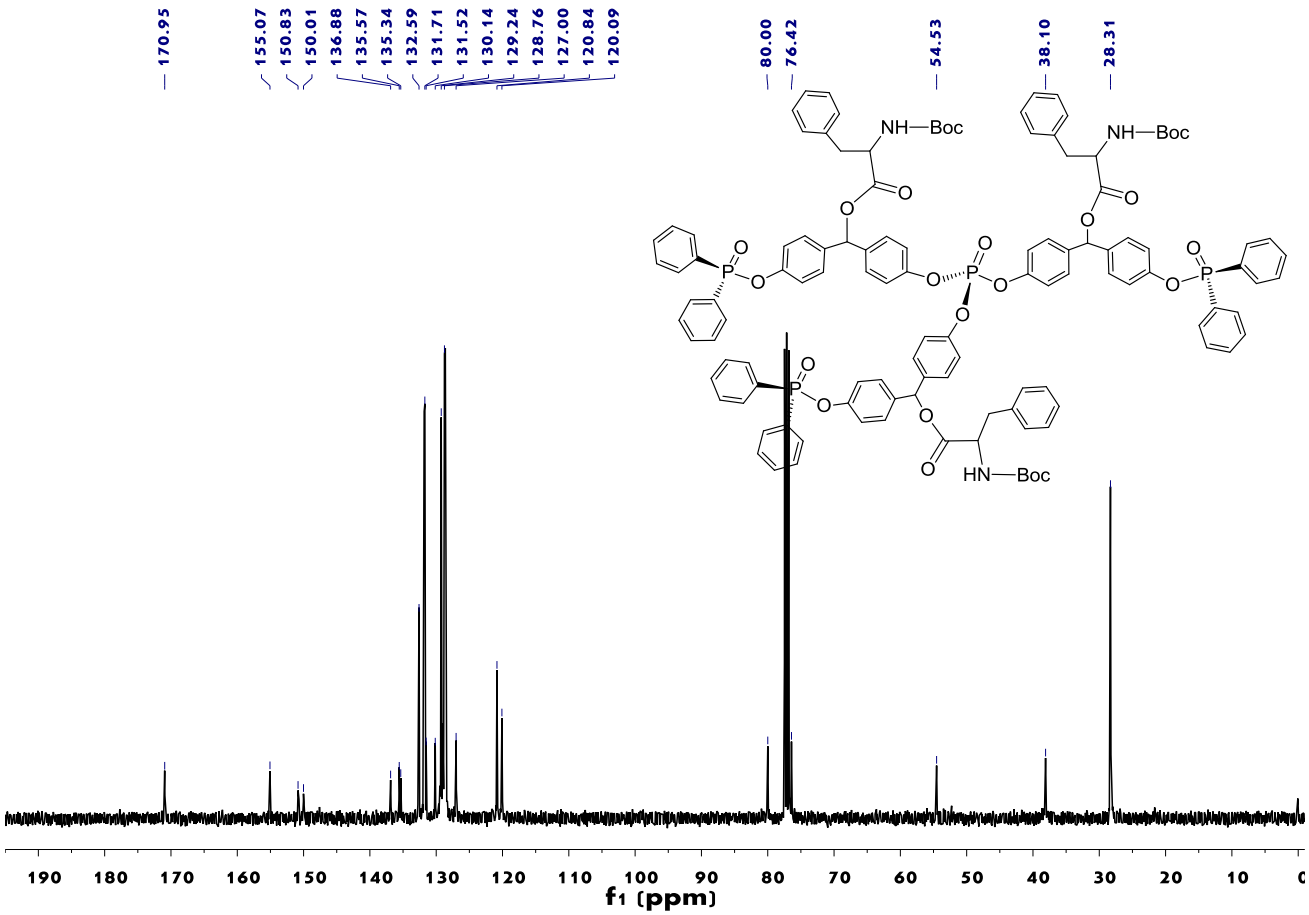

(Boc-Phe-O)$_3$-**TDPBP** ^{13}C NMR (100 MHz, $CDCl_3$)

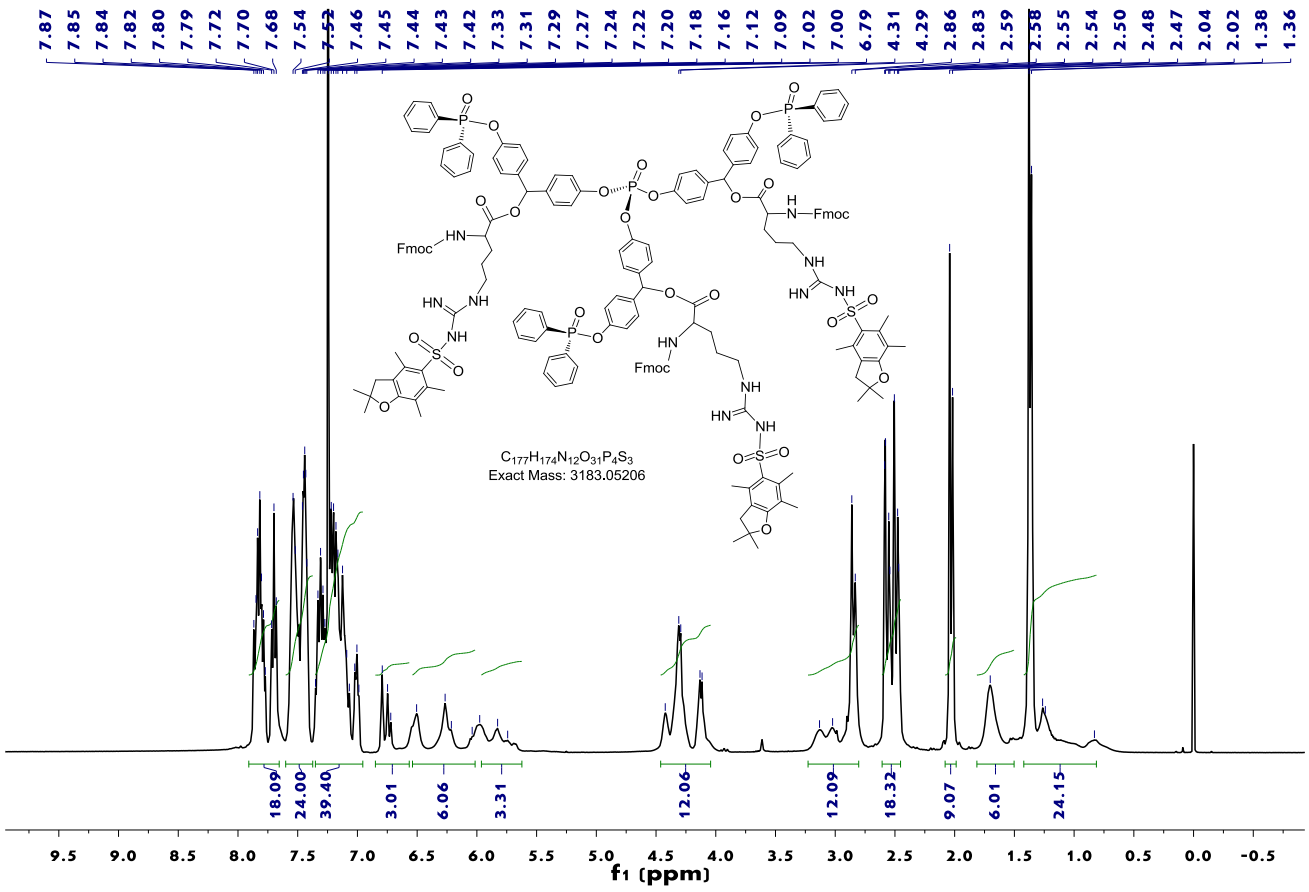

[Fmoc-Arg(Pbf)]$_3$-**TDPBP** ^{1}H NMR (400 MHz, $CDCl_3$)

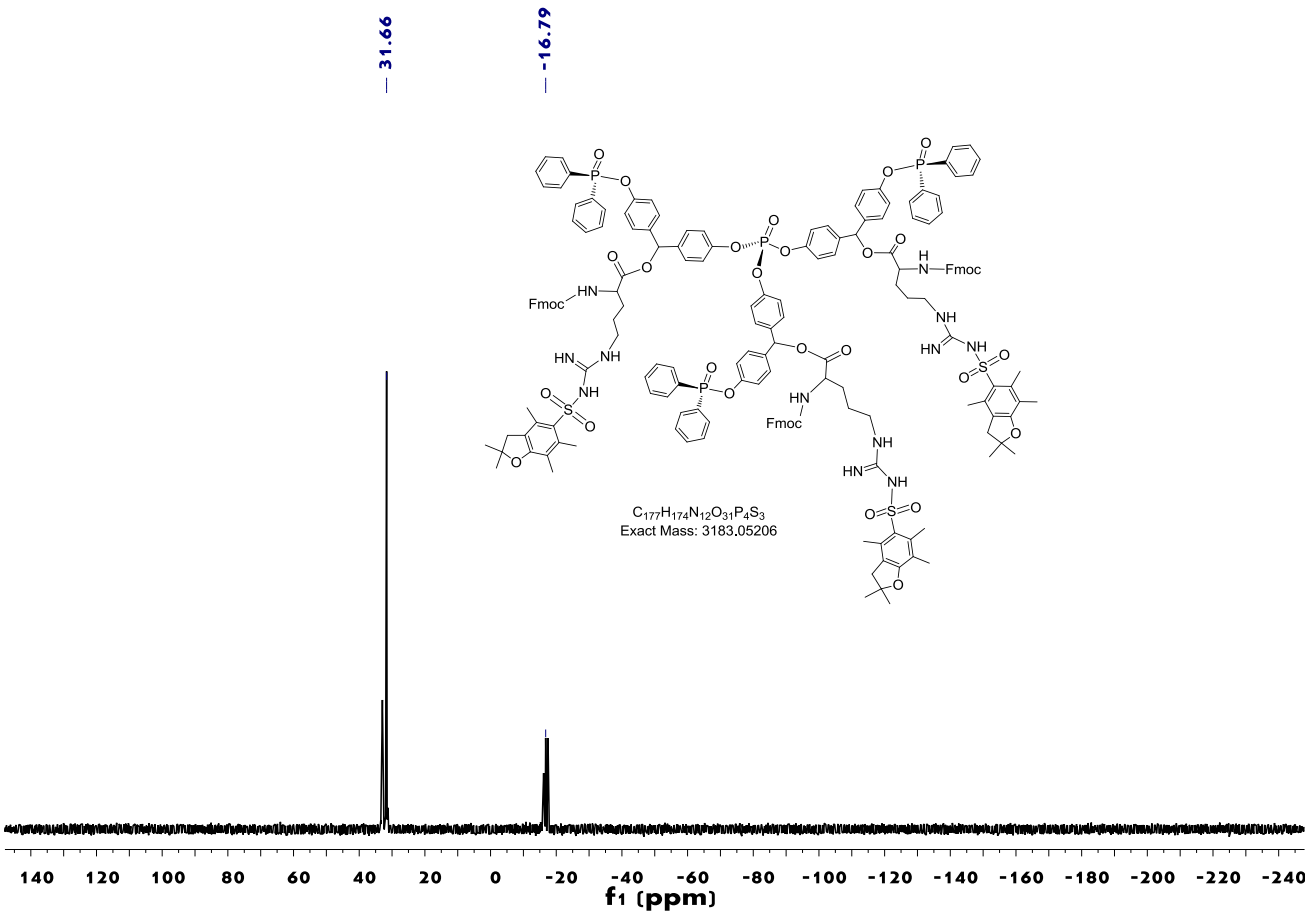

[Fmoc-Arg(Pbf)]$_3$-**TDPBP** ^{31}P NMR (162 MHz, $CDCl_3$)

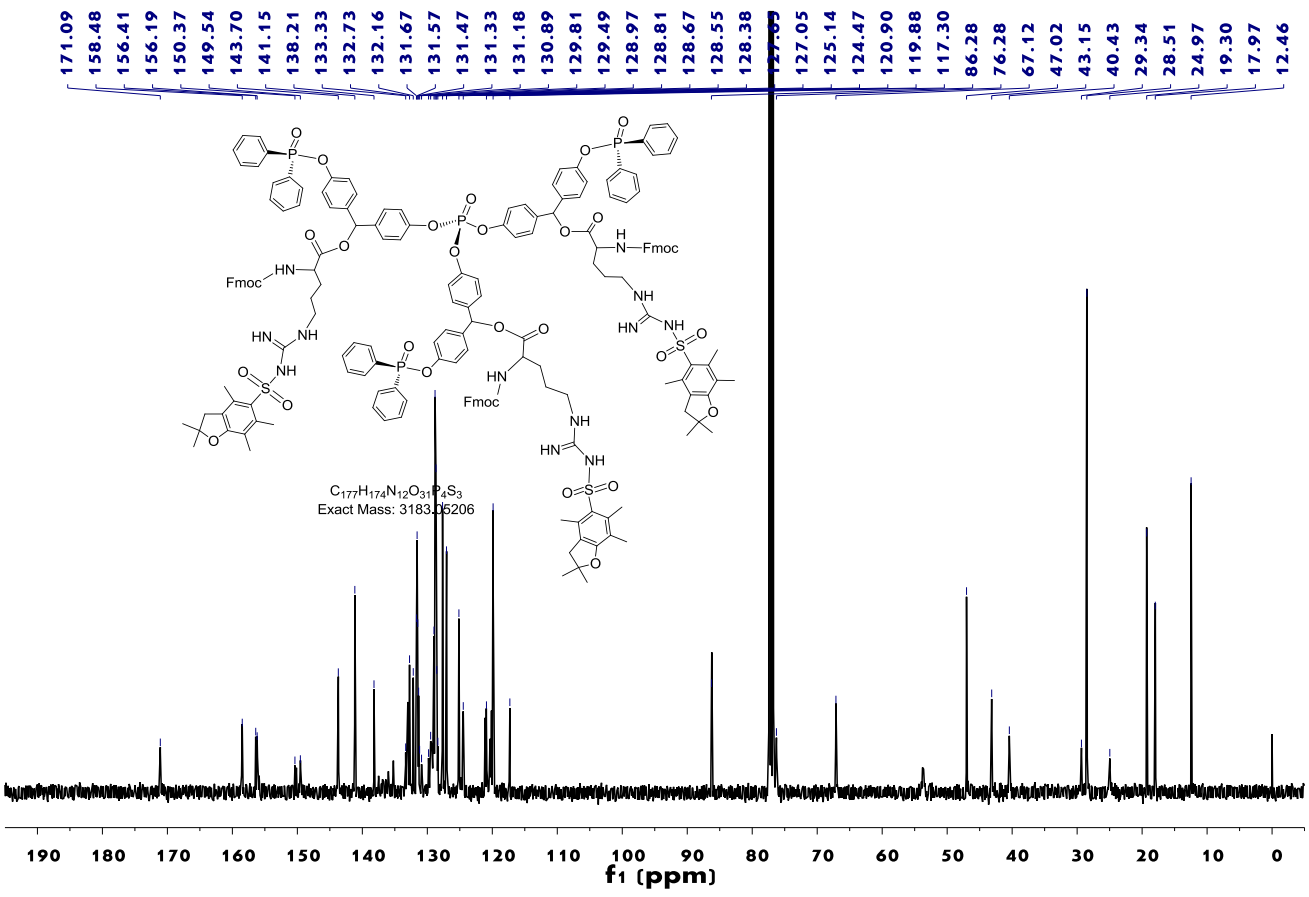

[Fmoc-Arg(Pbf)]$_3$-**TDPBP** ^{13}C NMR (100 MHz, $CDCl_3$)

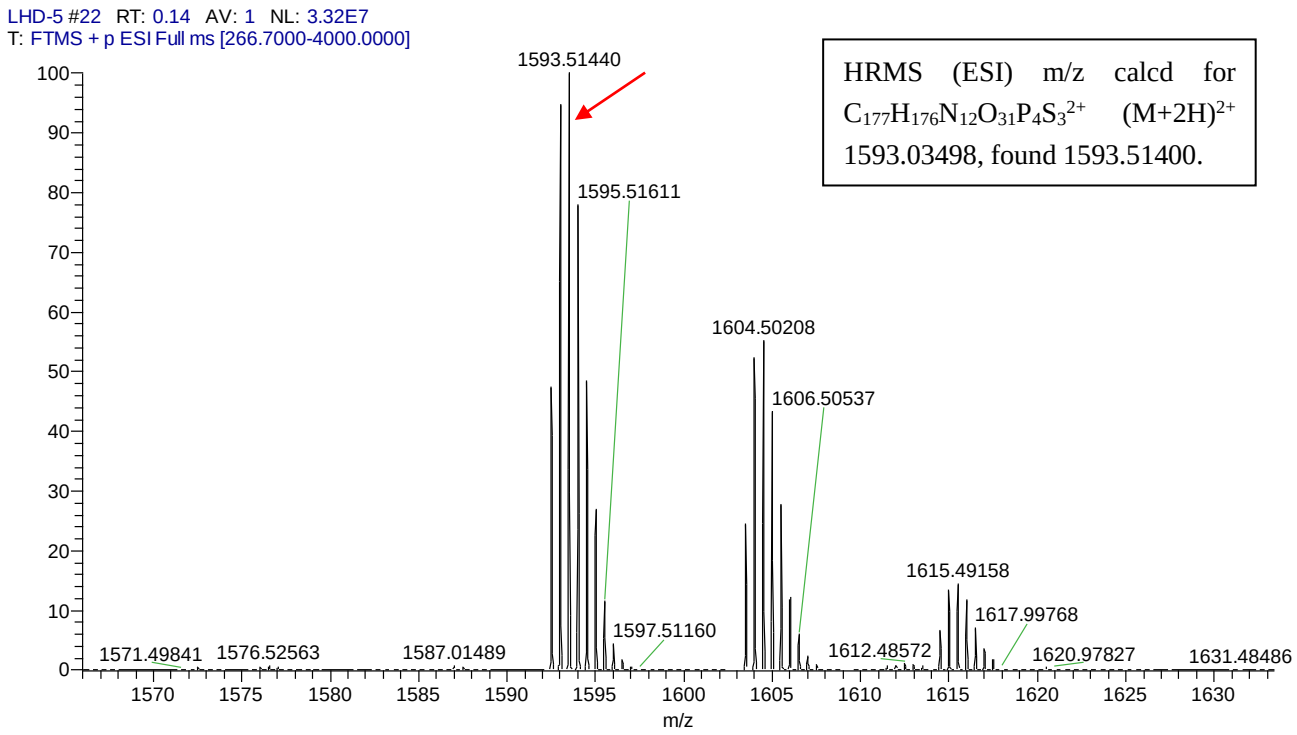

HRMS (ESI) m/z calcd for $C_{177}H_{176}N_{12}O_{31}P_4S_3^{2+}$ $(M+2H)^{2+}$ 1593.03498, found 1593.51400.

[Fmoc-Arg(Pbf)]$_3$-**TDPBP** HRMS (ESI)

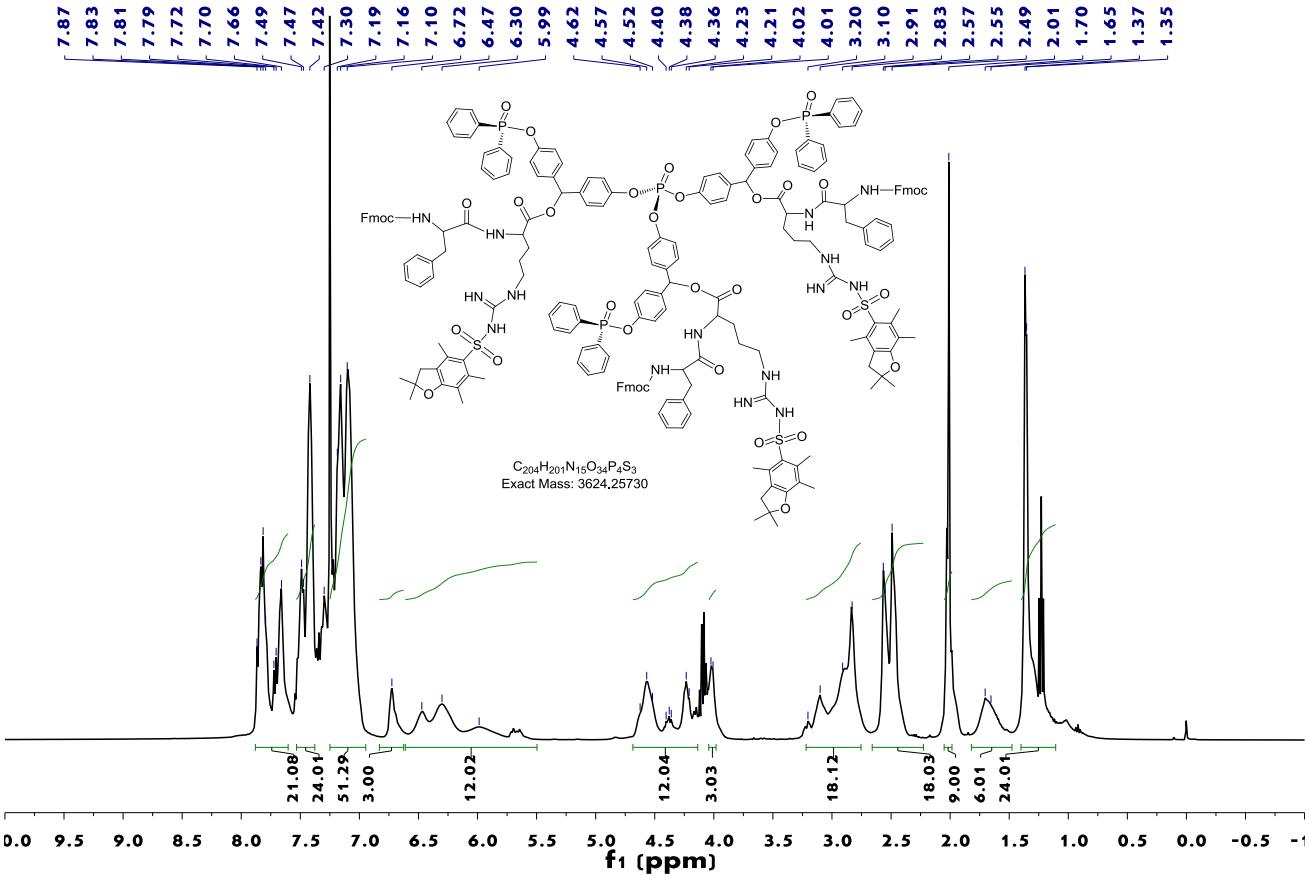

[Fmoc-Phe-Arg(Pbf)]$_3$-**TDPBP** ^{1}H NMR (400 MHz, $CDCl_3$)

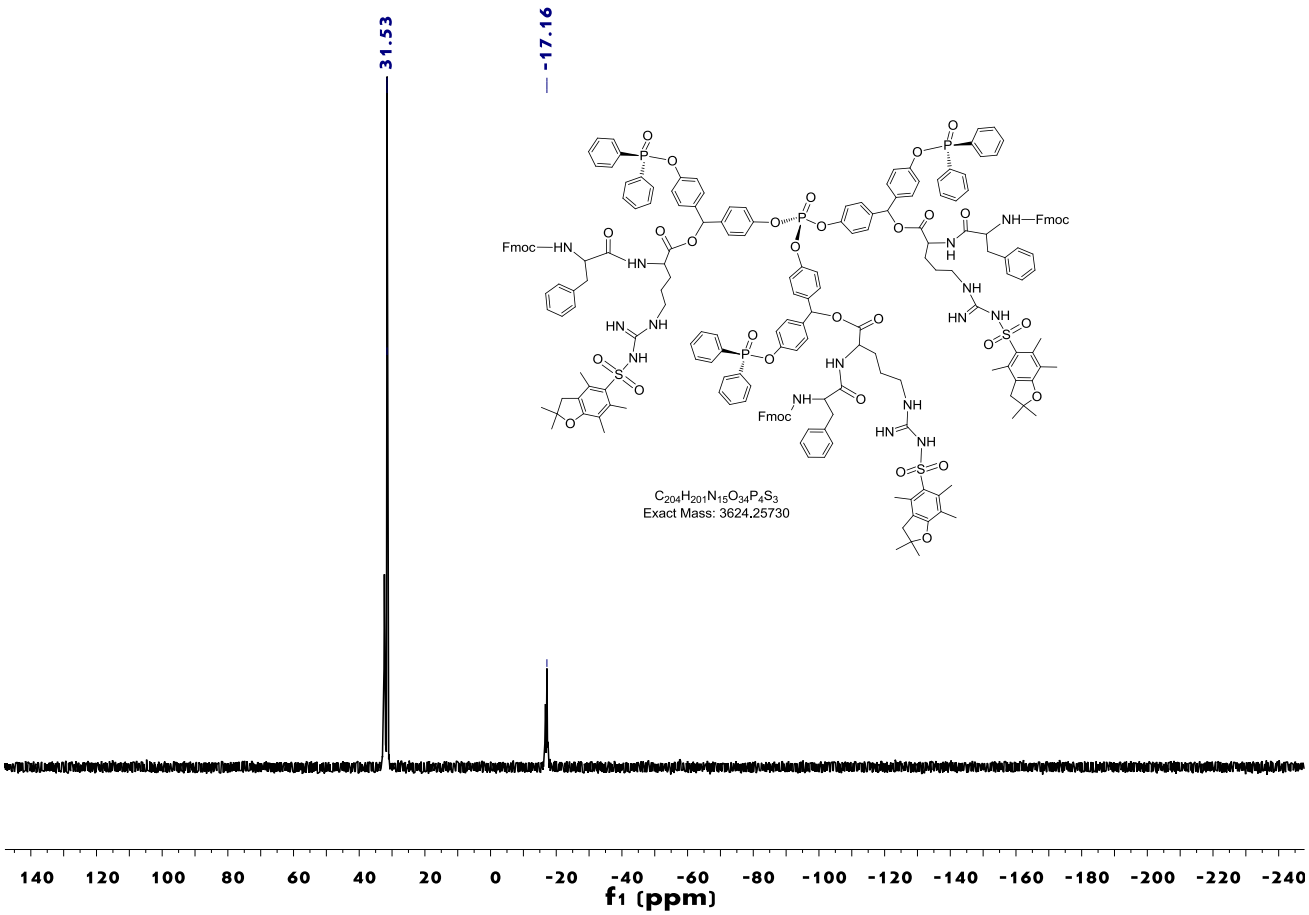

[Fmoc-Phe-Arg(Pbf)]$_3$-**TDPBP** ^{31}P NMR (162 MHz, $CDCl_3$)

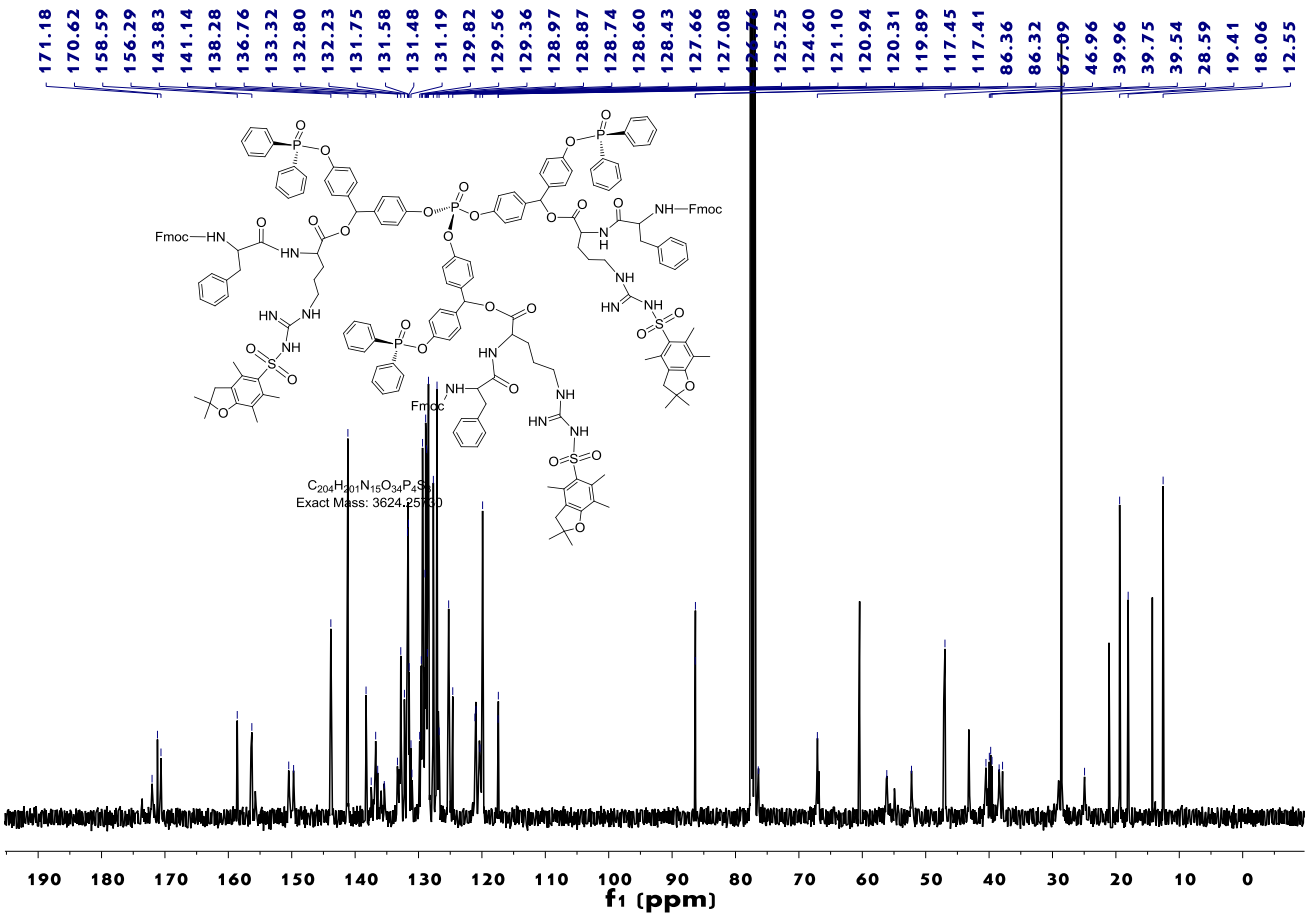

[Fmoc-Phe-Arg(Pbf)]$_3$-**TDPBP** ^{13}C NMR (100 MHz, $CDCl_3$)

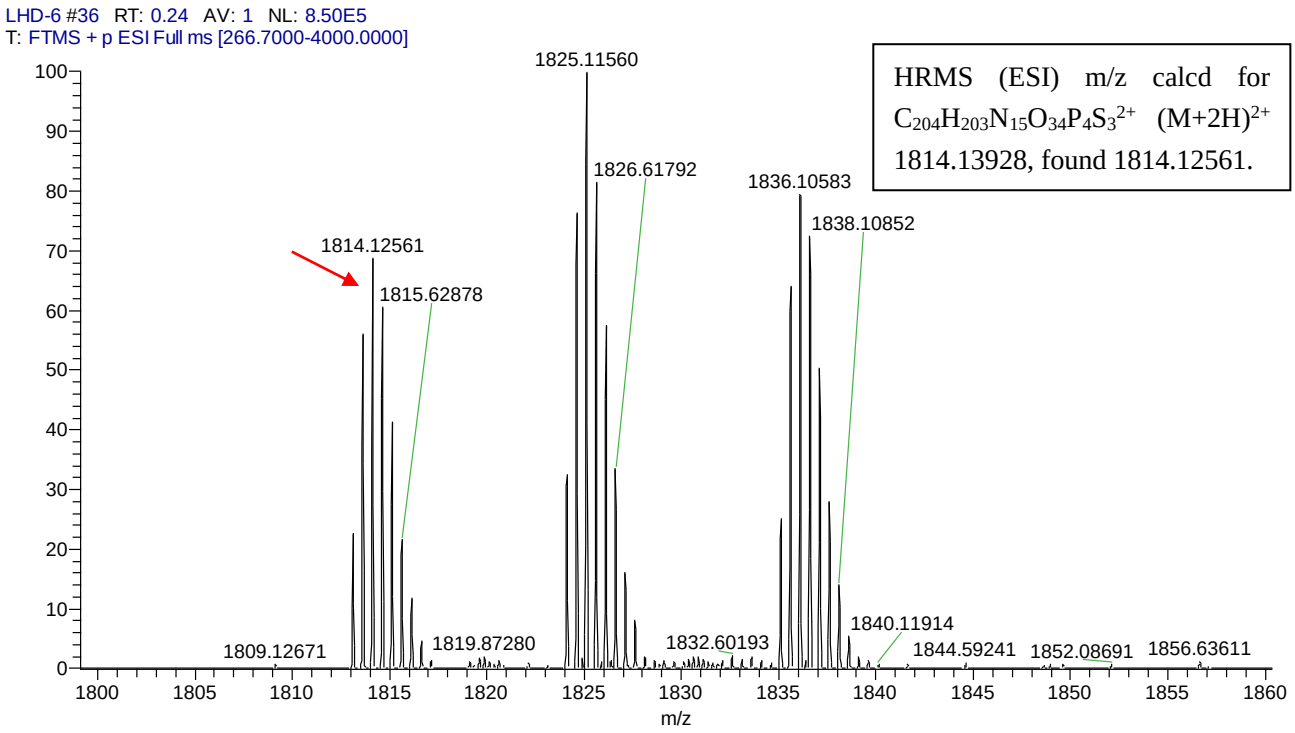

[Fmoc-Phe-Arg(Pbf)]$_3$-**TDPBP** HRMS (ESI)

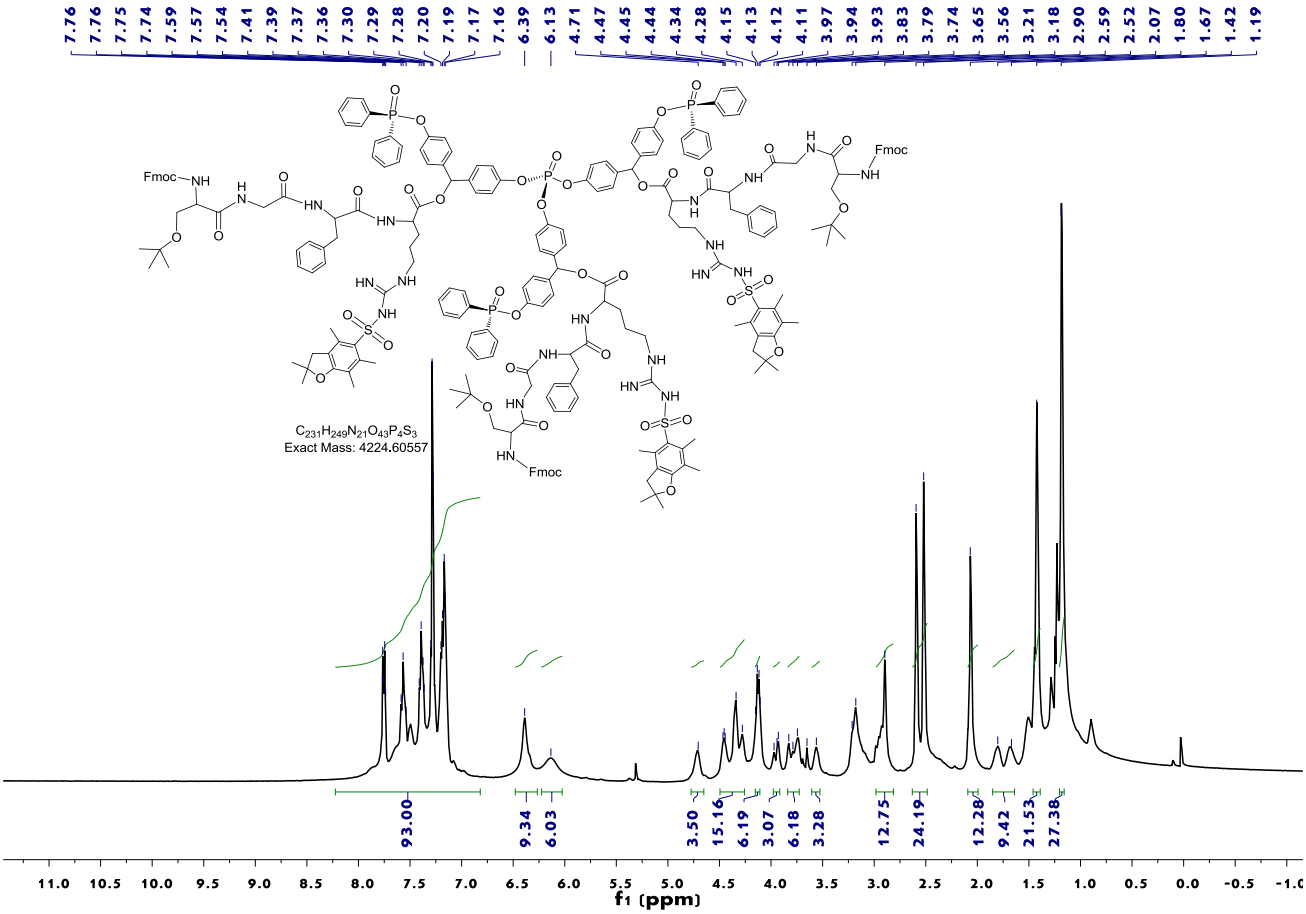

[Fmoc- -Ser(tBu)-Gly-Phe-Arg(Pbf)]$_3$-**TDPBP** ^{1}H NMR (400 MHz, $CDCl_3$)

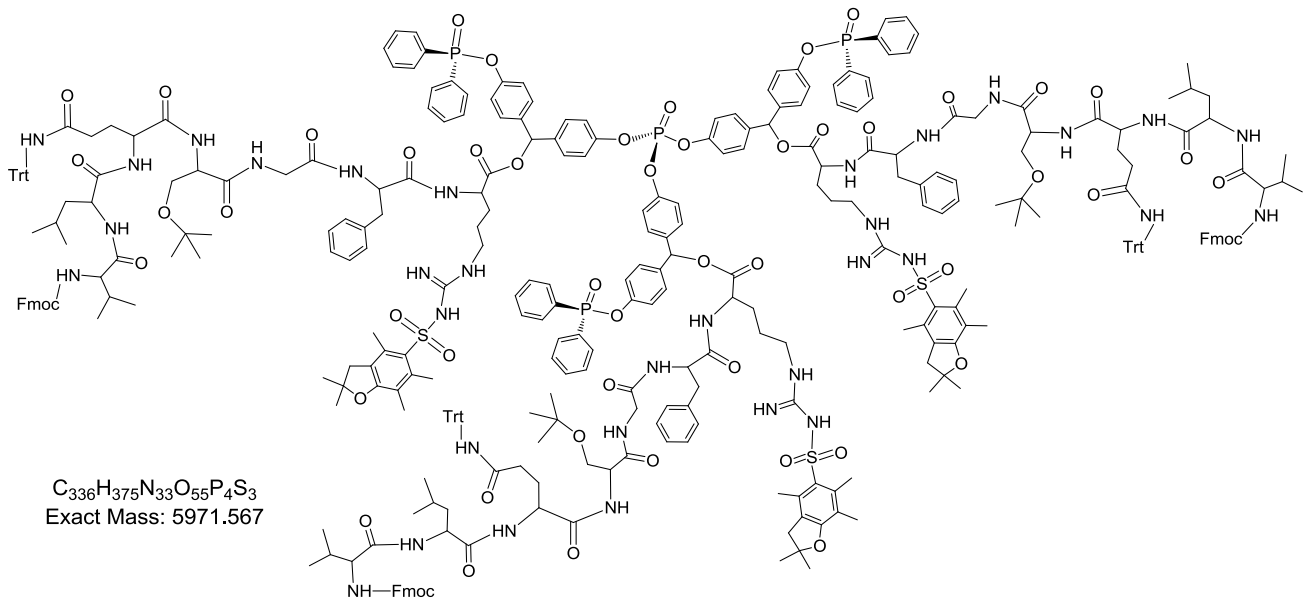

[Fmoc-Gln(Trt)-Ser(tBu)-Gly-Phe-Arg(Pbf)]$_3$-**TDPBP**

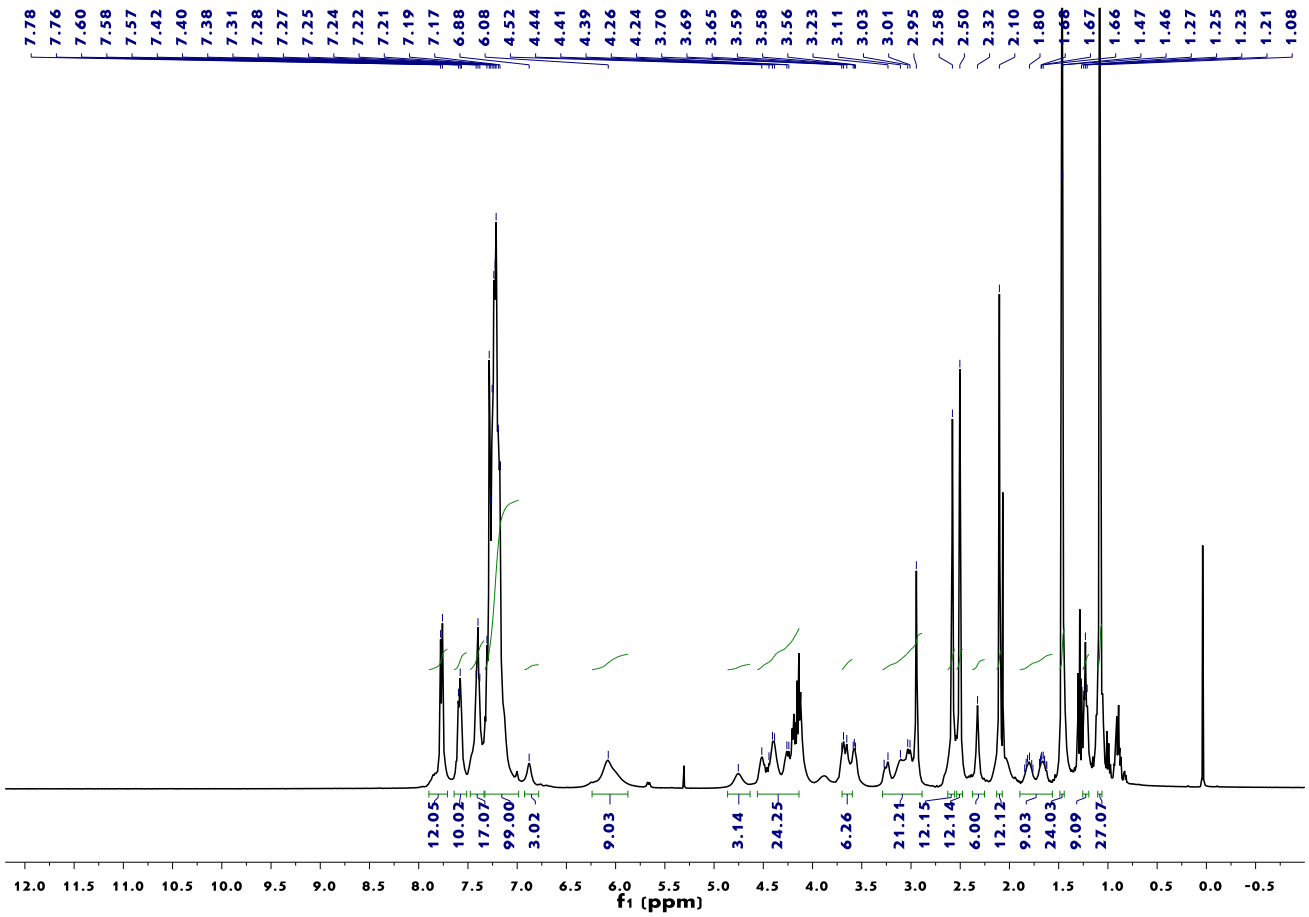

[Fmoc-Gln(Trt)-Ser(tBu)-Gly-Phe-Arg(Pbf)]$_3$-**TDPBP** ^{1}H NMR (400 MHz, $CDCl_3$)

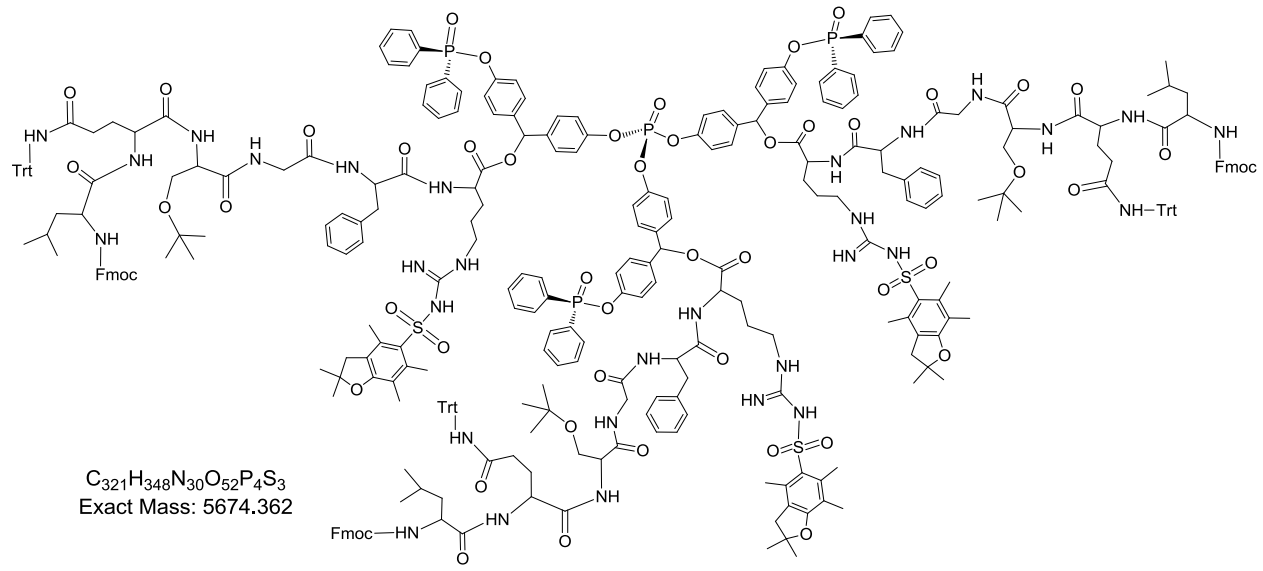

[Fmoc-Leu-Gln(Trt)-Ser(tBu)-Gly-Phe-Arg(Pbf)]$_3$-**TDPBP**

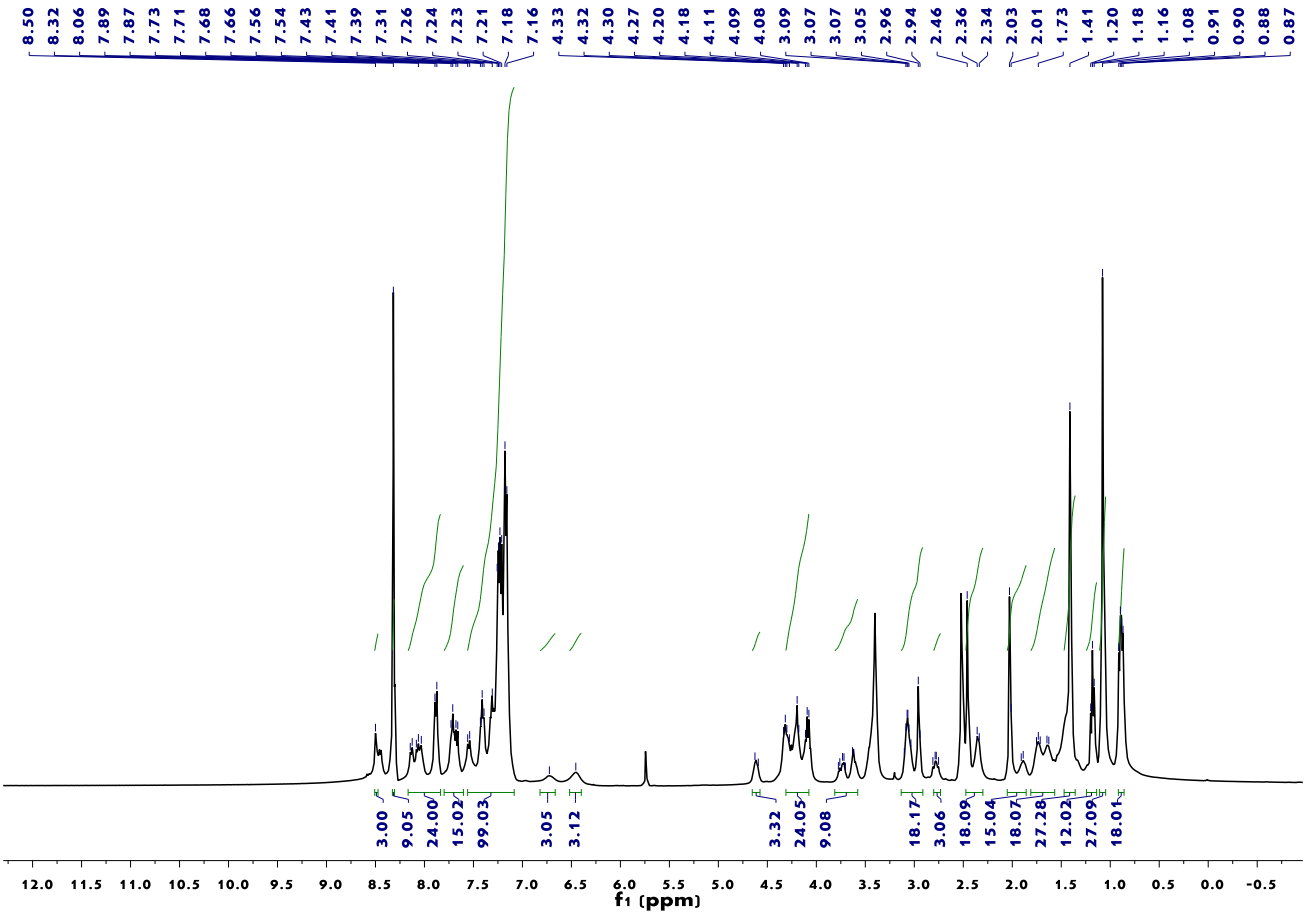

[Fmoc-Leu-Gln(Trt)-Ser(tBu)-Gly-Phe-Arg(Pbf)]$_3$-**TDPBP** ^{1}H NMR (400 MHz, DMSO-d_6)

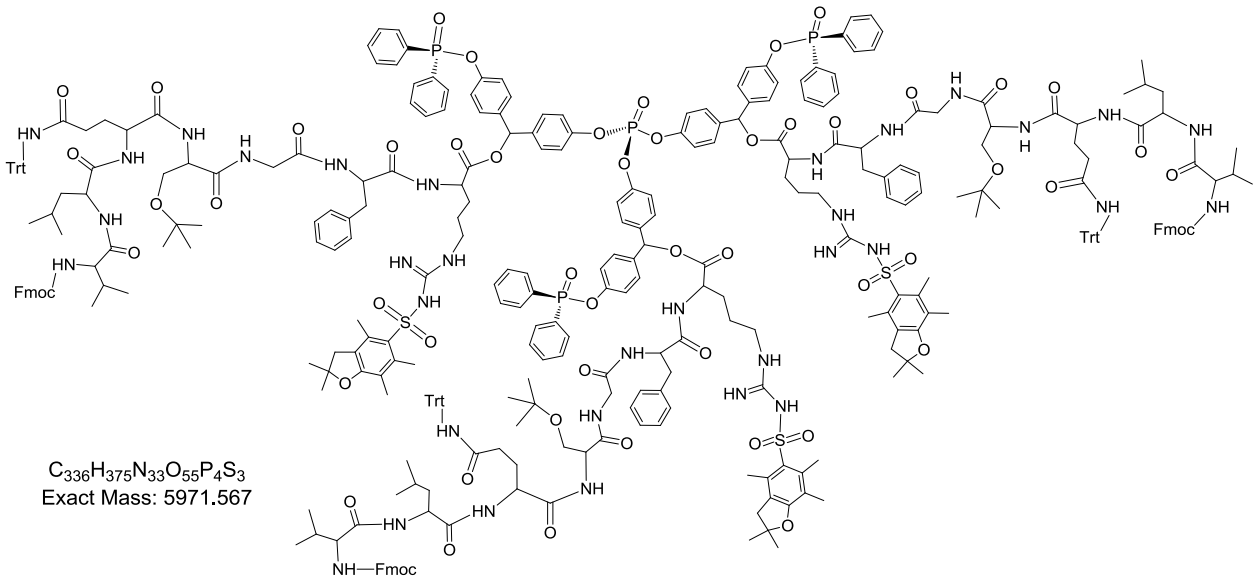

[Fmoc-Val-Leu-Gln(Trt)-Ser(tBu)-Gly-Phe-Arg(Pbf)]$_3$-**TDPBP**

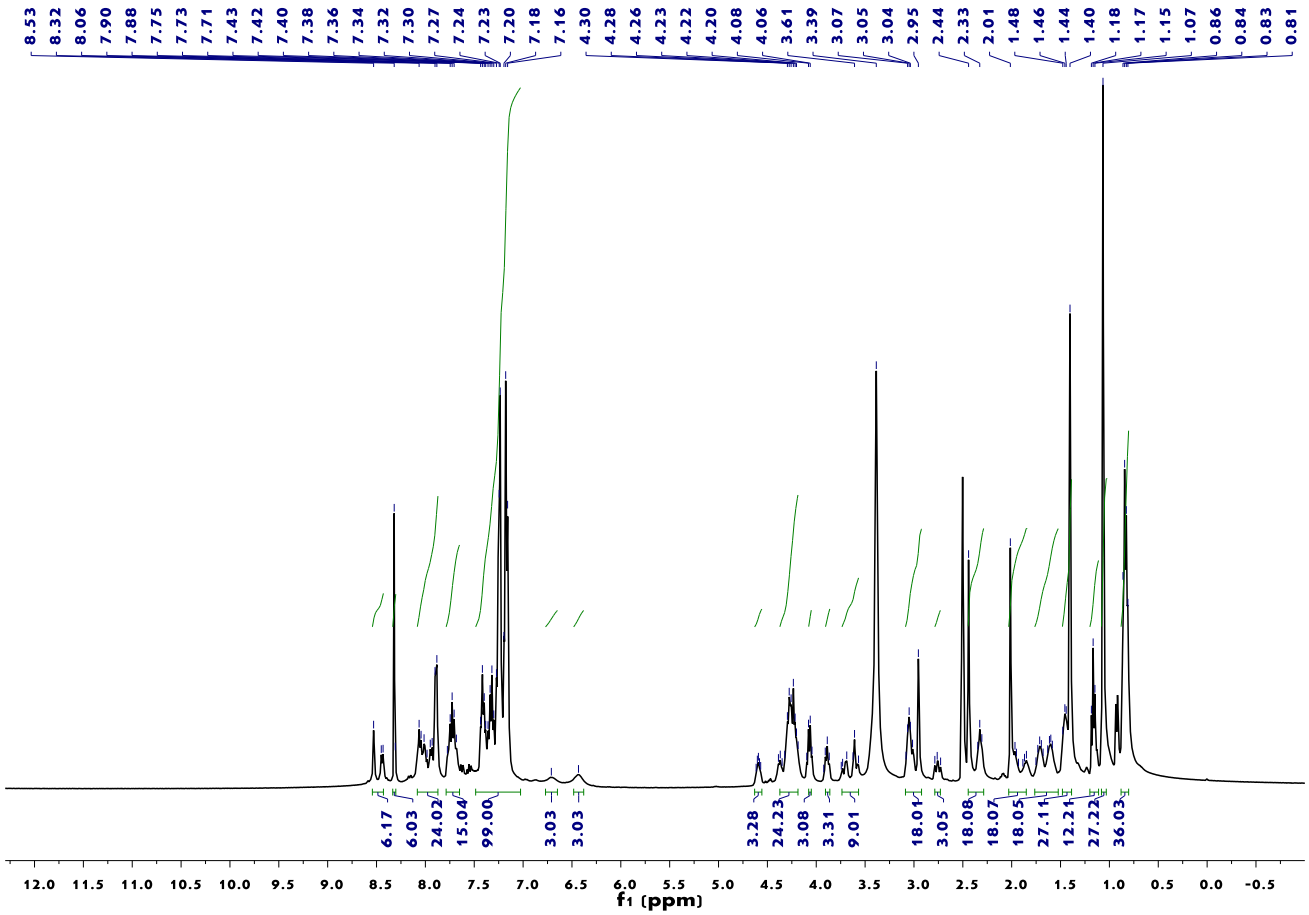

[Fmoc-Val-Leu-Gln(Trt)-Ser(tBu)-Gly-Phe-Arg(Pbf)]$_3$-**TDPBP** ^{1}H NMR (400 MHz, DMSO-d_6)

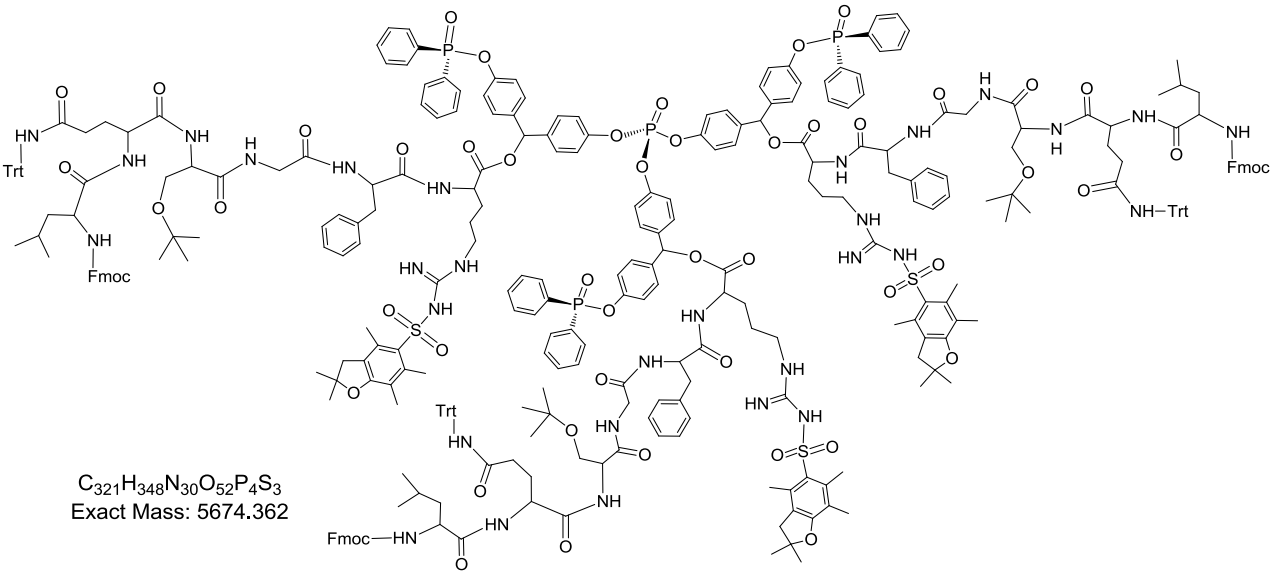

[Fmoc-Ala-Val-Leu-Gln(Trt)-Ser(tBu)-Gly-Phe-Arg(Pbf)]$_3$-**TDPBP**

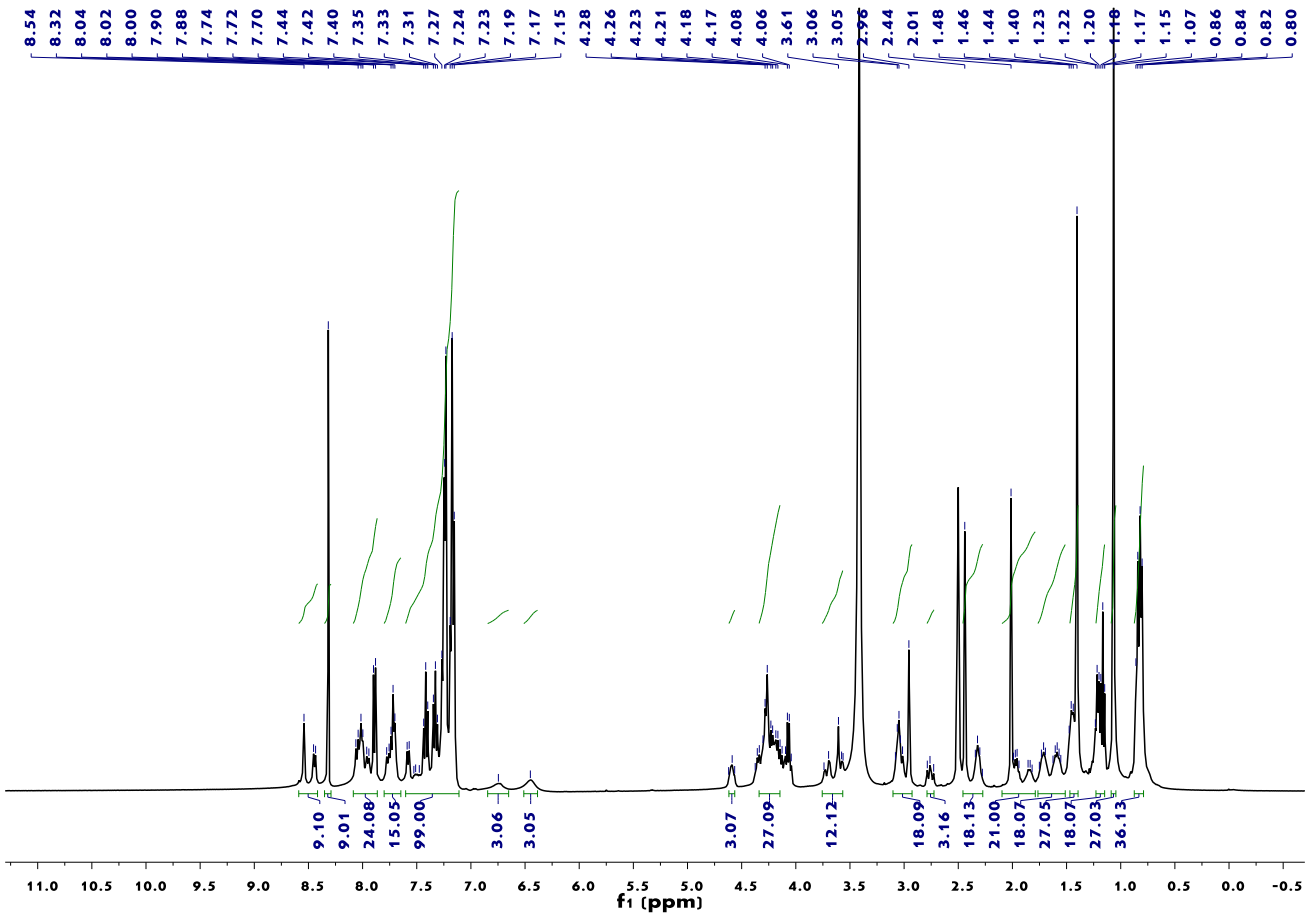

[Fmoc-Ala-Val-Leu-Gln(Trt)-Ser(tBu)-Gly-Phe-Arg(Pbf)]$_3$-**TDPBP** ^{1}H NMR (400 MHz, DMSO-d_6)

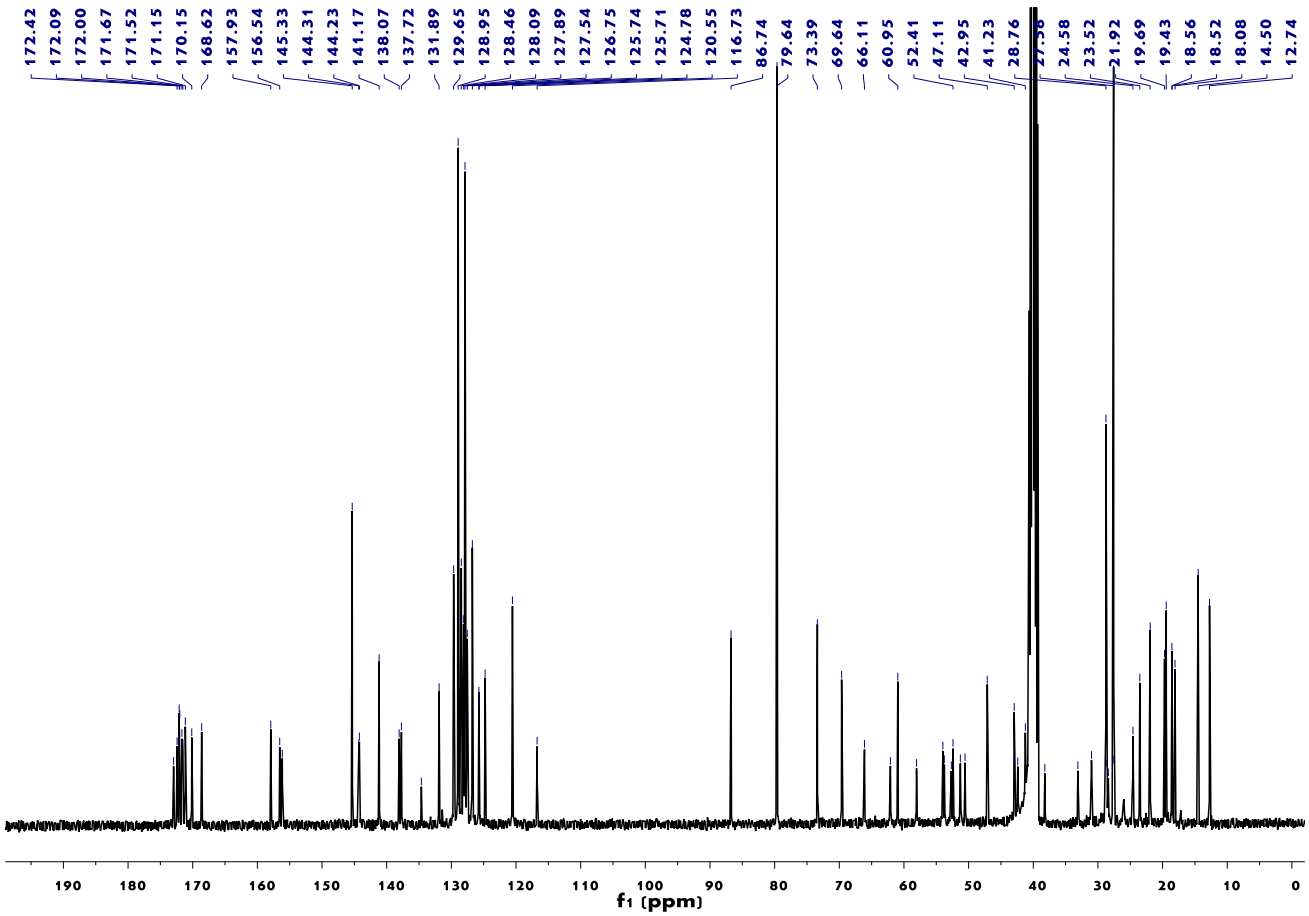

[Fmoc-Ala-Val-Leu-Gln(Trt)-Ser(tBu)-Gly-Phe-Arg(Pbf)]$_3$-**TDPBP** ^{13}C NMR (100 MHz, DMSO-*d*$_6$)

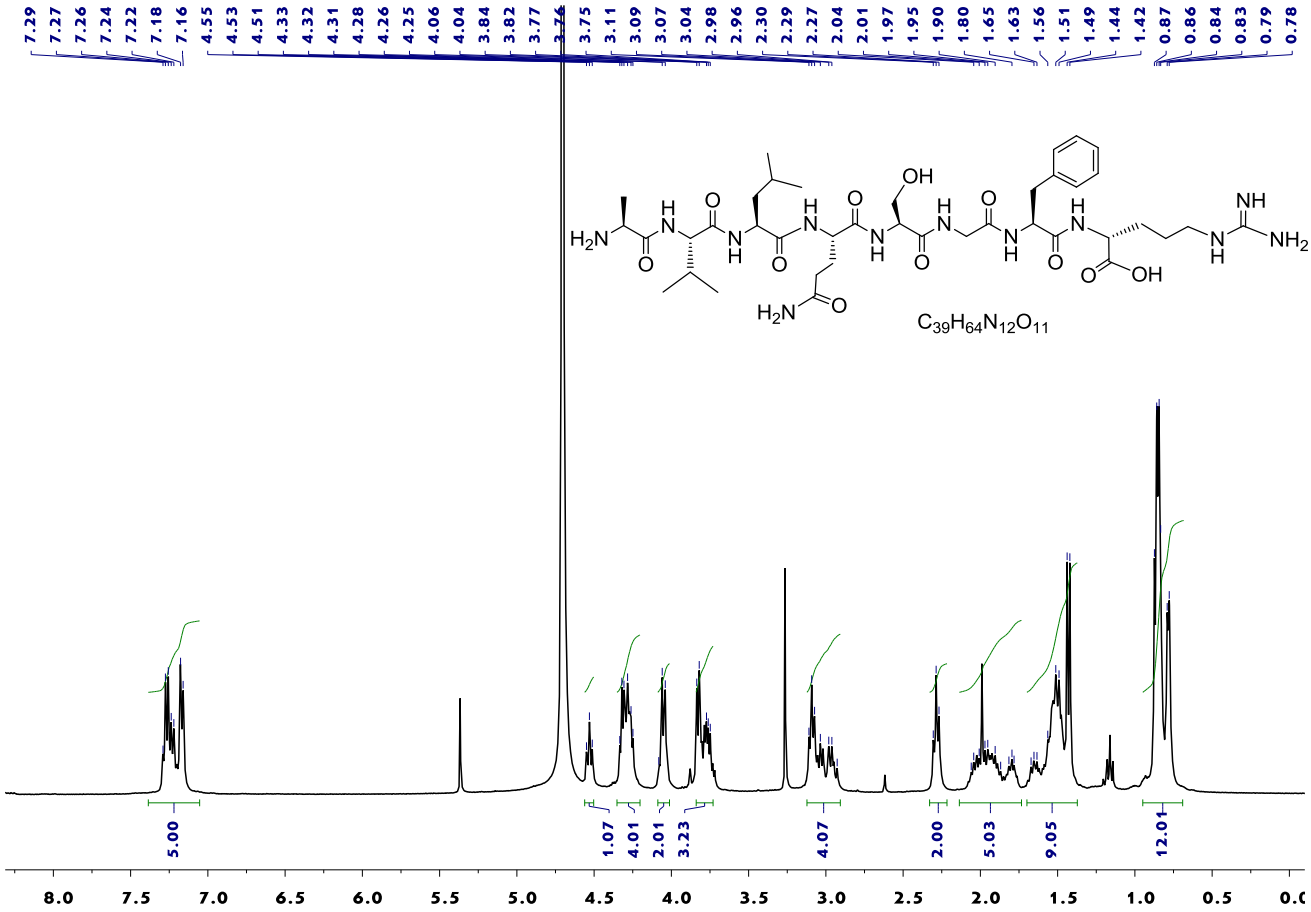

Anti-SARS octapeptide (2), H-AVLQSGFR-OH ^{1}H NMR (400 MHz, D_2O)

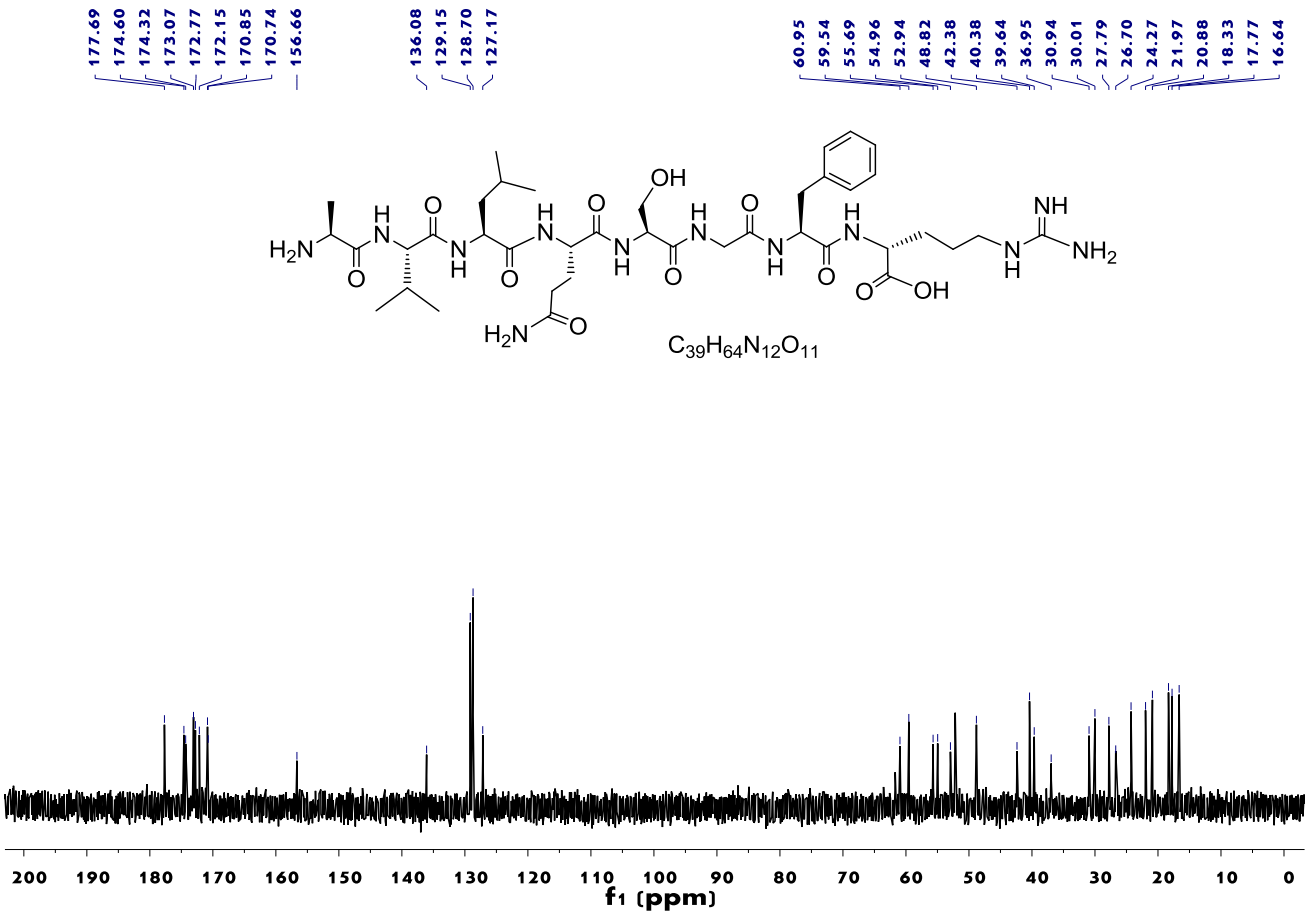

Anti-SARS octapeptide (2), H-AVLQSGFR-OH ^{13}C NMR (100 MHz, D_2O)

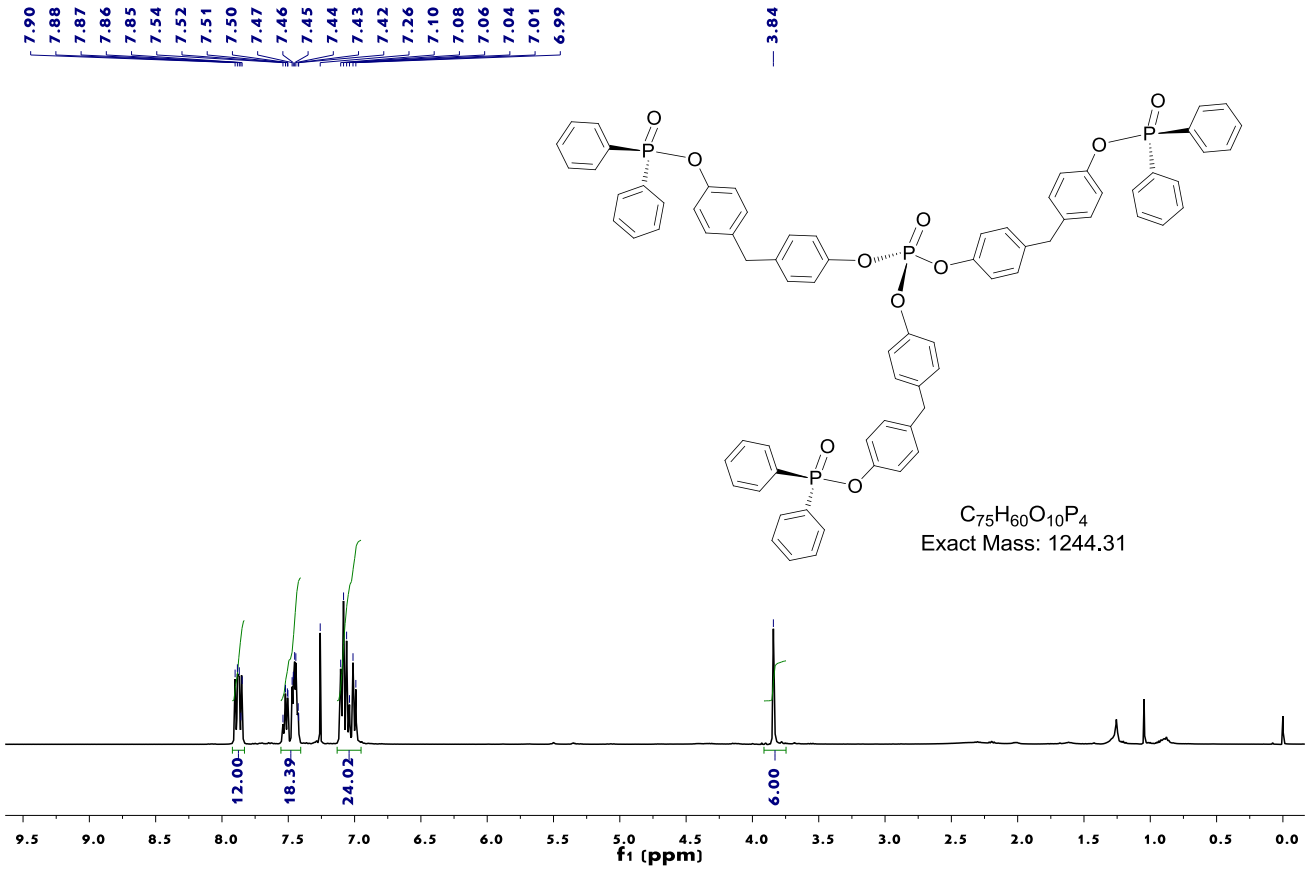

TDPBP residue ^{1}H NMR (400 MHz, $CDCl_3$)

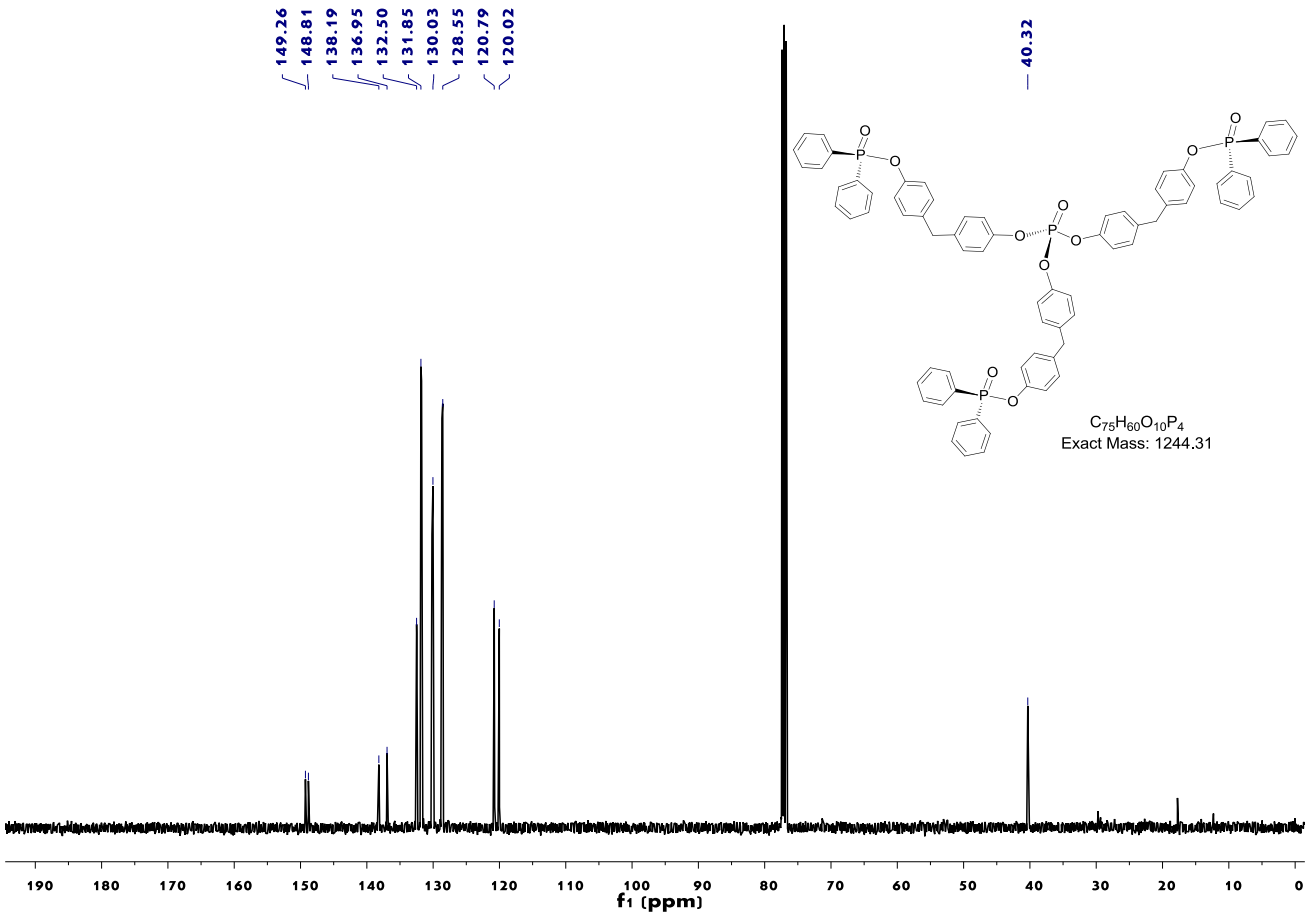

TDPBP residue ^{1}H NMR (400 MHz, $CDCl_3$)

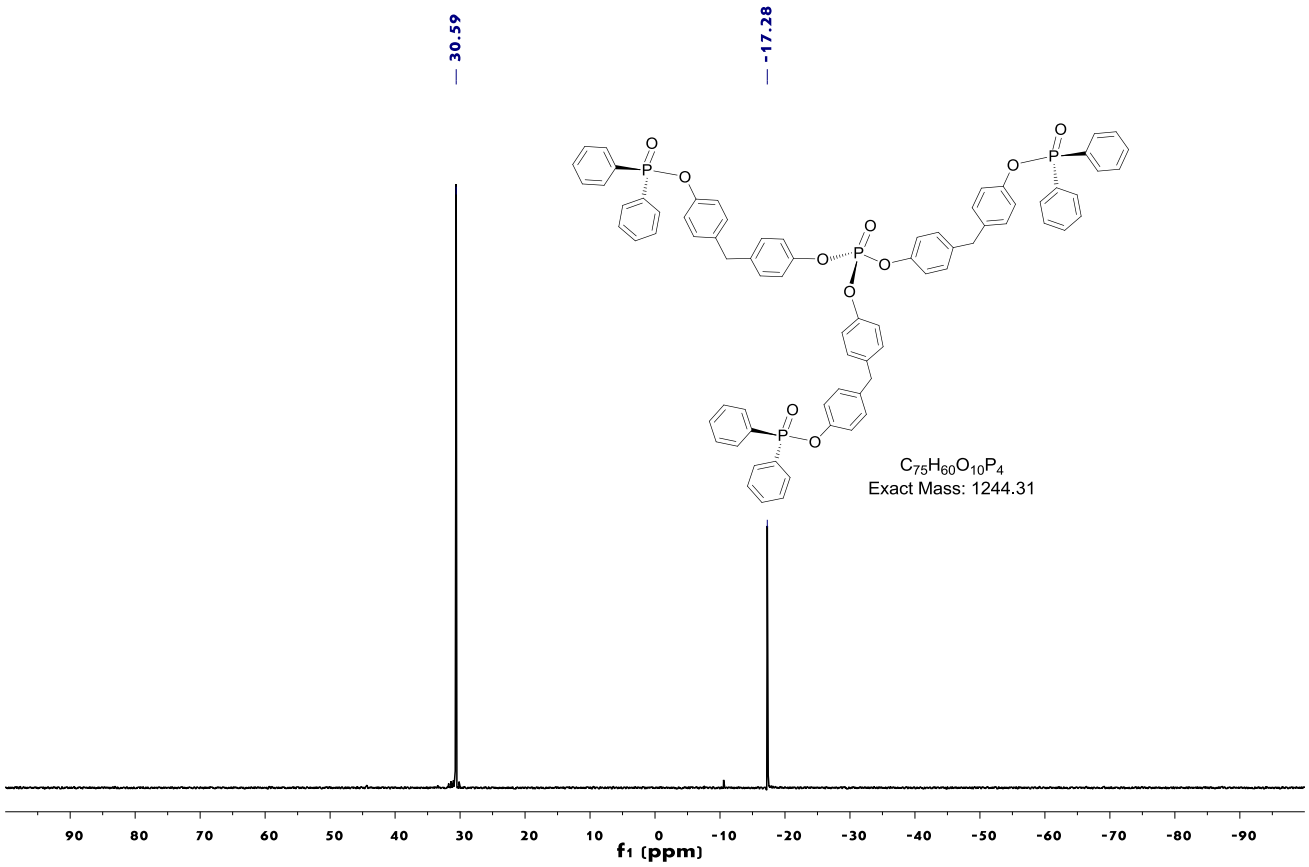

TDPBP residue ^{31}P NMR (162 MHz, $CDCl_3$)

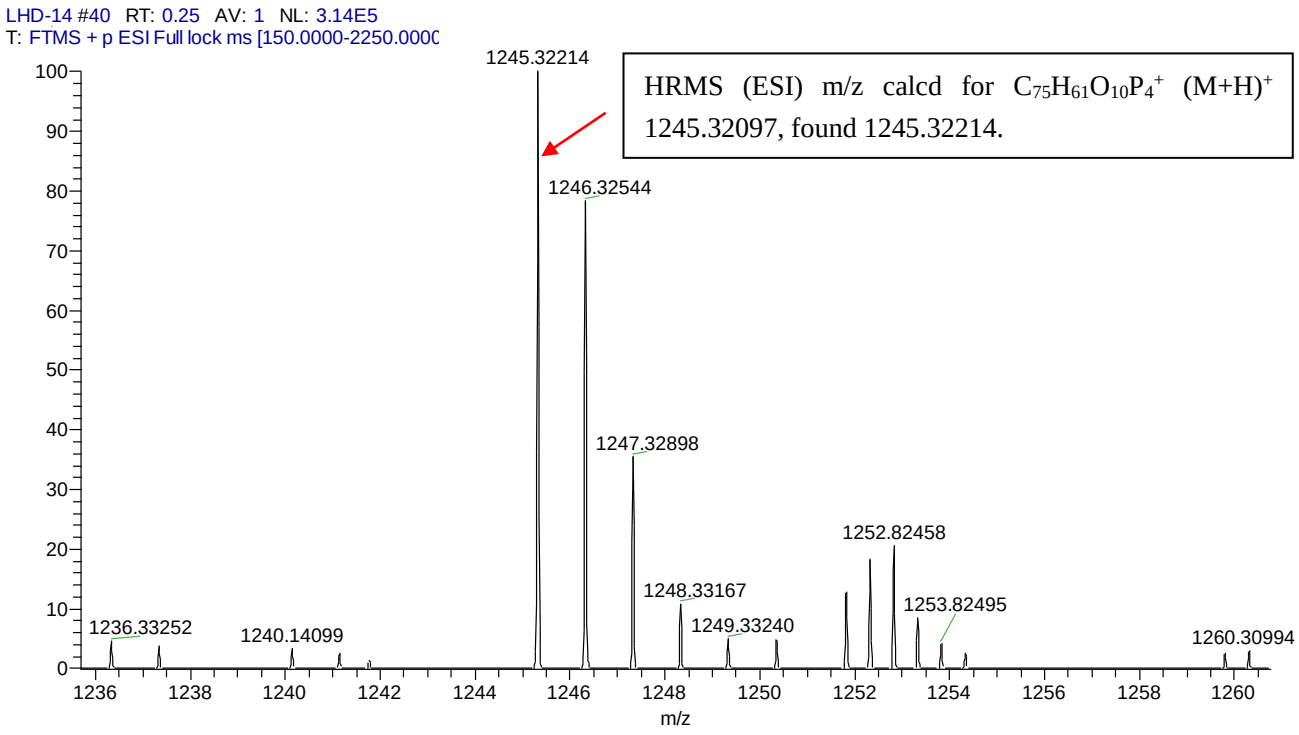

TDPBP residue HRMS (ESI)